Analysis of Microstructure and Growth Mechanism of Ion-Plated Cubic Boron Nitride Thin Film by Soft X-Ray Spectroscopy

Hidenori Kohzuki

Hyogo Prefectural Institute of Industrial Research

1995

Contents

Chapter 1
General Introduction

Cubic boron nitride (c-BN) was first successfully synthesized under the conditions of high pressure and temperature in 1957 by R.H.Wentorf, Jr. of General Electric Co. [1], and he and his coworkers had also first succeeded in synthesizing diamond under similar conditions to those that yield c-BN in 1955 [2]. Cubic boron nitride is one of crystalline phases of boron nitride (BN) and has been named "Borazon" by him [1].

Although BN has similar crystalline phases to those of carbon, BN does not exist in nature, unlike diamond and graphite [3]. The crystalline phases of BN are classified as cubic (zinc-blend, c-BN), wurtzite-type (w-BN), hexagonal (h-BN) and rhombohedral (r-BN), as shown in Fig. 1-1. In addition, the presences of turbostratic and amorphous BNs (t-BN and a-BN, respectively) are also known [4]. Cubic and wurtzite-type BNs are sp^3-bonded phases in which boron atoms combine with neighboring nitrogen atoms in four-fold coordination [5]. Hexagonal and rhombohedral BNs are sp^2-bonded phases in which boron atoms combine with neighboring nitrogen atoms in three-fold coordination [5]. Hexagonal BN is a layered graphite-like structure with planar six-membered rings of alternating boron and nitrogen atoms stacked in *AB AB* fashion (in a two-layered sequence). However, its structure differs slightly from that of graphite, and the hexagonal arrays are stacked directly above each other, each alternate layer being rotated by 30 degrees [5]. Rhombohedral BN has planar six-membered rings (like those of h-BN) stacked in a three-layered sequence (*ABC ABC*) [5]. Turbostratic BN consists of a random stacking of planar six-membered rings like those of h-BN [6, 7], and belongs to an sp^2-bonded phase. Pyrolytic BN (p-BN) which is synthesized by chemical vapor deposition is typical t-BN [8]. The B-N bonds in a-BN are considered to be sp^2-bonding [9], though a-BN does not exhibit a distinct crystal structure. Hexagonal BN has been already synthesized in 1842 and is well-known as "white graphite", since its properties are very similar to those of graphite [10]. Rhombohedral BN grows under similar conditions to those that yield h-BN, and has the

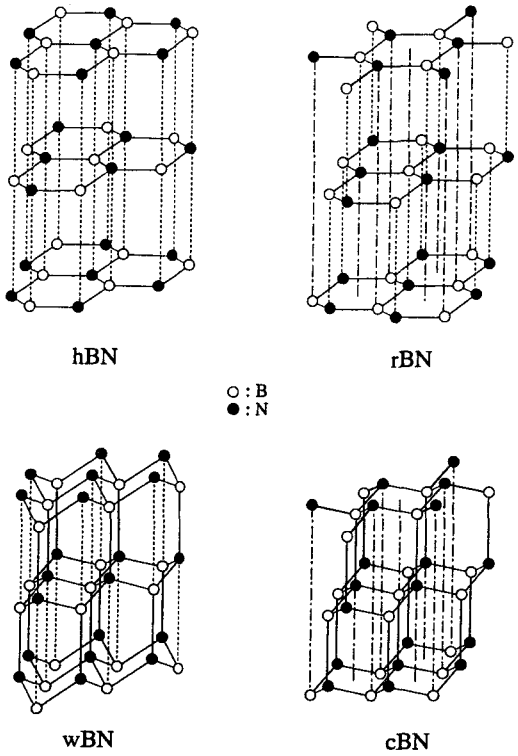

Fig. 1-1. The structures of hexagonal boron nitride (h-BN), rhombohedral boron nitride (r-BN), wurtzite-type boron nitride (w-BN) and cubic boron nitride (c-BN).

Table 1-1. The properties of cubic boron nitride (c-BN) and diamond.

Characteristics	c-BN	Diamond
Crystal structure	Zincblend	Diamond
Symmetry	$F\bar{4}3m$	$Fd3m$
Lattice constant (Å)	3.615	3.567
Density (g/cm^2)	3.48	3.515
Melting point (K)	3000	~ 4000
Vicker's hardness (kg/mm^2)	4695 ~ 8600	> 9000
Coefficient of linear expansion ($10^{-6}/K$)	4.3	4.5
Thermal conductivity (W/cm·K)	13	20
Refractive index	2.11	2.41
Dielectric constant	e_0 = 7.1 e_∞ = 4.5	5.58
Resistivity (Ω·cm)	10^2 ~ 10^{10}	$10 - 10^{16}$
Band gap (eV)	6.4 ~ 7.0	5.5

same properties as h–BN [5]. On the other hand, the crystal structures of c–BN and w–BN are similar to those of cubic and hexagonal diamond, respectively. As shown in Fig. 1–1, it is considered that c–BN and w–BN have zigzag six–membered rings of alternating boron and nitrogen atoms stacked in three–layered (*ABC ABC*) and two–layered (*AB AB*) sequences which correspond to those of r–BN and h–BN, respectively. Cubic BN is the high–pressure and high–temperature phase whereas w–BN is the high–pressure and low–temperature phase. Therefore, both BNs are metastable at ambient conditions whereas h–BN and r–BN are stable at ambient conditions. Cubic and wurtzite–type BNs are generally produced under static and dynamic compression, respectively [11].

BN is analogous to carbon materials, such as graphite and diamond, in many respects. However, BN is more chemically and thermally stable than carbon materials. For instance, carbon materials begin to be oxidized at about 600 °C whereas BN resists oxidation even at elevated temperatures up to about 900 °C [12]. Furthermore, carbon materials react readily with carbide–forming metals like ferrous alloys whereas BN is non–reactive with these metals [5]. Typical examples for practical uses of h–BN and t–BN are high–temperature solid lubricants, heating crucibles, microwave guide tubes, high–temperature insulators, *etc.* [9]. And the technical use of c–BN is mainly cutting tools because of its extreme hardness.

Since c–BN and diamond have low densities, extreme hardnesses, large thermal conductivities, wide band gaps and large resistivities, as shown in Table 1–1 [13], the both have been found to be useful for lots of applications. For example, they are excellent materials for cutting tool coatings and corrosion barriers because of their high hardnesses and chemical resistances, and for insulating and heat sinking films of semiconductors because of their large thermal conductivities and resistivities [14]. The advantage of c–BN is that it can be especially used to machine steel materials whereas diamond is not suitable. Their wide–ranging transparencies from ultraviolet to infrared are also preferable for optical applications, such as windows, lens coatings and x–ray lithography masks [14]. Moreover, possibilities as wide band gap semiconductors are quite attractive. In particular, c–BN can be doped both *p* and *n* type whereas diamond can only be doped *p* type [15, 16]. In addition, O.Mishima [17] has reported the manufacture from doped

c-BN crystals of an ultraviolet-emitting diode that functions up to 677 °C. These extensive potential applications have led to the intensive investigation of the synthesis of c-BN thin film using various vapor deposition process, because c-BN can only be manufactured in powder form and it is difficult to fabricate a bulky c-BN compact by normal pressure sintering and even by hot-pressing unless appropriate additives are mixed to pure c-BN powder [9].

In practice, the syntheses of diamond and c-BN films were subjects of study attracting the interest of many researchers, since S.Aisenberg *et al.* [18] had first reported about the diamond-like carbon film prepared by the C^+ ion beam deposition in the early 1970's. In particular, since S.Matsumoto *et al.* [19] had actually proved in 1981 that diamond film can be prepared from gaseous phase at low pressure, using the hot filament-assisted chemical vapor deposition, many researchers have begun to investigate extensively on the syntheses of these films using various physical and chemical vapor deposition (PVD and CVD) techniques [20]. The synthesis of c-BN film under low pressure was first reported in 1979 by M.Sokolowski [21], using a reactive pulse plasma deposition technique, and subsequently, C.Weissmantel [22] reported about the hard BN film deposited by an ion beam deposition technique, in 1981. Since then, there have been many investigations about its synthesis by many deposition techniques including reactive ion plating [23 - 27], radio-frequency (RF) sputtering [28 - 30], electron cyclotron resonance (ECR) plasma deposition [31], ion beam deposition [32 - 36], ion-assisted laser deposition [37 - 39] and plasma CVD [40 - 47]. However, it seems that the synthetic investigation of c-BN film is very smaller in number than that of diamond film, though many reports on the former synthesis have appeared from the 1980's [13, 48]. In the 1980's, the formation of c-BN film met with skepticism for the lack of sufficient characterization of the structure, composition and so on, whereas the formation of diamond film had been clearly evidenced by its Raman spectrum [19]. From the late 1980's to the early 1990's, some reports have shown the evidence of c-BN film formation by the detailed characterization [24 - 25, 49], and it has been recently gradually recognized that a c-BN film is formed by various PVD and CVD techniques. However, it is also considered that a Raman spectrum corresponding to a c-BN phase should be obtained from a c-BN film as perfect evidence for showing its formation, like a diamond film [50]. Unfortu-

nately, up to now, there is no report that the Raman spectrum has been measured on a c–BN film [25, 43, 51]. In reviewing the literature on c–BN films deposited by PVD and CVD techniques, it was noticed that a c–BN film had been successfully deposited by PVD rather than CVD techniques. A reactive ion–plating method has an advantage of that ceramic films with excellent adhesion force to a substrate, such as carbide, nitride and oxide, can be readily deposited on a large–area substrate at a high deposition rate, compared with other PVD techniques [52]. From these reasons, the author started a research on the deposition of c–BN film with a reactive ion–plating method for its application to cutting tool coatings, in 1988.

As mentioned above, the formation of c–BN film under low pressure could be scarcely believed for the lack of sufficient characterization of the structure and composition, when the author started the research. In those days, the phase identification of c–BN film was carried out mainly by infrared absorption spectroscopy and electron diffractometry [13, 40, 48, 53, 54]. Although x–ray diffractometry is superior and reliable analysis of the crystal structures of materials, this analysis could not be applied to the phase identification of c–BN film, because the deposited c–BN films were submicron thick and composed of fine crystallites of less than several tens nanometers [23 – 47] and because boron and nitrogen atoms are poor x–ray scatterers. However, it is very difficult to distinguish between c–BN and w–BN with infrared absorption spectroscopy, and to observe the weak reflections from the (200) and (222) planes of c–BN even with electron diffractometry because of a small difference between the atomic scattering factors of boron and nitrogen atoms [6]. Therefore, it is considered that infrared absorption spectroscopy and electron diffractometry are not always good analytical methods enough to identify the crystal structure of c–BN film. In addition to these analyses, there have been several attempts to identify the crystal structure of c–BN film with electron energy loss spectroscopy (EELS) and x–ray photoelectron spectroscopy (XPS) [50, 51, 55]. However, these analyses also were not always good means for its phase identification because c–BN exhibits the same EELS spectrum as w–BN [56, 57] and because there is little difference between the photoelectron energies of B *1s* or N *1s* of c–BN and h–BN [58]. The composition of c–BN film is determined by Auger electron spectroscopy [3, 25, 59], Rutherford backscattering spectroscopy [5, 10, 51], electron

microprobe analysis [24, 58] and x-ray photoelectron spectroscopy [29, 39, 60].

It is well-known that emission band spectra of characteristic x-rays reflect the electronic structures of materials and change in their spectral features with variation in chemical bond of elements [61 - 65]. Therefore, x-ray emission spectra have been measured on many materials in order to obtain the knowledge of their valence and electronic structures [66, 67]. The origin of K-emission band spectrum of boron (B K x-ray emission spectrum) is due to the electron transition to the *1s* from *2p* orbitals which is a valence one. It is, accordingly, known that its spectral feature changes with the variation in chemical bond of boron [68 - 72]. Thus, it is possible that the B K x-ray emission spectral feature changes depending on the crystal structure of BN, and it is expected to obtain the useful information about the chemical bonding states and microstructures of c-BN film from its B K x-ray emission spectral features. However, there is no report about the change of B K x-ray emission spectral feature depending on the crystal structure of BN, so far as the author knows.

Since it was not scientifically recognized that a c-BN film can be deposited under low pressure by PVD and CVD techniques and there were a few means of investigating the microstructure of the deposited BN thin film, this study has been undertaken with the following purposes.

(1) To verify that a c-BN film can be actually deposited by a reactive ion-plating method which is one of PVD techniques.

(2) To clarify that B K x-ray emission spectrum changes in the spectral feature depending on the crystal structure of BN.

(3) To elucidate the microstructures of the ion-plated c-BN thin films with soft x-ray spectroscopy using B K x-ray emission spectrum.

In chapter 2, the deposition conditions of c-BN film by the ion-plating method are described. BN films have been prepared under various deposition conditions by the reactive ion-plating method, and their crystal structures have been investigated by infrared absorption spectroscopy, electron diffractometry, electron energy loss spectroscopy, x-ray diffractometry and Raman spectroscopy. The c-BN film has been successfully deposited at self-bias voltages of -40 ~ -60 V, Ar/N_2 gas flow ratios of 2.0 ~ 3.0, ionization current of 14 A and electron-beam powers

(for boron evaporation) of 1.8 – 2.0 kW by the reactive ion–plating method.

In chapter 3, the changes of B K x–ray emission spectral features with kinds of atoms/ions combined to boron and depending on the crystal structure of BN are described. The B K x–ray emission spectra have been precisely measured by an electron probe microanalyzer using several boron compounds with different ligands of boron and BNs with different crystal structures, and it has been clarified that the B K x–ray emission spectrum changes in the spectral features with kinds of atoms/ions combined to boron and depending on the crystal structure of BN, such as the peak position, full width at half maximum and asymmetric index of the main band, the relative intensities and peak positions of the satellite bands. Furthermore, the characterization of ion–plated BN films has been carried out using the B K x–ray emission spectra.

In chapter 4, the adhesion improvement of the ion–plated c–BN film to a silicon substrate and its atmospheric degradation are described. The adhesion improvement has been investigated using three techniques, such as the formation of the buffer interlayer, the stress relief annealing and the ion implantation of boron and nitrogen ions to the substrate. The degradations of c–BN films exposed to air with different relative humidities have been investigated from SEM obser–vations and soft x–ray spectroscopic analyses of these films.

In chapter 5, the formation process of ion–plated c–BN film is described. Cubic BN films have been deposited by varying the deposition time, and it has been clarified by the soft x–ray spectroscopic analyses of these films that the sp^2–bonded BN film like h–BN forms at the initial stage of deposition prior to the growth of c–BN film.

In chapter 6, the reproductions of the measured B K x–ray emission spectra by the theoretical calculation with the discrete–variational Hartree–Fock–Slater (DV–Xα) method [73] are de–scribed. It has been clarified that the microstructure of the initially deposited BN film can be analyzed by the DV–Xα calculation of the B K x–ray emission spectrum.

In chapter 7, the growth mechanism of c–BN film deposited by the reactive ion–plating method is discussed from the knowledge obtained in this study, compared with the several arguments which have recently been suggested about those of c–BN films deposited by other PVD techniques [27, 31, 32, 35, 53].

References

[1] R.H.Wentorf, Jr., J. Chem. Phys., **26**, 956(1957).

[2] F.P.Bundy, H.T.Hall, H.M.Strong and R.H.Wentorf, Jr., Nature London, **176**, 51(1955).

[3] L.Guzman and M.Elena, Mater. Sci. Forum, **54&55**, 21(1990).

[4] A.Onodera, K.Inoue, H.Yoshihara, H.Nakae, T.Matsuda and T.Hirai, J. Mater. Sci., **25**, 4279(1990).

[5] T.A.Friedmann, P.B.Mirkarimi, D.L.Medlin, K.F.McCarty, E.J.Klaus, D.R.Boehme, H.A.Johnsen, M.J.Mills, D.K.Ottesen and J.C.Barbour, J. Appl. Phys., **76**, 3088(1994).

[6] D.L.Medlin, T.A.Friedmann, P.B.Mirkarimi, P.Rez, M.J.Mills and K.F.McCarty, J. Appl. Phys., **76**, 295(1994).

[7] B.E.Warren, Phys. Rev., **59**, 693(1941).

[8] H.Tanji and M.Hara, Boundary, **2**, 46(1986).

[9] K.Sugiyama and H.Itoh, Mater. Sci. Forum, **54&55**, 141(1990).

[10] F.Fujimoto, Mater. Sci. Forum, **54&55**, 45(1990).

[11] P.K.Lam, R.M.Wentzcovitch and M.L.Cohen, Mater. Sci. Forum, **54&55**, 165(1990).

[12] S.Komatsu, T.Yoshida and K.Akashi, Proc. 9th Symp. on ISIAT '85, Tokyo, (1985), p.421.

[13] H.Saitoh and Y.Ichinose, Bull. Jpn. Inst. Met., **27**, 720(1988).

[14] T.Ichiki, T.Momose and T.Yoshida, J. Appl. Phys., **75**, 1330(1994).

[15] R.M.Chrenko, Phys. Rev., **B7**, 4560(1973).

[16] D.K.Ferry, Phys. Rev., **B12**, 2361(1975).

[17] O.Mishima, Mater. Sci. Forum, **54&55**, 313(1990).

[18] S.Aisenberg and R.W.Chabot, J. Appl. Phys., **42**, 2953(1971).

[19] S.Matsumoto, Y.Sato, M.Kamo and N.Setaka, Jpn. J. Appl. Phys., **21**, L183(1982).

[20] R.C.DeVries, *Diamond and Diamond-like Films and Coatings* (Plenum, New York, 1991).

[21] M.Sokolowski, J. Cryst. Growth, **46**, 136(1979).

[22] C.Weissmantel, J. Vac. Sci. Technol., **18**, 179(1981).

[23] B.Rother, H.D.Zscheile, C.Weissmantel, C.Heiser, G.Holzhüter, G.Leonhardt and P.Reich,

Thin Solid Films, **142**, 83(1986).

[24] K.Inagawa, K.Watanabe, H.Ohsone, K.Saitoh and A.Itoh, J. Vac. Sci. Technol., **A5**, 2696(1987).

[25] T.Ikeda, Y.Kawate and Y.Hirai, J. Vac. Sci. Technol., **A8**, 3168(1990).

[26] M.Murakawa and S.Watanabe, Surf. Coat. Technol., **43/44**, 128(1990).

[27] D.R.McKenzie, W.D.McFall, W.G.Sainty, C.A.Davis and R.E.Collins, Diamond Relat. Mater., **2**, 970(1993).

[28] C.Weissmantel, K.Bewilogua, K.Breuer, D.Dietrich, U.Ebersbach, H.-J.Erler, B.Rau and G.Reisse, Thin Solid Films, **96**, 31(1982).

[29] M.Mieno and T.Yoshida, Jpn. J. Appl. Phys., **29**, L1175(1990).

[30] H.Windischmann, J. Vac. Sci. Technol., **A9**, 2431(1991).

[31] A.Weber, U.Bringmann, R.Nikulski and C.-P.Klages, Surf. Coat. Technol., **60**, 493(1993).

[32] C.Weissmantel, Thin Solid Films, **92**, 55(1982).

[33] M.Satou and F.Fujimoto, Jpn. J. Appl. Phys., **22**, L171(1983).

[34] K.Miyoshi, D.H.Buckley and T.Spalvins, J. Vac. Sci. Technol., **A3**, 2340(1985).

[35] D.J.Kester and R.Messier, J. Appl. Phys., **72**, 504(1992).

[36] D.J.Kester, K.S.Ailey, R.F.Davis and K.L.More, J. Mater. Res., **8**, 1213(1993).

[37] G.Kessler, H.-D.Bauer, W.Pompe and H.-J.Scheibe, Thin Solid Films, **147**, L45(1987).

[38] G.L.Doll, J.A.Sell, C.A.Taylor and R.Clarke, Phys. Rev., **B43**, 6816(1991).

[39] K.Kaneda and K.Shibata, Jpn. J. Appl. Phys., **32**, 5652(1993).

[40] K.L.Chopra, V.Agarwal, V.D.Vankar, C.V.Deshpandey and R.F.Bunshah, Thin Solid Films, **126**, 307(1985).

[41] A.Chayahara, H.Yokoyama, T.Imura and Y.Osaka, Jpn. J. Appl. Phys., **26**, L1435(1987).

[42] H.Saitoh, T.Hirose, H.Matsui, Y.Hirotsu and Y.Ichinose, Surf. Coat. Technol., **39/40**, 265(1989).

[43] S.Komatsu, Y.Moriyoshi, M.Kasamatsu and K.Yamada, J. Appl. Phys., **70**, 7078(1991).

[44] A.Bath, P.J. van der Put, J.G.M.Becht, J.Schoonman and B.Lepley, J. Appl. Phys., **70**, 4366(1991).

[45] L.Maya, J. Am. Ceram. Soc., **75**, 1985(1992).

[46] H.Saitoh, H.Morino and Y.Ichinose, Jpn. J. Appl. Phys., **32**, L1684(1993).

[47] S.V.Nguyen, T.Nguyen, H.Treichel and O.Spindler, J. Electrochem. Soc., **141**, 1633(1994).

[48] S.P.S.Arya and A.D'Amico, Thin Solid Films, **157**, 267(1988).

[49] D.R.McKenzie, W.G.Sainty and D.Green, Mater. Sci. Forum, **54&55**, 193(1990).

[50] M.Mieno and T.Yoshida, Pro. Symp. on Synthesis of Cubic Boron Nitride, Tokyo, (1991), p.1.

[51] W.D.Halverson, T.G.Tetreault and J.K.Hirvonen, Mater. Sci. Forum, **54&55**, 71(1990).

[52] R.F.Bunshah, J.M.Blocher, Jr., D.M.Mattox, T.D.Bonifield, G.E.McGuire, J.G.Fish, M.Schwartz, P.B.Ghate, J.A.Thornton, B.E.Jacobson and R.C.Tucker, Jr., *Deposition Technologies for Films and Coatings* (Noyes, New Jersey, 1982), p.244.

[53] C.Weissmantel, K.Bewilogua, D.Dietrich, H.-J.Erler, H.-J.Hinneberg, S.Klose, W.Nowick and G.Reisse, Thin Solid Films, **72**, 19(1980).

[54] H.Miyamoto, M.Hirose and Y.Osaka, Jpn. J. Appl. Phys., **22**, L216(1983).

[55] D.R.McKenzie, D.J.H.Cockayne, D.A.Muller, M.Murakawa, S.Miyake, S.Watanabe and P.Fallon, J. Appl. Phys., **70**, 3007(1991).

[56] J.Hosoi, T.Oikawa, M.Inoue, Y.Matsui and T.Endo, J. Electron Spectrosc. Relat. Phenom., **27**, 243(1982).

[57] S.Saito, K.Higeta and T.Ichinokawa, J. Microscopy, **142**, 141(1986).

[58] K.Nakamura, Mater. Sci. Forum, **54&55**, 111(1990).

[59] K.Inagawa, K.Watanabe, K.Saitoh, Y.Yuchi and A.Itoh, Surf. Coat. Technol., **39/40**, 253(1989).

[60] M.Okamoto, H.Yokoyama and Y.Osaka, Jpn. J. Appl. Phys., **29**, 930(1990).

[61] D.J.Fabian, *Soft X-Ray Band Spectra* (Academic Press, London, 1968).

[62] D.J.Fabian, L.M.Watson and C.A.W.Marshall, Rep. Progr. Phys., **34**, 601(1972).

[63] D.J.Nagel, Advan. X-Ray Anal., **13**, 182(1970).

[64] Y.Gohshi, J. Spectrosc. Soc. Jpn., **18**, 235(1969).

[65] W.L.Baun, Appl. Spectry. Rev., **1**, 379(1968).

[66] D.W.Fisher, Advan. X-Ray Anal., **13**, 159(1969).

[67] M.Motoyama and G.Hashizume, J. Spectrosc. Soc. Jpn., **29**, 92(1980).

[68] D.J.Joyner and D.M.Hercules, J. Chem. Phys., **72**, 1095(1980).

[69] M.Okusawa, K.Ichikawa, T.Matsumoto and K.Tsutsumi, J. Phys. Soc. Jpn., **51**, 1921(1982).

[70] S.Luck and D.S.Urch, Physica Scripta, **41**, 970(1990).

[71] R.D.Carson and S.E.Schnatterly, Phys. Rev. Lett., **59**, 319(1987).

[72] B.M.Davis, F.Bassani, F.C.Brown and C.G.Olson, Phys. Rev., **B24**, 3537(1981).

[73] H.Adachi, *Ryoshi-Zairyo-Kagaku-Nyumon* (means an introduction to quantum chemistry for materials), (Kyoritsu-Shuppan, Tokyo, 1991).

Chapter 2
Deposition of Cubic Boron Nitride Film by Reactive Ion-Plating Method

2-1. Introduction

Since a diamond film was prepared by hot filament-assisted chemical vapor deposition [1], there are many investigations on the synthesis of a cubic boron nitride (c-BN) film from gaseous phase at low pressure by various physical or chemical vapor depositions (PVD or CVD) [2], such as reactive ion plating [3 - 6], radio-frequency (RF) sputtering [7], ion beam-assisted deposition [8 - 10] and plasma-enhanced CVD deposition [11 - 18]. Unlike a diamond film, it seems that a c-BN film is successfully deposited by PVD rather than CVD [10].

The advantage of a reactive ion-plating method is to be able to coat metallic or ceramic films like carbide, nitride and oxide with excellent adhesion to a substrate at a high deposition rate on a large-area substrate, compared with other PVD techniques [19]. Therefore, it is considered that a reactive ion-plating method is more practical than other PVD techniques for c-BN coatings. The deposition by a reactive ion-plating method is generally performed using various plasmas for the ionization of species, such as a glow discharge, RF discharge, arc discharge, hollow cathode discharge and thermoelectron-assisted discharge. It is known that a thermoelectron-assisted plasma discharge can occur in vacuum of the order of 10^{-2} Pa and ionize efficiently species [19]. It is, therefore, considered that a thermoelectron-assisted plasma discharge is superior to other plasma discharges for the stable electron-beam evaporation of boron, which can be obtained in vacuum of less than 10^{-1} Pa, and for the ionization of boron and nitrogen. In this study, thus, the deposition of c-BN film was attempted by the reactive ion-plating method using a thermoelectron-assisted DC plasma discharge for the ionization of species such as boron, nitrogen and argon in terms of the practical c-BN coatings.

Although there have been several reports on the deposition of c-BN film by reactive ion-plating methods [3 - 6], the detailed effects of the ion-plating parameters on the formation of c-BN film have not been sufficiently investigated, and the formation of c-BN film by a reactive ion-

plating method has not always been verified because of the lack of sufficient characterization of the structure, composition and so on. Thus, in order to grasp the deposition conditions of c-BN film by the reactive ion-plating method and to verify its formation, BN films were deposited on a silicon substrate by varying the ion-plating parameters such as the substrate bias voltage, electron-beam power for boron evaporation, Ar/N_2 gas flow ratio introduced into the deposition chamber, *etc.*, and were characterized by infrared absorption spectroscopy, electron diffractometry, electron energy loss spectroscopy, x-ray diffractometry and Raman spectroscopy.

2-2. Effects of Ion-Plating Parameters on Deposition of Cubic BN Film

Boron nitride is a good insulator. In the case of the BN film deposition by the reactive ion-plating method using a thermoelectron-assisted DC plasma discharge, it is difficult to keep the plasma discharge stable throughout deposition because the insulated BN film is deposited on an ionization electrode. Therefore, in order to obtain the stable plasma discharge throughout deposition, a pair of magnets were attached to the ion-plating apparatus for generating a magnetic field parallel to the electric field between a thermoelectron radiating filament (hot cathode) and an opposed anode with a positive voltage. The method using this apparatus is, hereafter, called the reactive ion-plating method with a hot cathode plasma discharge in a parallel magnetic field.

In order to grasp the deposition conditions of the c-BN film by this ion-plating method, the BN films were deposited on Si substrates by varying the ion-plating parameters such as RF power applied to the substrate, electron-beam (EB) power for boron evaporation and ionization current which flows to the anode from the hot cathode. The phase identification of the deposited BN film was mainly carried out by Fourier transform infrared spectroscopy (FTIRS).

Consequently, it was found that the application of high RF power to the substrate and the addition of argon gas into a nitrogen gas plasma are required for the formation of c-BN film, although any BN films cannot be deposited at the excessive RF power due to resputtering.

Experimental Procedure

Ion-plating apparatus

Figure 2-1 shows the schematic diagram of the ion-plating apparatus used. A plasma is produced near the substrate by a hot cathode, an anode and a pair of magnets. Without the pair of magnets, the maximum ionization current obtained was only about 2 A, moreover, the current decreased with deposition progress and finally did not flow due to the insulated BN film deposited on the anode. Thus, in order to make thermoelectrons screw motion from the hot cathode toward the anode, a pair of magnets were attached to the apparatus for generating a magnetic field parallel to the electric field between the anode and the hot cathode [20]. Consequently, the plasma was enhanced by the magnetic field, and the maximum ionization current attained to about 15 A. The anode and the hot cathode are made of a molybdenum (Mo) plate of 100 x 10 x 2 mm and a tungsten (W) filament of 1mm$^{\phi}$, respectively. The pair of magnets (1100 x 50 x 12 mm) are made of strontium ferrite, and cooled by water. The distance between the magnets is about 180 mm. The magnetic field at the center of the two magnets is about 30 Ga. Figure 2-2 shows the relationship between the ionization voltage applied to the anode and the ionization current at various W filament powers. On this apparatus, the insulated BN film is prevented from depositing on the anode at an ionization current of 7 A or more, and the plasma can be kept stable throughout the deposition.

Preparation of BN film

Deposition chamber was pre-evacuated to the order of 10^{-4} Pa by a oil diffusion pump with a liquid nitrogen trap and rotary pump system. Before deposition, argon (Ar) plasma was generated for 5 minutes for cleaning the substrate which was a mirror-polished Si wafer. Nitrogen (N_2, purity 99.99%) and Ar (purity 99.99%) gases were introduced into the deposition chamber through the gas flow controllers of float type, and the working gas pressure was $6 \times 10^{-2} \sim 1 \times 10^{-1}$ Pa. The BN films were deposited on the substrates for 20 minutes by reaction of the EB-evaporated boron (purity 99.9%) with nitrogen ions generated in the plasma. The distance between the evaporation source and the substrate is 400 mm. RF (13.56 MHz) power was

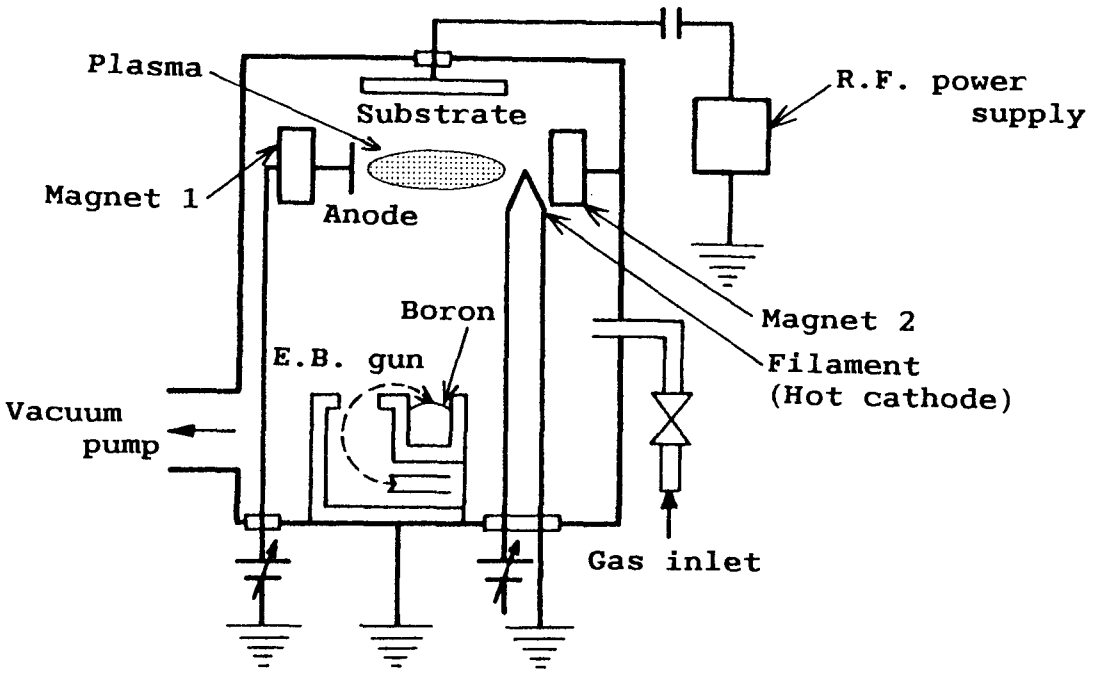

Fig. 2-1. Schematic diagram of the ion-plating apparatus.

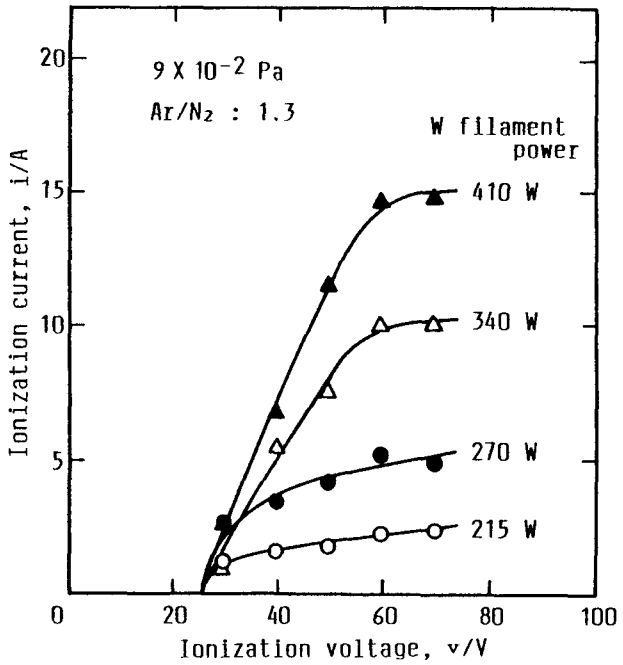

Fig. 2-2. Relation between the ionization voltage and current at various W filament powers.

applied to the substrate for generating a negative self-bias voltage so as to accelerate nitrogen and argon ions and promote the reaction. However, in this experiment, the self-bias voltage could not be actually measured, as the voltmeter was not attached to the apparatus. During the deposition, the ionization voltage was kept constant at 60 V, and the ionization current was controlled by varying W filament power. Although the substrate was not heated, its temperature during the deposition was presumed to be more than 523 K, since the temperature of the back face of the substrate holder was measured immediately after the deposition to be 523 K. Experimental conditions are summarized in Table 2-1.

Table 2-1. Experimental conditions for the depositions of BN films.

Substrate	Si wafer
Temperature	> 523 K
E.B. power	1.4 ~ 2.0 kW
E.B. evaporant	99.9 % boron
Ionization voltage	60 V
Ionization current	5 ~ 14 A
W filament power	215 ~ 410 W
R.F. power	0 ~ 150 W (13.56 MHz)
Pressure	$6 \times 10^{-2} \sim 1 \times 10^{-1}$ Pa
Ar/N_2 gas flow ratio	1 ~ 1.3

Results and Discussion

Analysis of BN film

Boron nitride has various kinds of crystal structures which are correspond to those of carbon. The crystalline phases of BN are classified as cubic (zincblend, c-BN), wurtzite-type (w-BN), hexagonal (h-BN), turbostratic (t-BN), rhombohedral (r-BN) and amorphous (a-BN) [21].

For identification of a crystalline phase, x-ray diffractometry is generally superior and reliable. It is, however, difficult to perform the phase identification of BN film by x-ray diffractometry, because BN films deposited by various PVD and CVD processes are very thin films of

less than 0.5 μm, and consist of fine crystallites of less than tens nanometers, and moreover, of light elements [22]. Therefore, the phase identification of BN film is generally performed by FTIRS or electron diffractometry [23]. In this experiment, it was carried out by FTIRS.

Figures 2–3 and 2–4 show the infrared (IR) absorption spectra of different BN powders used as standard samples. In these samples, c–BN, h–BN and t–BN powders are commercially available, c–BN powder is synthesized at high temperature and high pressure and t–BN powder is pyrolytic BN synthesized by thermal CVD [24]. Wurtzite–type BN powder is synthesized by shock compression [25], r–BN and a–BN powders are synthesized in nitrogen atmosphere at 1173 K from $NaBH_4$ + NH_4Cl and KBH_4 + NH_4Cl, respectively [26, 27]. Each BN powder was mixed with KBr and formed into a disk. The IR spectrum was measured in transmittance mode using the disk.

Cubic BN and w–BN, which are sp^3–bonded phases, have a reststrahlen band at about 1050 cm^{-1}, while h–BN, r–BN, t–BN and a–BN, which are sp^2–bonded phases, have two absorption bands at about 1380 cm^{-1} due to the B–N stretching vibration and at about 800 cm^{-1} due to B–N–B bending vibration [28, 29]. By the IR spectrum, an sp^3–bonded phase can be distinguished distinctly from an sp^2–bonded phase, however, it is difficult to distinguish between c–BN and w–BN or among h–BN, r–BN, t–BN and a–BN.

Figure 2–5 shows the examples of IR spectra obtained from the BN films deposited by the ion–plating method. These IR spectra were measured in transmittance mode using the disks into which were formed from the mixture of KBr and each BN film peeled off from the substrate. Most of these spectra have three absorption peaks at about 1050 cm^{-1} corresponding to an sp^3–bonded phase, and at about 1380 and 800 cm^{-1} corresponding to an sp^2–bonded phase. Judging from these spectra, most of the BN films are considered to consist of the mixture of sp^2– and sp^3–bonded BN phases. As above–mentioned, it is difficult to distinguish between c–BN and w–BN with the IR spectrum. In this experiment, however, the IR absorption peak at 1050 cm^{-1} in the IR spectrum of the BN film is considered to be due to a c–BN phase, as described later in section 2–3. The percentage of c–BN phase content $R(c)$ in the film was calculated simply using the IR absorption intensities of each band, $I(c)$ at 1050 cm^{-1} and $I(h)$ at 1380 cm^{-1}. The

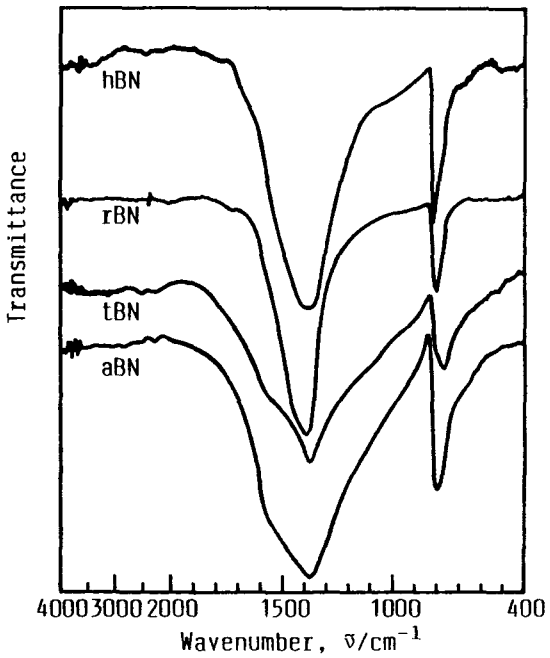

Fig. 2-3. Infrared absorption spectra of the BN powders with different crystalline phases.

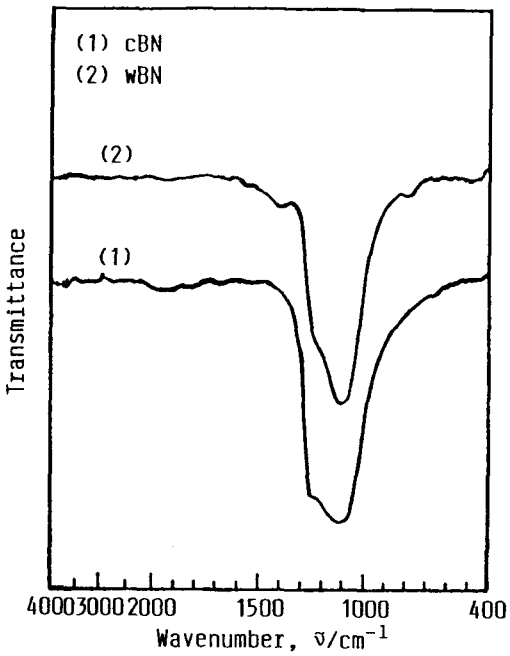

Fig. 2-4. Infrared absorption spectra of c-BN powder synthesized at high temperature and pressure, and of w-BN powder synthesized by shock compression.

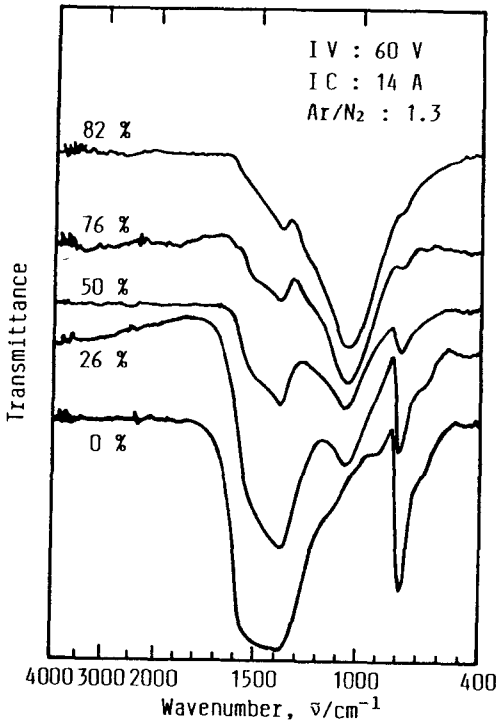

Fig. 2-5. Infrared absorption spectra of the BN films deposited by the ion-plating method. Cubic BN phase contents in each film denoted in this figure were estimated by the infrared absorption intensities of each band at 1050 and 1380 cm^{-1}.

definition of $R(c)$ is as follows [4, 30].

$$R(c) = I(c) / [\, I(c) + I(h) \,] \times 100\ \%$$

In Fig. 2–5, $R(c)$ values calculated from each IR spectrum are noted . In this experiment, the maximum percentage of c–BN phase content in the film attained to about 82 %.

Effects of ion–plating parameters on c–BN phase content

A c–BN phase was not observed to form in the BN film deposited in a nitrogen gas plasma. Therefore, Ar gas in addition to N_2 gas was introduced into the deposition chamber during the deposition, because the addition of Ar gas into a nitrogen gas plasma has been reported to be effective against the c–BN film deposition by many PVD techniques [3 – 10]. However, since the gas flow controllers of float type were used to adjust the flow rates of Ar and N_2 gases, the Ar/N_2 gas flow ratio could not be exactly adjusted. Thus, the depositions were performed at Ar/N_2 gas flow ratios of about 1.0 ~ 1.3 in this experiment.

By the addition of Ar gas, a c–BN phase was observed to form in the BN film. Figure 2–6 shows the effect of the ionization current on the c–BN phase content in the film deposited at several RF powers applied to the substrate. The c–BN phase content increases as the ionization current increases, and the maximum content was obtained in the film deposited at a current of 14 A at every RF powers. However, it was difficult to keep the plasma stable at an ionization current of more than 14 A because of an anomalous discharge. Thus, the depositions were, hereafter, performed at the fixed current of 14 A.

Figure 2–7 shows the effect of the applied RF power to the substrate on the c–BN phase content in the film deposited at the EB powers of 1.7 and 2.0 kW for the evaporation of boron. A c–BN phase was observed to form in the film when the depositions were performed at an RF power of more than 80 W, and the c–BN phase content in the film increased abruptly with increasing the RF power. But, any BN films could not be deposited on the substrate under the excessive RF power, because of the resputtering of growing film predominantly caused by ions impinging on the film. Figure 2–8 shows the effects of RF and EB powers on the c–BN phase content. The predominant resputtering of growing film occurs at the lower RF power as the EB

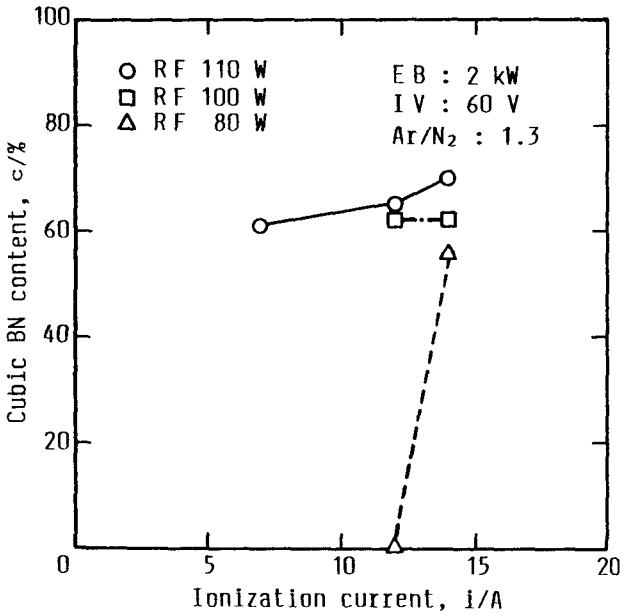

Fig. 2-6. Effect of the ionization current on c-BN phase content in the BN film deposited by the ion-plating method.

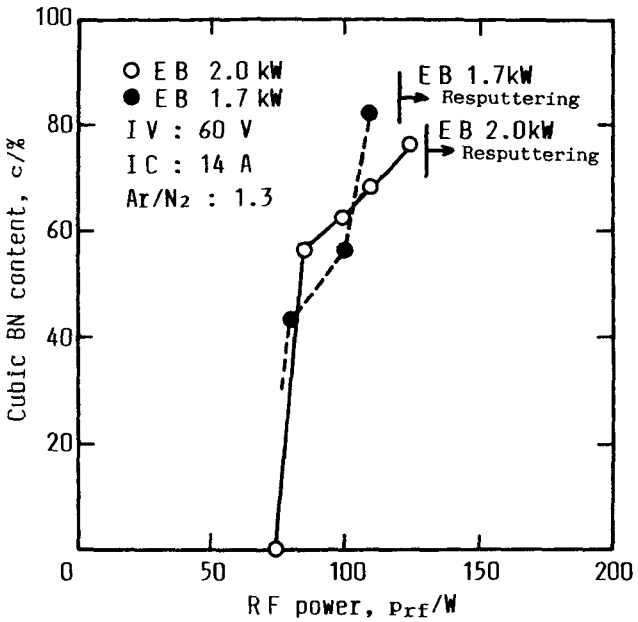

Fig. 2-7. Effect of radio-frequency (RF) power applied to the substrate on c-BN phase content in the BN film deposited by the ion-plating method.

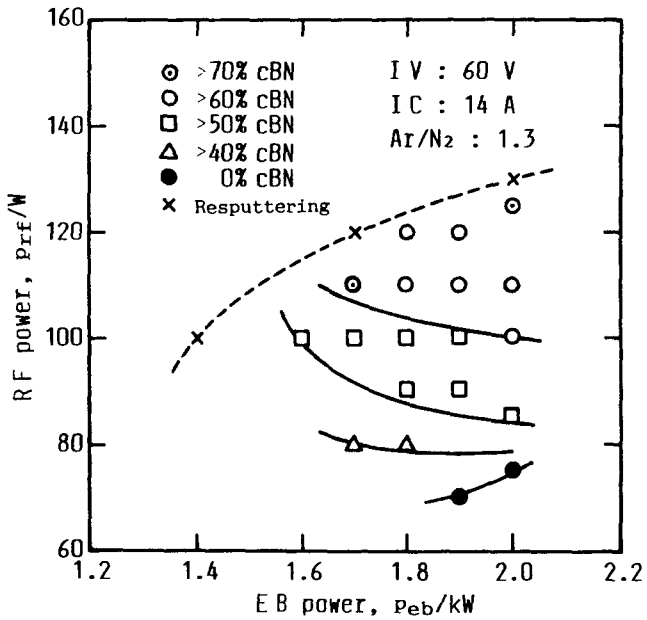

Fig. 2-8. Effects of radio-frequency (RF) power applied to the substrate and electron-beam (EB) power for boron evaporation on c-BN phase content in the BN film deposited by the ion-plating method.

power (*i.e.*, the evaporation rate of boron) decreases. On the other hand, the c–BN phase content increases at every EB powers with increasing the RF power. Consequently, in order to form a c–BN phase in the film, it is necessary to deposit at the higher RF power within the range of the power which makes it possible to deposit the film, and to introduce Ar gas together with N_2 gas into the evaporation chamber during the deposition.

2–3. Effects of Ar/N_2 Gas Flow Ratio and Self–Bias Voltage on Cubic BN Phase Content

It has been suggested that bombarding the growing BN film with an Ar ion plays a significant role for the formation of c–BN film [3, 6, 10]. The degree of Ar ion bombardment is considered to depend immediately on the magnitude of the self–bias voltage (V_{DC}) generated by the applied RF power to the substrate, and on the amount of Ar gas introduced together with N_2 gas into the deposition chamber during the deposition. Thus, in order to investigate the effects of V_{DC} and Ar/N_2 gas flow ratio on the formation of c–BN phase in the film, the BN films were deposited on Si substrates by varying these parameters. The characterization of the BN film was carried out by electron diffractometry and electron energy loss spectroscopy (EELS), besides FTIRS. Further, its characterization was performed by x–ray diffractometry and Raman spectroscopy.

Consequently, the deposited BN film was identified as a c–BN film by electron and x–ray diffractometry, Raman spectroscopy, EELS and FTIRS, and it was verified that the c–BN film can be deposited by the reactive ion–plating method. It is very important to control appropriately the V_{DC} and Ar/N_2 gas flow ratio in order to form a c–BN phase in the film, and it was found that the BN film with a c–BN phase content of more than 70 % can be deposited at V_{DC} of –40 ~ –60V, Ar/N_2 gas flow ratios of 2.0 ~ 3.0 and EB powers of 1.8 ~ 2.0 kW by the reactive ion–plating method with a hot cathode plasma discharge in a parallel magnetic field. However, the c–BN films always contained a small amount of h–BN phase, a 100% c–BN film could not be deposited under any deposition conditions by this ion–plating method. Further, it was found from an EPMA measurement that the c–BN films contain a small amount of carbon, oxygen and argon as impurities.

Experimental Procedure

Details of the ion-plating system and deposition procedures have been described in section 2-2. In order to exactly control the V_{DC} and Ar/N_2 gas flow ratio, a V_{DC} controller and the mass flow controllers for Ar and N_2 gases were attached to the ion-plating apparatus. By using the V_{DC} controller, the V_{DC} can be set in 1 V steps from 0 V to -2 kV and kept constant during deposition. By using the mass flow controllers, the Ar and N_2 gas flow rates can be set in 1 sccm steps from 0 to 100 sccm and in 0.5 sccm steps from 0 to 50 sccm, respectively.

The BN films were deposited on the Si substrates for 20 minutes by varying the V_{DC} and Ar/N_2 gas flow ratios in the range from 0 V to -80 V and from 1.3 to 4, respectively. All depositions were carried out at the ionization voltage and the ionization current kept constant at 66 V and 14 A, respectively. Total gas pressure was $6 \times 10^{-2} \sim 1 \times 10^{-1}$ Pa. The preparation conditions of the BN films are summarized in Table 2-2. The c-BN phase contents in the films were calculated using the IR absorption intensities at 1380 and 1050 cm^{-1}, measured with the same procedure as mentioned in section 2-2. Besides FTIRS, the phase identification of the BN film was carried out by selected area electron diffractometry (SAED, accelerative voltage 200kV) and

Table 2-2. Preparation conditions of the BN films by the ion-plating method.

Substrate	Si wafer
Temperature	> 523 K
E.B. power	1.7 ~ 2.3 kW
E.B. evaporant	99.9 % boron
Ionization voltage	66 V
Ionization current	14 A
W filament power	360 ~ 540 W
R.F. power	13.56 MHz
Self-bias voltage	0 ~ -80 V
Ar gas flow	14 ~ 20 sccm
N_2 gas flow	5 ~ 11 sccm
Ar/N_2 gas flow ratio	1.3 ~ 4.0

EELS (accelerative voltage 100kV), using a thin leaf of the BN film peeled off from the substrate. The N/B ratios of the BN films were measured by an electron probe microanalyzer (EPMA, accelerative voltage 15 kV). Further, the x-ray diffraction pattern and Raman spectrum were measured on the BN films with a buffer interlayer described later in section 4-2.

Results and Discussion

Preparation of c-BN film

In order to investigate the effect of V_{DC} on the formation of c-BN phase, BN films were deposited at an Ar/N_2 gas flow ratio of 2.0 and an EB power of 2.0 kW by varying the V_{DC}. Figure 2-9 shows the c-BN phase contents in the films plotted against the V_{DC} together with the N/B ratio of each BN film. It is seen in Fig. 2-9 that there is a favorable range of V_{DC}, from -40 V to -60 V, which is necessary to grow the film that is predominantly a c-BN phase, and that the BN films deposited in this range of V_{DC} have an N/B ratio of more than 0.8. On the other hand, the BN films deposited out of the favorable range of V_{DC}, *i.e.*, at V_{DC} of less than -40 V or of more than -60 V, are an h-BN phase and substoichiometric with respect to nitrogen. At a V_{DC} of more than -80 V, any BN films could not be deposited on the substrates because the resputtering of the growing film is predominant over the deposition. It is reported in the many other PVD techniques that there is a favorable range of the substrate bias voltage for the formation of c-BN film [4 - 6, 10, 18, 31]. D.J.Kester *et al.* [10] have especially reported that the important factor for the c-BN formation is the momentum transferred into the film per a depositing boron atom, namely, that a c-BN phase forms predominantly at more than the lower threshold momentum, and that the resputtering of the growing film or the transition of c-BN to h-BN takes place at more than the upper threshold momentum. According to their results, it is considered in this experiment that the momentum required for the c-BN formation is obtained by ion bombardment within the range of V_{DC} from -40 V to -60 V, although the value of the momentum could not be evaluated because it is hard to measure the flux of ions impinging on the substrate and the deposition rate of boron.

Next, in order to investigate the effect of Ar/N_2 gas flow ratio on the c-BN formation, BN

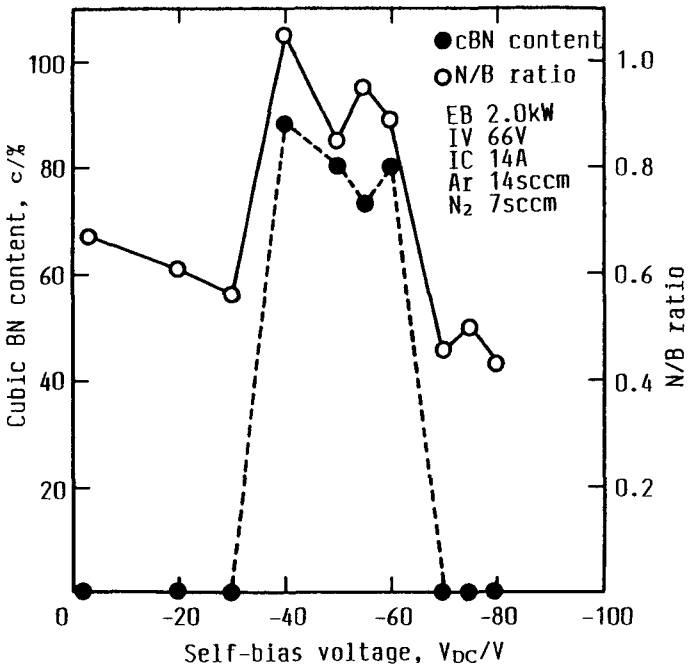

Fig. 2-9. Effect of self-bias voltage applied to the substrate on c-BN phase content and N/B ratio in the BN film deposited by the ion-plating method.

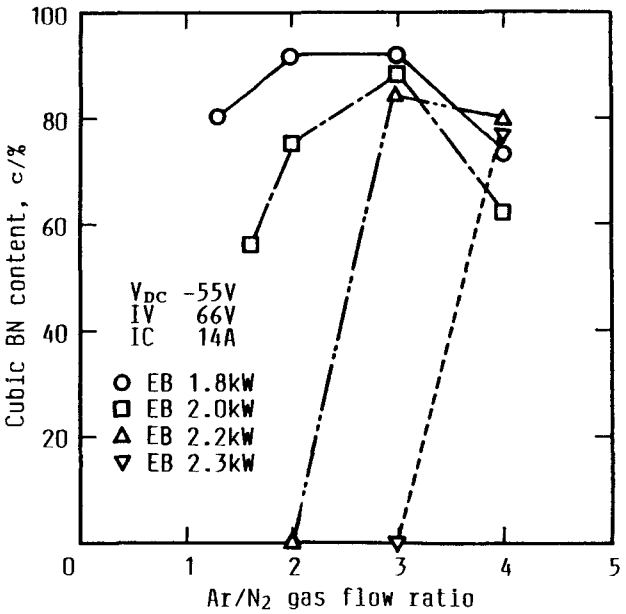

Fig. 2-10. Effect of Ar/N_2 gas flow ratio on c-BN phase content in the BN film deposited by the ion-plating method.

films were deposited at a V_{DC} of −55 V by varying the Ar/N_2 gas flow ratio at several EB powers. The results are shown in Fig. 2–10. At an EB power of 1.8kW, an about 90 % c–BN film was deposited in the range of Ar/N_2 gas flow ratios from 2.0 to 3.0. It is also seen in Fig. 2–10 that there is a favorable range of Ar/N_2 gas flow ratio for the c–BN formation, and that the favorable range shifts to the larger side of Ar/N_2 gas flow ratio with increasing EB power, *i.e.*, the evaporation rate of boron.

It is found that the BN film with a c–BN phase content of more than 70 % can be deposited at V_{DC} of −40 ~ −60 V, an Ar/N_2 gas flow ratios of 2.0 ~ 3.0 and EB powers of 1.8 ~ 2.0 kW by the reactive ion–plating method with a hot cathode plasma discharge in a parallel magnetic field, and that it is very important to control appropriately the V_{DC} applied to the substrate and the Ar/N_2 gas flow ratio in order to form a c–BN phase in the film.

Analysis of c–BN film

As mentioned in section 2–2, c–BN cannot distinguish from w–BN with FTIRS. Thus, the phase identification of BN film is carried out by SAED and EELS, besides FTIRS.

In Fig. 2–11, the diffraction pattern by SAED and TEM micrograph of the BN film with a c–BN phase content of about 90 % are shown together with the patterns of c–BN powder synthesized at high temperature and high pressure, and w–BN powder synthesized by shock compression. The diffraction rings are observed in these patterns by SAED. The diffraction pattern of the BN film is distinctly close to that of c–BN powder, rather than of w–BN powder. The *d*–spacings are calculated from these diffraction rings. The *d*–spacings of BN film and c–BN powder are shown in Table 2–3, compared with reported values [32, 33]. Most of the *d*–spacings of the BN film are close to those of c–BN powder. But the diffuse ring is observed in the most interior side of the diffraction pattern of the BN film, and its *d*–spacing is estimated to be about 0.334 nm, which is close to 0.332813 nm of the (0002) plane of h–BN [34]. Therefore, this BN film is considered from an SAED measurement to be almost a c–BN film which contains a small amount of h–BN composed probably of amorphous–like or fine crystallites. In the diffraction pattern of the BN film, the reflections corresponding to the (200) and (222) planes of

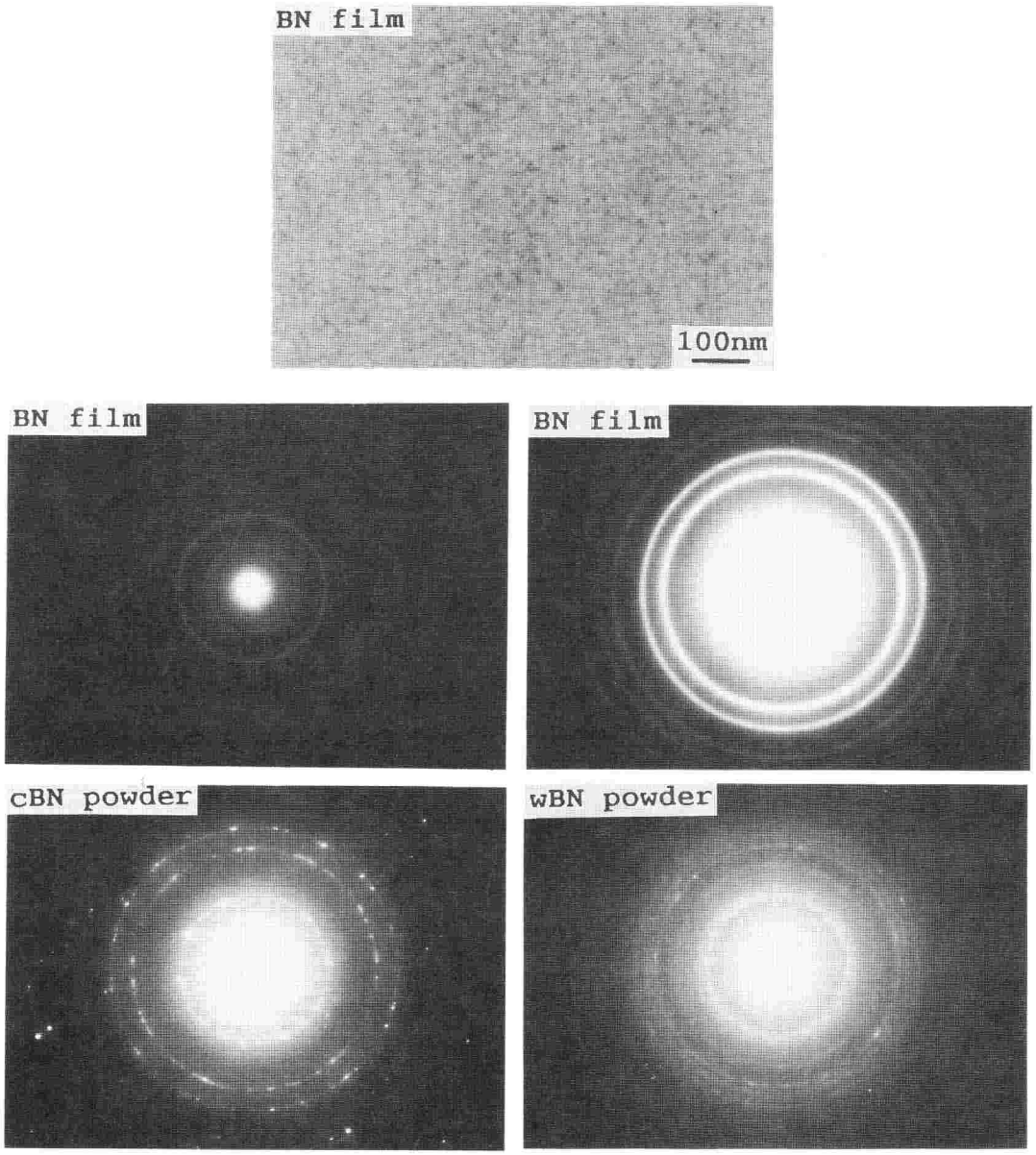

Fig. 2-11. TEM micrograph and selected area electron diffraction pattern of the BN film with c-BN phase content of about 90 %, and selected area electron diffraction patterns of c-BN powder synthesized at high temperature and pressure and of w-BN powder by shock compression.

Table 2-3. The *d*-spacings of the BN film with c-BN phase content of about 90 % and c-BN powder synthesized at high temperature and pressure, calculated for the selected area electron diffraction rings, compared with reported values.

Observed value				Reported value				(hkl)
BN film		cBN powder		JCPDS25-1033		JCPDS35-1365		
d(nm)	I/I_0	d(nm)	I/I_0	d(nm)	I/I_0	d(nm)	I/I_0	
0.334	w							
0.208	vs	0.208	vs	0.2088	100	0.20872	100	(111)
-		0.180	vw	0.1808	2	0.18081	5	(200)
0.128	s	0.128	s	0.12785	6	0.12786	24	(220)
0.109	w	0.109	s	0.10901	3	0.10900	8	(311)
-		0.104	vw	0.10443	1	-		(222)
0.0909	vw	0.0908	vw	0.09041	1	0.09039	2	(400)
0.0846	vw	0.0831	vw	0.08297	3	0.08296	3	(331)
0.0744	vw	0.0739	vw					
0.0704	vw	0.0697	vw					

vs ; very strong, s ; strong, w ; weak, vw ; very weak

c-BN could not be observed. The reason is considered to be due not to the preferred orientation of c-BN crystallite but to the essentially very weak reflections, since the reflections corresponding to these planes, which are originally forbidden in diamond structure, take place owing to a small difference between the atomic scattering factors of boron and nitrogen [35].

Figure 2-12 shows the dark field image taken from the BN film using a ring indexed as the (111) reflection of c-BN. The size of c-BN crystallite in the film was estimated from this image to be less than 30 nm.

Figure 2-13 shows the EELS spectra in the vicinity of the boron and nitrogen K-edge for the BN film, c-BN and h-BN powders. These spectra are occurred by the transition of a K-shell electron to an unoccupied level and reflect the density of electronic states in the unoccupied bands [36]. Hexagonal BN has a sharp and narrow π^* band in the spectra of both boron and nitrogen, but c-BN does not [37]. Therefore, the π^* band is a good indicator of the presence of h-BN phase. It is, however, very hard to distinguish between c-BN and w-BN using the EELS spectrum because both spectral features are very similar [37]. In the EELS spectra of both

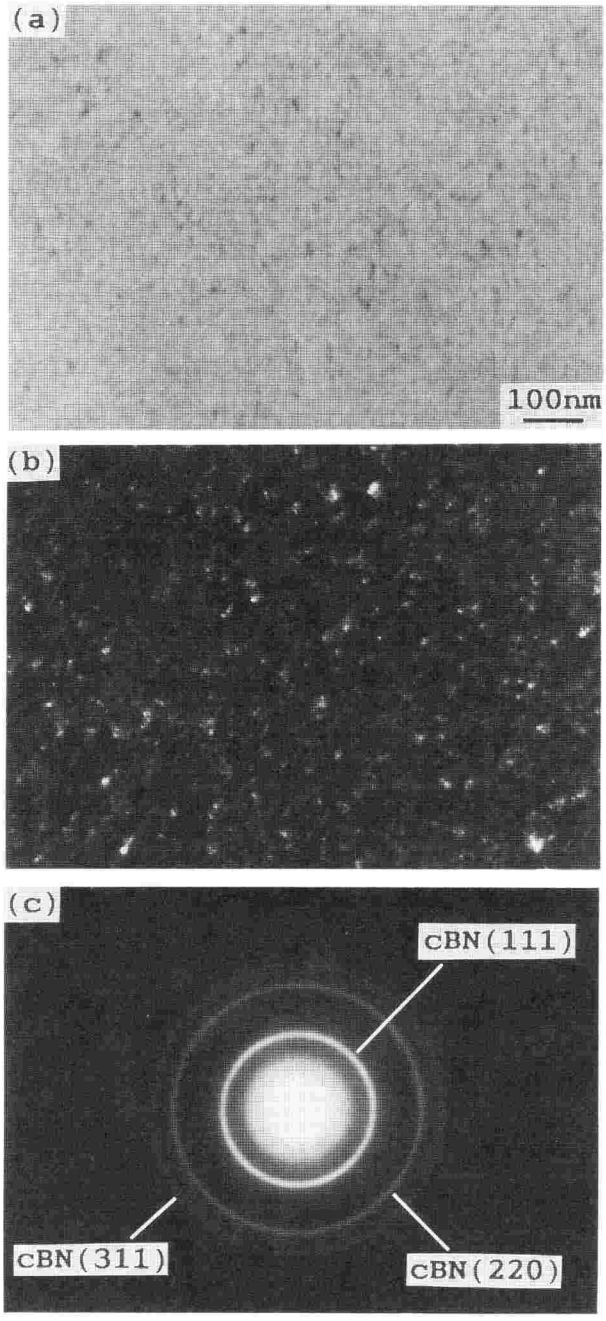

Fig. 2-12. Bright field (a) and dark field (b) images and selected area electron diffraction pattern (c) of the BN film with c-BN phase content of about 90 % deposited by the ion-plating method.

boron and nitrogen for the BN film, the small π^* band can be observed, and the spectral feature of σ^* band is very similar to that of c-BN powder rather than of h-BN powder. Thus , it is also confirmed from the EELS spectrum that the BN film is predominantly a c-BN phase and contains a small amount of h-BN phase.

Table 2-4 shows the chemical composition of the BN film determined quantitatively by an EPMA. The BN film has an N/B ratio of about 0.9 and contains a small amount of carbon, oxygen and argon as impurities. Argon is considered to be incorporated with nitrogen from the plasma gas mixture. However, it is unknown whether carbon is contained really in the film, because carbon contamination occurs on the surface of the BN film during an EPMA measurement.

Until now, the c-BN film with a thickness of more than 0.2 μm could not be prepared because of its poor adhesion to a substrate. Therefore, the only broad x-ray diffraction peak corresponding to the (111) plane of c-BN could be observed even by an x-ray diffractometer equipped with the attachment for a thin film, and also no Raman peak could be observed [6. 38]. Thus, the c-BN film with about 0.5 μm thickness was prepared by forming a buffer interlayer with gradually increasing nitrogen concentration between the substrate and the film, as described later in section 4-2. Figures 2-14 and 2-15 show the x-ray diffraction pattern and Raman spectrum obtained from this film, respectively. The x-ray diffraction pattern was measured with an incident angle of Cu Kα x-rays at 0.5 degrees for the film surface by using the attachment for a thin film. It can be seen in Fig. 2-14 that diffraction peaks corresponding to the (111), (200), (220) and (311) planes of c-BN are obtained. The Raman spectrum was measured with an argon-ion laser beam (wavelength 488 nm, output power 200 mW) by Raman spectrometer, using a charge coupled device (CCD) detector. In Fig. 2-15, two weak peaks are visible at 1056 and 1307 cm^{-1} corresponding to the TO and LO (transverse and longitudinal optics) modes of the c-BN lattice, respectively [39]. No peak can be observed at the h-BN position of 1366 cm^{-1} [39]. The abrupt rising of the Raman spectrum at the left side in Fig. 2-15 is due to the luminescence of the silicon substrate. Up to now, no reports have appeared showing that x-ray diffraction peaks of more than two and a Raman peak corresponding to c-BN were observed

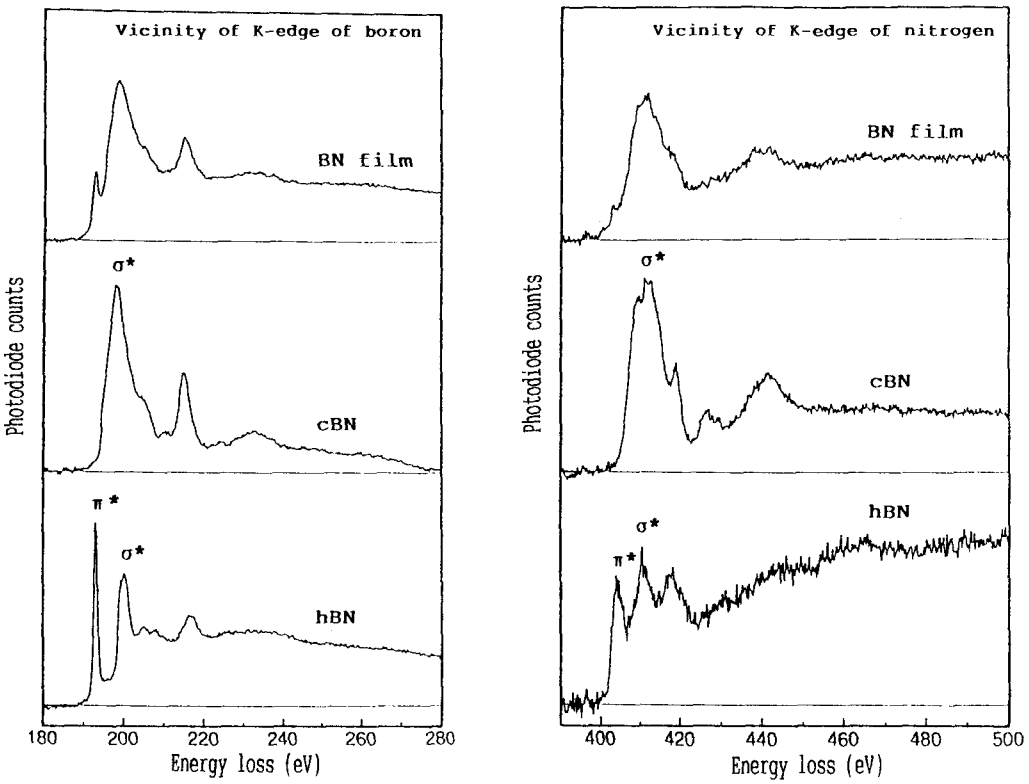

Fig. 2-13. Electron energy loss spectra in the vicinities of the K-edges of boron and nitrogen, measured on the BN film with c-BN phase content of about 90 %, c-BN powder synthesized at high temperature and pressure, and h-BN powder.

Table 2-4. Chemical composition and N/B ratio of the BN film with c-BN phase content of about 90 %.

(mol %)

B	N	Ar	C	O	N/B ratio
51	45	1.2	1.9	0.6	0.9

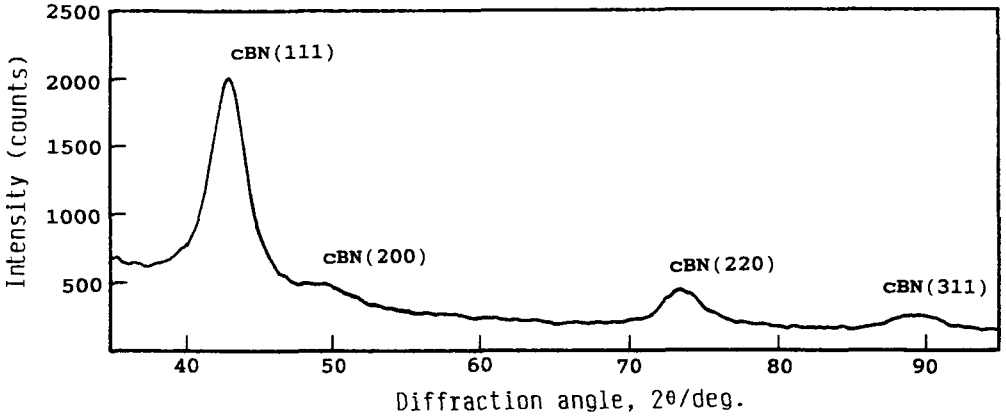

Fig. 2-14. X-ray diffraction pattern measured on the c-BN film with buffer interlayer with an incident angle of Cu Kα x-rays at 0.5 degrees for the film surface, using the attachment for thin film.

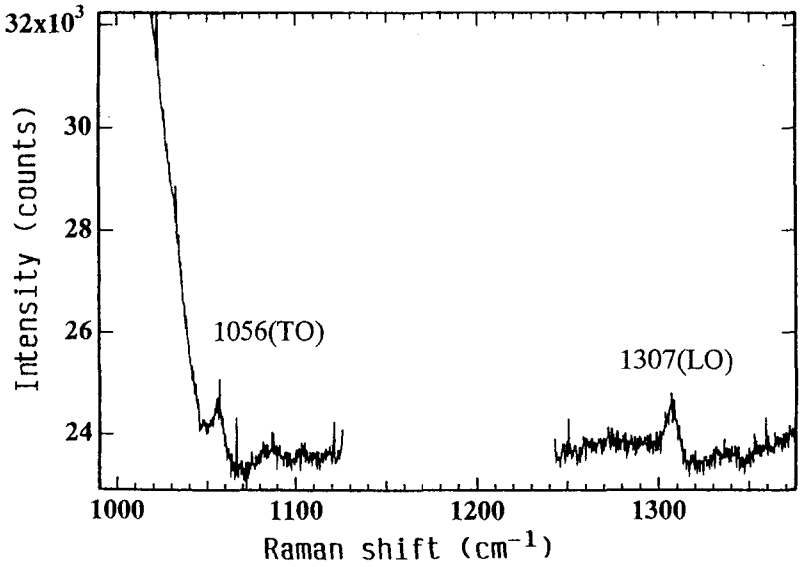

Fig. 2-15. Raman spectrum measured on the c-BN film with buffer interlayer using an argon-ion laser beam (wavelength 488 nm, output power 200 mW).

from c-BN films deposited by various PVD and CVD techniques.

In summary, the deposition condition of c-BN film by the reactive ion-plating method with a hot cathode plasma discharge in a parallel magnetic field could be clarified. In order to deposit the c-BN film, it is important to introduce a desired amount of Ar gas with N_2 gas into the deposition chamber and to control appropriately the V_{DC} applied to the substrate. It was revealed from FTIRS, SAED and EELS measurements that the prepared c-BN film contains a small amount of h-BN phase and composes of fine crystallites of less than 30 nm, and from an EPMA measurement that the film has an N/B ratio of about 0.9 and contains a small amount of oxygen, carbon and argon as impurities. It is, however, unknown whether carbon is contained really in the film or not. Furthermore, the four x-ray diffraction peaks and two Raman peaks corresponding to c-BN could be observed from the c-BN film with about 0.5 μm thickness and with the buffer interlayer. Therefore, it is considered that the c-BN film can be undoubtedly deposited by the reactive ion-plating method.

References

[1] S.Matsumoto, Y.Sato, M.Kamo and N.Setaka, Jpn. J. Appl. Phys., **21**, L183(1982).

[2] S.P.S.Arya and A.D'Amico, Thin Solid Films, **157**, 267(1988).

[3] B.Rother, H.D.Zscheile, C.Weissmantel, C.Heiser, G.Holzhüter, G.Leonhardt and P.Reich, Thin Solid Films, **142**, 83(1986).

[4] K.Inagawa, K.Watanabe, H.Ohsone, K.Saitoh and A.Itoh, J. Vac. Sci. Technol., **A5**, 2696(1987).

[5] M.Murakawa and S.Watanabe, Surf. Coat. Technol., **43/44**, 128(1990).

[6] T.Ikeda, Y.Kawate and Y.Hirai, J. Vac. Sci. Technol., **A8**, 3168(1990).

[7] M.Mieno and T.Yoshida, Jpn. J. Appl. Phys., **29**, L1175(1990).

[8] C.Weissmantel, K.Bewilogua, D.Dietrich, H.-J.Erler, H.-J. Hinneberg, S.Klose, W.Nowick and G.Reisse, Thin Solid Films, **72**, 19(1980).

[9] M.Satou and F.Fujimoto, Jpn. J. Appl. Phys., **22**, L171(1983).

[10] D.J.Kester and R.Messier, J. Appl. Phys., **72**, 504(1992).

[11] A.Chayahara, H.Yokoyama, T.Imura and Y.Osaka, Jpn. J. Appl. Phys., **26**, L1435(1987).

[12] G.Kessler, H.-D.Bauer, W.Pompe and H.-J.Scheibe, Thin Solid Films, **147**, L45(1987).

[13] H.Saitoh, T.Hirose, H.Matsui, Y.Hirotsu and Y.Ichinose, Surf. Coat. Technol., **39/40**, 265(1989).

[14] S.Komatsu, Y.Moriyoshi, M.Kasamatsu and K.Yamada, J. Appl. Phys., **70**, 7078(1991).

[15] A.Bath, P.J. van der Put, J.G.M.Becht, J.Schoonman and B.Lepley, J. Appl. Phys., **70**, 4366(1991).

[16] L.Maya, J. Am. Ceram. Soc., **75**, 1985(1992).

[17] S.V.Nguyen, T.Nguyen, H.Treichel and O.Spindler, J. Electrochem. Soc., **141**, 1633(1994).

[18] T.Ichiki, T.Momose and T.Yoshida, J. Appl. Phys., **75**, 1330(1994).

[19] R.F.Bunshah, J.M.Blocher, Jr., D.M.Mattox, T.D.Bonifield, G.E.McGuire, J.G.Fish, M.Schwartz, P.B.Ghate, J.A.Thornton, B.E.Jacobson and R.C.Tucker, Jr., *Deposition Technologies for Films and Coatings* (Noyes, New Jersey, 1982), p.244.

[20] R.F.Bunshah, J.M.Blocher, Jr., D.M.Mattox, T.D.Bonifield, G.E.McGuire, J.G.Fish,

M.Schwartz, P.B.Ghate, J.A.Thornton, B.E.Jacobson and R.C.Tucker, Jr., *Deposition Technologies for Films and Coatings* (Noyes, New Jersey, 1982), p.28.

[21] F.Fujimoto, Mater. Sci. Forum, **54&55**, 45(1990).

[22] C.R.Aita, Mater. Sci. Forum, **54&55**, 1(1990).

[23] K.L.Chopra, V.Agarwal, V.D.Vankar, C.V.Deshpandey and R.F.Bunshah, Thin Solid Films, **126**, 307(1985).

[24] Y.Kubota, Boundary, **3**, 38(1986).

[25] P.K.Lam, R.M.Wentzcovitch and M.L.Cohen, Mater. Sci. Forum, **54&55**, 165(1990).

[26] T.Sato, Proc. Jpn. Acad., **61**, **Ser.B**, 459(1985).

[27] A.Onodera, N.Takahashi, H.Yoshihara, H.Nakae, Y.Matsunami and T.Hirai, J. Mater. Sci. **25**, 4157(1990).

[28] R.Geich, C.H.Perry and G.Rupprecht, Phys. Rev., **146**, 543(1966).

[29] P.J.Gielisse, S.S.Mitra, J.N.Plendl, R.D.Griffis, L.C.Mansur, R.Marshall and E.A.Pascoe, Phys. Rev., **155**, 1039(1967).

[30] A.Weber, V.Bringmann, R.Nikulski and C.-P.Klages, Surf. Coat. Technol., **60**, 493(1993).

[31] H.Yokoyama, M.Okamoto and Y.Osaka, Jpn. J. Appl. Phys., **30**, 344(1991).

[32] Joint Committee on Powder Diffraction Standards (JCPDS, Swarthmore, PA), pattern 25-1033.

[33] Joint Committee on Powder Diffraction Standards (JCPDS, Swarthmore, PA), pattern 35-1365.

[34] Joint Committee on Powder Diffraction Standards (JCPDS, Swarthmore, PA), pattern 34-421.

[35] B.D.Cullity, *Elements of X-Ray Diffraction* (Addison-Wesley, Massachusetts, 1956), p.479.

[36] D.R.McKenzie, W.G.Sainty and D.Green, Mater. Sci. Forum, **54&55**, 193(1990).

[37] J.Hosoi, T.Oikawa, M.Inoue, Y.Matsui and T.Endo, J. Electron Spectrosc. Relat. Phenom., **27**, 243(1982).

[38] W.D.Halverson, T.G.Tetreault and J.K.Hirvonen, Mater. Sci. Forum, **54&55**, 71(1990).

[39] D.R.Clarke and F.Adar, Mater. Sci. Res., **15**, 199(1983).

Chapter 3

Soft X-Ray Spectroscopic Analysis of Boron Compounds and Cubic Boron Nitride Thin Films

3-1. Introduction

Boron nitride (BN) has various kinds of crystal structures which are similar to those of carbon polymorphs, respectively. The crystalline phases of BN are classified as zincblend-type (c-BN), wurtzite-type (w-BN), graphite-like (h-BN), turbostratic (t-BN), rhombohedral (r-BN) and amorphous (a-BN) [1]. Zincblend-type BN is a useful material that has such low density, extreme hardness, large thermal conductivity, wide band gap and large resistivity as diamond [2].

Like a diamond film, recently the synthesis of c-BN film has been investigated using various PVD and CVD techniques [3 - 11]. It is generally reported that c-BN films with a thickness of less than 0.5 μm can be only deposited because of poor adhesion to a substrate due to their large compressive stress [3, 12 - 14], and that they compose of fine crystallites with a size of several tens nanometers [2, 6, 13, 15, 16]. Further, both of boron and nitrogen atoms are poor x-ray scatterers. Therefore, it is difficult to perform the phase identification of BN thin film with x-ray diffractometry, although this method is superior and reliable as analysis of the crystal structures of materials. So far, its phase identification is mainly performed by infrared spectroscopy and electron diffractometry [17]. However, it is very difficult to distinguish between c- and w-BN phases or among h-, r-, t- and a-BN phases with infrared spectroscopy, and to observe the Bragg-reflections from the (200) and (222) planes of a c-BN phase even with electron diffractometry because of a small difference between the atomic scattering factors of boron and nitrogen atoms [16]. These methods are not always tools enough to identify the crystal structure of a BN film.

It is well-known that x-ray emission band spectra reflect the electronic structures of materials and change in their spectral features with the chemical bonds of elements [18 - 21]. Therefore, x-ray spectroscopy has been applied to many materials in order to obtain the knowledge of

their valence and electronic structures [22, 23]. Since the origin of K–emission band spectrum of boron (B K x–ray spectrum) is due to the electron transition to the *1s* orbital from the *2p* orbital which is a valence orbital, its spectral feature should change with variation in the chemical bond of boron [24 – 28]. Thus, it is expected to obtain the useful informations about a chemical bonding state and a microstructure of BN film from B K x–ray emission spectrum.

In this work, B K x–ray emission spectra were measured precisely on BNs with different crystal structures and other boron compounds by an electron probe microanalyzer (EPMA), in order to investigate the change in the spectral feature with variation in the chemical bonding state of boron. Furthermore, B K x–ray emission spectra of BN films deposited by different ion–plating methods were also measured by an EPMA, and these spectral features were discussed in comparison with those of BNs and boron compounds.

3–2. B K X–Ray Emission Spectra of Boron Compounds

B K x–ray emission spectra of metallic boron (M.B), boron carbide (B_4C), boron nitride (BN), boron oxide (B_2O_3) and sodium tetrafluoroborate ($NaBF_4$) were precisely measured by an EPMA, in order to investigate the changes in the spectral features with variation in the chemical bonding state of boron. Compared with the B K x–ray emission spectrum of M.B, the main peak positions of these boron compounds shifted to longer wavelength side, and the satellite bands were observed at both sides of the main bands. The B K x–ray emission spectra of these compounds change obviously in the spectral features with variation in the chemical bonding state of boron, such as the peak positions and asymmetric indices of the main bands, or the peak positions and relative intensities of the satellite bands. In particular, the peak position of the satellite band at the long wavelength side shifts to longer wavelength side with increasing the electronegativity of the ligand in the boron compound. Thus, its peak position can be used to identify the ligand. The B K x–ray emission spectrum of $NaBF_4$ changed in the spectral feature during the EPMA measurement with the electron beam–induced decomposition of $NaBF_4$ which resulted in the formation of a similar B–B bond to that of M.B. However, the change in the spectral feature

can be depressed by continuous moving the analytical area of the sample at a fast speed during the EPMA measurement.

Experimental Procedure

The boron compounds used for B K x-ray emission measurements are B_4C (purity 99 %), BN (hexagonal structure, purity 99.5 %), B_2O_3 (purity 99.999 %) and $NaBF_4$ (purity 98 %) which are commercially available. These compounds were pressed into the disks of 5 mm^{ϕ} x 3 mm with flat planes, and coated with carbon in vacuum of the order of 10^{-3} Pa. The flat plane of each disk was used for EPMA measurements. After M.B (purity 99.9%) was melted by electron beam and solidified in vacuum of the order of 10^{-3} Pa, its cleavage plane was used without the carbon coating for an EPMA measurement.

Using an EPMA, B K x-ray emission spectra were measured on these samples at an accelerative voltage of 15 kV and sample currents of 0.002 ~ 0.2 μA. A multilayer pseudo-crystal of lead stearate ($2d$=10 nm) was used as an analyzing element, and scanned from 8.0 to 6.0 nm in wavelength at a speed of 0.001 nm/s. B K x-ray emission spectra were detected at a take-off angle of 52.5 degrees with a PR gas (Ar 90 % + CH_4 10 %)- flow type proportional counter and recorded on a strip chart after passing through a pulse height analyzer in order to prevent from the overlap of the third order spectrum of oxygen with the B K x-ray spectrum.

The wavelength calibration was performed using the 10th and 7th order emission bands of Al Kα band with the peak positions at 8.337 and 5.836 nm in wavelength, respectively. The peak position of B K x-ray emission spectrum could be read off to the nearest 0.004 nm in wavelength, and its variation was below 0.01 nm in wavelength for five measurements.

The B K x-ray emission spectrum of $NaBF_4$ was recorded with continuous moving the analytical area of the sample during the EPMA measurement, in order to depress the change of the spectral feature caused by the electron beam-induced damage of this sample. The analytical area of the sample was moved by sliding the sample and scanning the electron beam normal to the sliding direction of the sample.

Results and Discussion

B K x-ray emission spectra of M.B and boron compounds

Figure 3-1 shows the B K x-ray emission spectra of M.B and boron compounds. The characteristics of these spectra are summarized in Table 3-1. Figure 3-2 shows the definitions of the spectral characteristics such as peak position, full width at half maximum (FWHM) and asymmetric index (A.I.). The relative intensity of satellite band is expressed in percentage to the peak intensity of the main band.

The B K x-ray emission spectrum of M.B composes of the main band only, while those of the boron compounds compose of the main band and the satellite bands which exist in both sides of the main band. On the B K x-ray emission spectra of boron compounds, the peak positions of the main bands of BN, B_2O_3 and $NaBF_4$ shift to longer wavelength side than those of M.B and B_4C, and there are also small differences in the peak position among those of BN, B_2O_3 and $NaBF_4$. Furthermore, the spectra of M.B, B_4C, BN, B_2O_3 and $NaBF_4$ differ from one another in the spectral features of the main band such as A.I. and FWHM. The origin of the main band is due to the electron transition to the *1s* from the *2p* orbitals of boron, and its spectral feature reflects mainly the electronic structure of the *2p* orbital which is a valence orbital [26]. Consequently the changes in the spectral feature of the main band are attributable to the change of the density of state (DOS) of the *2p* orbital with variation in the chemical bond of boron. On the other hand, regarding the satellite band at the long wavelength side, its peak position shifts distinctly to longer wavelength side in this order: B_4C, BN B_2O_3 and $NaBF_4$, namely as the electronegativity of the ligand in these compound is larger. The change in the peak position of this satellite band is larger and more regular than that of the main band. Therefore, the peak position of this satellite band can be used to identify the ligand in the boron compounds. There have been several investigations on this satellite band, and its origin is considered to be due to the electron transition to the *1s* orbital of boron from the *2p* orbital of boron which hybridized with the *2s* orbital of the ligand [26, 29]. And this matter was confirmed in this study, as described later in chapter 6. Thus, the change in the peak position of this satellite band is considered to be brought about due to the difference in the energy level of *2s* orbital of the ligand.

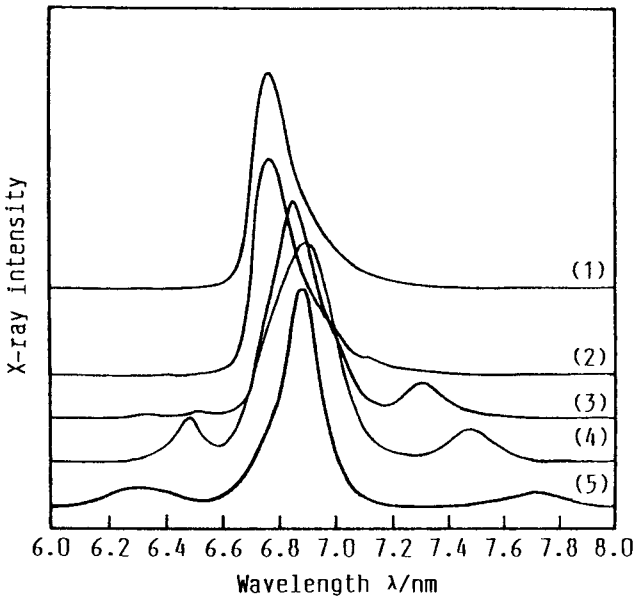

Fig. 3-1. B K x-ray emission spectra measured by an EPMA on metallic boron (1), B_4C (2), h-BN (3), B_2O_3 (4) and $NaBF_4$ (5).

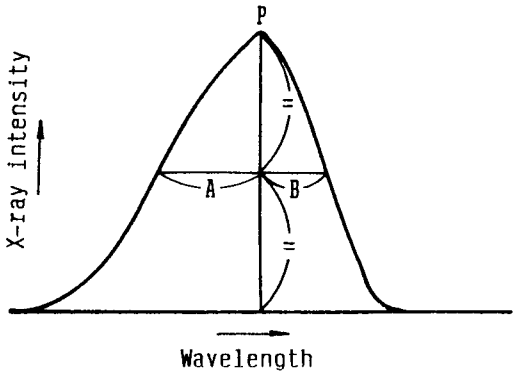

Fig. 3-2. Definition of spectral characteristics.
(1) P : peak position, (2) A+B : full width at half maximum (FWHM), (3) B/A : asymmetric index (A.I.).

Table 3-1. Characteristics of B K x-ray emission spectra measured by an EPMA on metallic boron (B) and the various boron compounds.

Samples	Main peak			Satellite peak					
	Position (nm)	FWHM (nm)	Asymmetric index	Position (nm)			Intensity (%)		
B	6.76	0.16	1.82	-	-	-	-	-	-
B_4C	6.76	0.17	1.76	6.42	6.53	7.11	0.3	1.0	7.5
hBN	6.86	0.20	1.12	6.34	6.52	7.31	1.6	2.9	16.6
B_2O_3	6.88	0.27	0.83	-	6.48	7.47	-	20.0	14.0
$NaBF_4$	6.89	0.15	0.81	6.30	-	7.71	9.0	-	7.0

The two weak satellite bands are observed at the short wavelength side in the B K x-ray emission spectra of B_4C and BN whereas the only strong satellite band is observed in the spectra of B_2O_3 and $NaBF_4$, and moreover, the satellite bands of these compounds differ from one another in their peak positions. In particular, the satellite band of B_2O_3 at the short wavelength side exhibits the strongest intensity among these compounds. S.Luck *et al.* [26] have reported that this satellite band is prominently strong in the boron compounds such as $AlBO_3$, $B(OH)_3$ and B_2O_3 where boron is in the three-hold coordination, and suggested that it is a resonance or core-exciton peak. But its origin has been not made clear yet. As described later in section 6-2, the origin of the satellite band of h-BN at the short wavelength side is considered to be due to the electron transition to the *1s* orbital of boron from the unoccupied antibonding molecular orbital after the excitation of electrons in the occupied orbitals of boron to this antibonding orbital with electron-beam irradiation. Since the satellite bands at the short wavelength side change with variation in the chemical bond of boron in the spectral features such as their positions, relative intensities and number, these satellite bands can be also used for the chemical state analysis of the boron compound.

In the case of B_4C, although the satellite band at the long wavelength side can be observed as a weak shoulder in the tail of the main band, and two weak satellite bands can be observed at the short wavelength side, the spectral feature of main band is almost similar to that of M.B with respect to the peak position, A.I. and FWHM. This is considered to be due to the fact that most of boron atoms in B_4C have identical B-B bonds to those of M.B, because 8-icosahedrons constructed of 12-boron atoms, which are similar to those of M.B, are combined with 3-carbon atoms into the rhombohedral structure of B_4C [30]. The weak satellite bands are considered to appear due to a few B-C bonds in B_4C.

In this experiment, it was found that B K x-ray emission spectra of the boron compounds change with variation in the chemical bond of boron in the spectral feature such as the peak position, FWHM and A.I. of the main band, and the relative intensity and peak position of the satellite band, and that the spectral features can be used to distinguish the boron compounds. It is especially important that the peak position of the satellite band at the long wavelength side can

be used to identify the ligand in the boron compound.

Depression of change in B K x-ray emission spectral feature of $NaBF_4$ with electron beam-induced damage

$NaBF_4$ is one of the materials that are damaged readily by electron-beam irradiation. The chemical state analysis of materials by a fine structure of x-ray emission spectrum is generally performed in order to obtain the informations about the valence and electronic structures of elements [22, 23], Therefore, when an x-ray emission spectrum is measured by an EPMA on the sample that is damaged readily by electron-beam irradiation, it is important to reduce its electron beam-induced damage so as not to change the spectral feature. In this experiment, it was attempted to reduce the electron beam-induced damage of $NaBF_4$ with continuous moving the analytical area of the sample during the EPMA measurement. The analytical area was moved by sliding the sample and scanning the electron beam normal to the sliding direction of the sample.

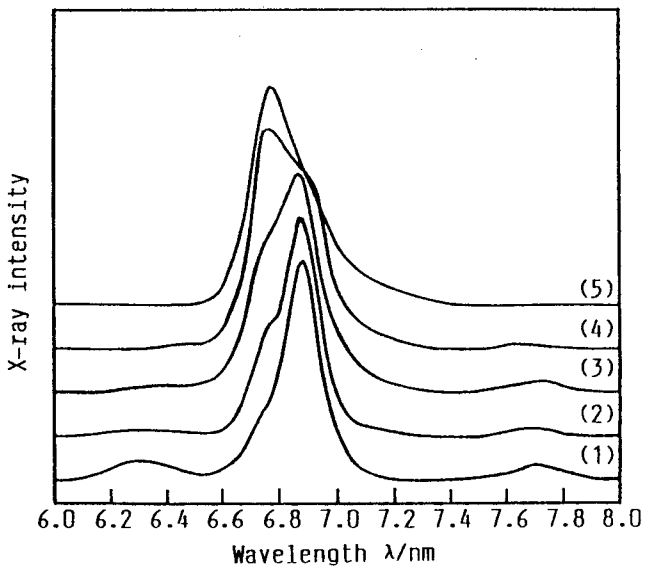

Fig. 3-3. Change in the B K x-ray emission spectral feature with decomposition of $NaBF_4$ during electron-beam irradiation. The simultaneously measured intensities of F K x-rays were 21989 cps (1), 18960 cps (2), 1667 cps (3), 12080 cps (4) and 5787 cps (5).

Figure 3–3 shows the B K x–ray emission spectra of $NaBF_4$ measured with continuous moving the analytical area at different sliding speeds and scanning widths. The B K x–ray emission spectra denoted by the numbers of (1) ~ (5) in Fig. 3–3 were measured (1) at a sliding speed of 6 μm/s and a scanning width of 0.16 mm, (2) at 0.4 μm/s and 0.16mm, (3) at 0.4 μm/s and 0.08 mm, (4) at 0.4 μm/s without the scan, and (5) with fixing the sample and the electron beam, respectively. The K–emission x–ray intensities of fluorine (F K x–ray intensity), which were simultaneously measured as an indicator of the degree of the electron beam–induced damage of $NaBF_4$, were (1) 21989 cps, (2) 18960 cps, (3) 16667 cps, (4) 12080 cps, and (5) 5787 cps, respectively. It is considered that more electron beam–induced damage of $NaBF_4$ is brought about as F K x–ray intensity becomes weaker. The B K x–ray emission spectrum (5) in Fig. 3–3, which was measured without moving the analytical area, composes only of the main band with the peak position at 6.77nm, and no satellite band can be observed in this spectrum. Although this spectrum has larger FWHM (2.26 nm) and A.I. (2.01) than those of M.B, the spectral feature is almost similar to that of M.B. Therefore, it is considered that electron–beam irradiation gives rise to decompose $NaBF_4$ and to form a similar B–B bond to that of M.B. On the other hand, the B K x–ray emission spectrum (1) in Fig. 3–3, which were measured with continuous moving the analytical area at the fastest speed in this experiment, differs distinctly from the spectrum (5) in the spectral feature, and has the main band with the peak position at about 6.89 nm and the satellite bands at both sides of the main band. Although, the spectral feature of the spectrum (1) is slightly affected by the electron beam–induced damage because the small shoulder can be observed at about 6.77 nm, it is considered that the electron beam–induced damage of $NaBF_4$ can be almost reduced by continuous moving the analytical area of the sample at a fast speed during the EPMA measurement, and that its B K x–ray emission spectrum can be measured almost correctly by an EPMA.

In summary, it was found that B K x–ray emission spectrum changes with variation in the chemical bond of boron in the spectral feature such as the peak position, FWHM and A.I. of the main band, and moreover, the peak position and relative intensity of the satellite band. Therefore, the spectral feature can be used to distinguish the boron compounds. In particular, the peak

position of the satellite band at the long wavelength side is considered to be a superior tool to identify the ligand in the boron compound. In the case of an EPMA measurement, electron-beam irradiation occasionally gives rise to the damage of a sample which results in the change of x-ray emission spectral feature. However, with continuous moving the analytical area of the sample at a fast speed during the measurement, it is possible to reduce the electron beam-induced damage and to measure the almost correct x-ray emission spectrum.

3-3. B K X-Ray Emission Spectra of BN Powders with Different Crystal Structures

B K x-ray emission spectra were precisely measured on boron nitride (BN) powders with different crystal structures by an EPMA, in order to investigate the changes in the spectral features depending on their crystal structures. Consequently, it was clarified that the B K x-ray emission spectra of BN powders change in the spectral features, such as the peak position and asymmetric index (A.I.) of the main band, and the relative intensities of the satellite bands which are observed at both sides of the main band, and that the B K x-ray emission spectrum can be used to identify the crystal phase of BN depending on the crystal structure.

The observations of polarized B K x-ray emission spectra were attempted using the BN samples with such a layered hexagonal structure as graphite by an EPMA. Unfortunately, the polarized emission of B K x-ray could not be clearly recognized from these samples.

Experimental Procedure

The BN samples used for B K x-ray emission measurements are c-BN powder (zincblend structure), w-BN powder (wurtzite structure), h-BN powder (hexagonal structure), t-BN plate (turbostratic structure, 5 x 5 x 1.3 mm), r-BN powder (rhombohedral structure) and a-BN powder (amorphous structure). In these samples, c-, h- and t-BN samples are commercially available, c-BN powder is synthesized at high temperature and high pressure, and a t-BN plate is pyrolytic BN synthesized by thermal CVD [31]. Wurtzite-type BN powder is synthesized by shock compression [32], r- and a-BN powders are synthesized in nitrogen atmosphere at 1173 K

from $NaBH_4$ + NH_4Cl and KBH_4 + NH_4Cl, respectively [33, 34]. For this experiment, w- and a-BN powders were provided by Dr. A.Onodera of Faculty of Engineering Science, Osaka University, and r-BN powder by Dr. T.Sato of National Institute for Research in Inorganic Materials. Metallic boron (M.B) melted by electron beam and solidified in vacuum of the order of 10^{-3} Pa was used too.

B K x-ray emission spectra were measured on these samples by an EPMA. For the measurements, BN powders were pressed into the disk of 5 mm^{ϕ} x 3 mm with flat plane, and then these disks and a t-BN plate were coated with carbon in vacuum of the order of 10^{-3} Pa. M.B was used without the carbon coating for the measurement. Details of the measurement conditions have been described in section 3-2. The B K x-ray emission spectra of BN powders were excited with sample currents of 0.07 ~ 0.13 μA. The B K x-ray intensities of BN powders were 650 ~ 8000 cps. On c-, w- and h-BN samples, K-emission band spectra of nitrogen (N K x-ray emission spectra) were also measured. Since h- and t-BN exhibit a similar layered hexagonal structure to that of graphite, the observations of polarized B K x-ray emission spectra were attempted using the t-BN plate and the h-BN single crystal with a size of about 5 μm. The polarized B K x-ray emission spectra were measured by both perpendicular and parallel excitations to the basal planes of these BNs.

Results and Discussion

N K x-ray emission spectra of c-, w- and h-BN powders

Figure 3-4 shows the N K x-ray emission spectra obtained from c-, w- and h-BN powders. The characteristics of these spectra are summarized in Table 3-2. Although the N K x-ray emission spectra were measured with similar exciting conditions to those of B K x-ray emission spectra, the former intensities were 1/4 to 1/5 of the latter ones. All N K x-ray emission spectra composed of the main band only, and no satellite band could be observed. Although the A.I. of the main band of the N K x-ray emission spectrum of w-BN powder is larger than those of c- and h-BN powders, there are few differences in the peak position and the FWHM of the main band among c-, w- and h-BN powders. Because a multilayer pseudo-crystal of lead stearate

used as an analyzing element has a low resolution in the region of the wavelength of N K x-ray, it is considered that the N K x-ray emission spectrum dose not change very much in the spectral feature depending on the crystal structure of BN.

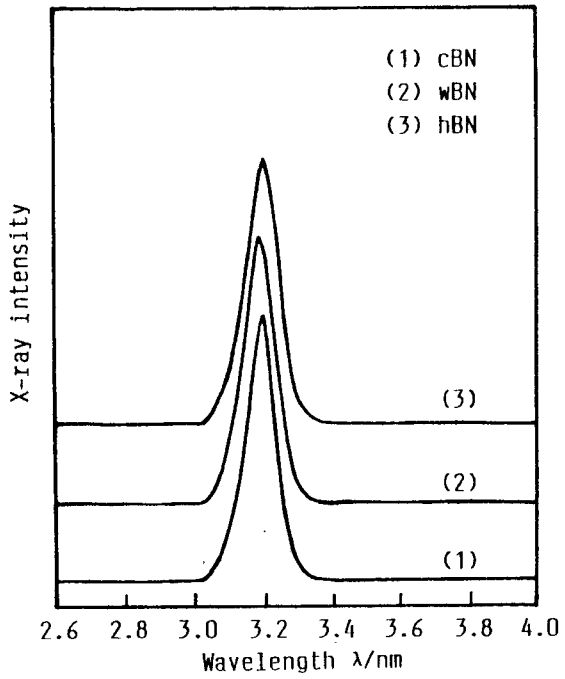

Fig. 3-4. N K x-ray emission spectra measured by an EPMA on c-BN powder (1), w-BN powder (2) and h-BN powder (3).

Table 3-2. Characteristics of N K x-ray emission spectra of c-BN, w-BN and h-BN powders.

Samples	Main peak		
	Position (nm)	FWHM (nm)	Asymmetric index
cBN	3.20	0.09	0.88
wBN	3.20	0.10	1.02
hBN	3.21	0.11	0.87

B K x-ray emission spectra of BN powders

Figures 3-5, 3-6 and 3-7 show the B K x-ray emission spectra obtained from M.B and BN powders with different crystal structures, and the characteristics of these spectra are summarized in Table 3-3. The relative intensity of satellite band was expressed in percentage to the peak intensity of the main band, and the variation was below 10 % of the relative intensity for five measurements.

The B K x-ray emission spectrum of M.B composes of the main band only, and no satellite band can be observed. In the cases of BN powders, the B K x-ray emission spectra compose of the main band and satellite bands at both sides of the main band, and the peak positions of main

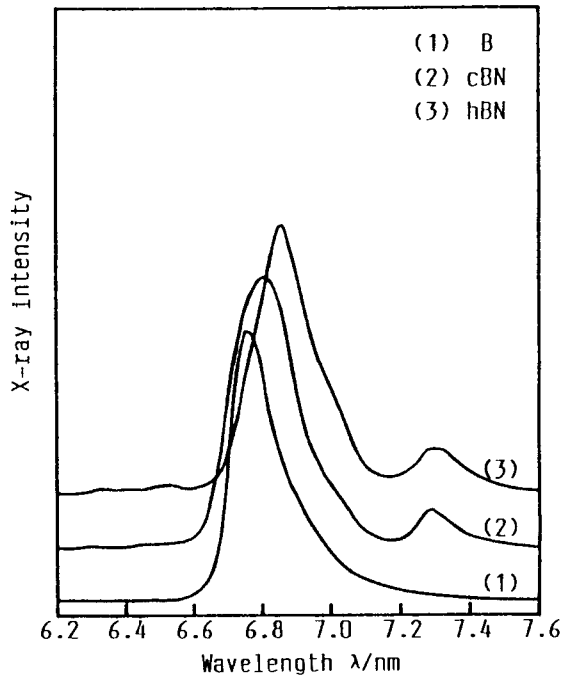

Fig. 3-5. B K x-ray emission spectra measured by an EPMA on metallic boron (1), c-BN powder (2) and h-BN powder (3).

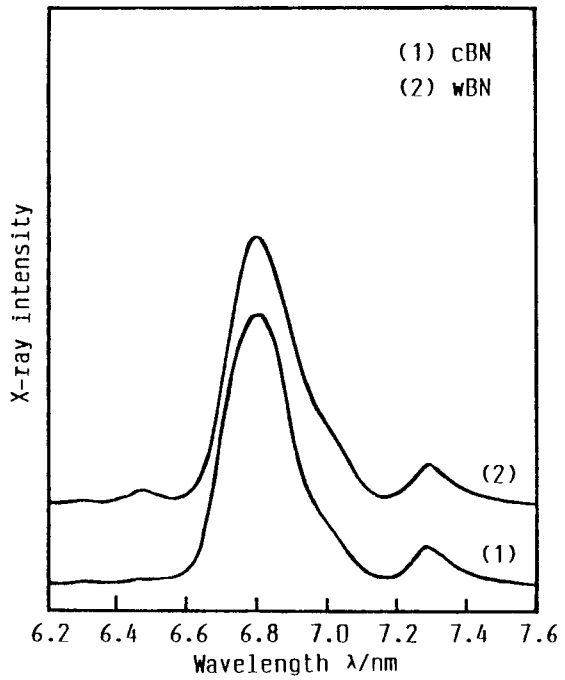

Fig. 3-6. B K x-ray emission spectra measured by an EPMA on c-BN powder (1) and w-BN powder (2).

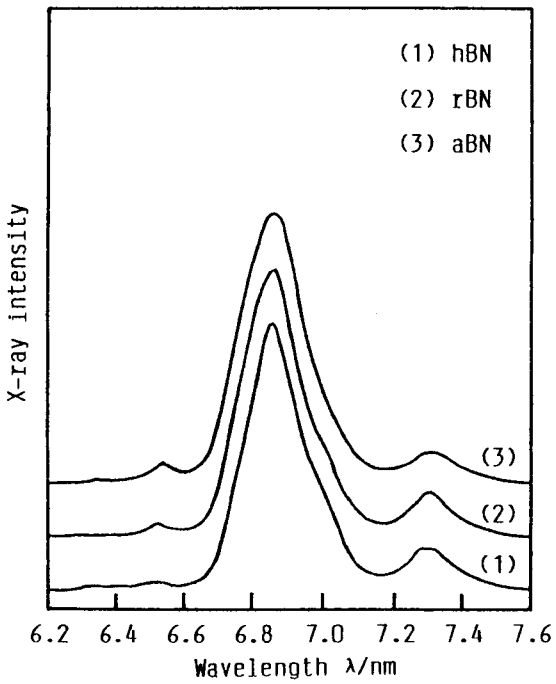

Fig. 3-7. B K x-ray emission spectra measured by an EPMA on h-BN powder (1), r-BN powder (2) and a-BN powder (3).

Table 3-3. Characteristics of B K x-ray emission spectra measured by an EPMA on metallic boron (B) and the various boron nitrides.

Samples	Main peak			Satellite peak					
	Position (nm)	FWHM (nm)	Asymmetric index	Position (nm)			Relative intensity (%)		
B	6.76	0.16	1.82	-	-	-	-	-	-
cBN	6.81	0.21	0.95	6.34	6.51	7.29	0.6	1.4	14.4
wBN	6.80	0.22	1.35	6.32	6.47	7.29	0.8	5.2	15.8
hBN	6.86	0.20	1.12	6.34	6.52	7.31	1.6	2.9	16.6
rBN	6.86	0.21	0.85	6.34	6.53	7.31	0.6	4.8	17.0
aBN	6.86	0.21	1.20	6.34	6.53	7.30	1.0	7.3	11.9

bands shift to longer wavelength side than that of M.B. The main bands of c- and h-BN powders differ distinctly from each other in the peak positions which are at 6.81 nm and 6.86 nm, respectively. There is, however, no significant difference in the peak positions between c- and w-BN powders, and among h-, r- and a-BN powders. Although the FWHMs of the main bands of BN powders are larger than that of M.B, there is no significant difference among those of BN powders, which are in the range from 0.20 nm to 0.22 nm. The asymmetric indices of the main bands of BN powders are smaller than that of M.B, and vary from 0.85 to 1.35 with the crystal structure of BN powder. There is especially some difference in the A.I. between c- and w-BN powders, and also among h-, r- and a-BN powders, even though the FWHM and the peak position of the main band scarcely differ.

The B K x-ray emission spectra of BN powders have two satellite bands at the short wavelength side and one satellite band at the long wavelength side. As mentioned in section 3-2, though the peak position of the satellite band at the long wavelength side changes with the ligand in boron compounds such as boron carbide, nitride and oxide, there is no significant difference among the peak positions of BN powders which are at about 7.30 nm. However, the relative intensity of this satellite band varies slightly with the crystal structure of BN powder, and a-BN powder shows the weakest relative intensity among these BN powders. The peak positions of

the satellite bands at the short wavelength side are at about 6.34 and 6.50 nm. The satellite bands near 6.34 nm of all BN powders are very weak, and there is little difference in its peak position and relative intensity among BN powders, while the satellite bands near 6.50 nm of w–, r– and a–BN powders are distinctly stronger than those of c– and h–BN powders.

As mentioned above, it was clarified that the B K x–ray emission spectral feature of BN powder changes depending on its crystal structure, and that the spectral feature can be used to identify the structure types of BN. That is to say, c– and w–BN are distinguished from h–, a– and r–BN by the peak position of the main band. Although the peak position of the main band of c–BN is similar to that of w–BN, c–BN is distinguished from w–BN by both the A.I. of the main band and the relative intensity of the satellite band near 6.50 nm. In the cases of h–, r– and a–BN, h–BN is distinguished from the latter two polymorphs by the relative intensity of the satellite band near 6.50 nm, and r–BN is distinguished from a–BN by both the A.I. of the main band and the relative intensity of the satellite band near 7.30 nm.

The crystal structure of c–BN is similar to that of diamond and belongs to a face–centered cubic structure [35], while that of w–BN is similar to that of hexagonal diamond and belongs to a close–packed hexagonal structure [36]. However, both c– and w–BN are sp^3–bonded BN phases, and boron atoms in both BNs combine with neighboring nitrogen atoms in four–fold coordination [11]. On the other hand, h– and r–BN are sp^2–bonded BN phases with a layered hexagonal structure, although both BNs differ from each other in the stacking sequence of the planar hexagonal networks constructed of six–membered rings of alternating boron and nitrogen atoms which are in three–fold coordination [11]. Amorphous BN is also an sp^2–bonded BN phase, though a–BN dose not exhibit a distinct crystal structure [37]. The origin of the main band of B K x–ray emission spectrum is due to the electron transition to the *1s* from the *2p* orbitals in a boron atom, and the spectral feature of the main band reflects mainly the electronic structure of *2p* orbital in a boron atom [26]. Since the *2p* orbital of boron is a valence orbital, its electronic structure should change with whether a boron atom in BN has an sp^2– or sp^3–hybridized orbital. Therefore, it is considered that the sp^2– and sp^3–bonded BN phases differ distinctly from each other in the peak position of the main band, of which the sp^2– and sp^3–bonded BN

phases are at about 6.86 and 6.80 nm, respectively. The origin of the satellite band near 7.3 nm is attributable to the electron transition to the *1s* orbital of boron from the *2p* σ molecular orbital of BN formed by the hybridization of the *2p* orbital of boron with the *2s* orbital of nitrogen, as described later in section 6–2. On the other hand, the origins of the satellite bands near 6.5 and 6.34 nm are due to the electron transition to the *1s* orbital of boron from the *2p* π* and σ* anti–bonding molecular orbitals of BN , as also described later in section 6–2. Although, it is assumed that the reason why these satellite bands change in the relative intensity depending on the crystal structure of BN is that the electron transition probability depends on the crystal structure, this assumption could not be unfortunately verified in this study.

Polarized B K x–ray emission spectra of h– and t–BN

It is well–known that K–emission band spectra of carbon (C K x–ray emission spectra) from the single crystal of graphite excited perpendicular and parallel to its basal plane differ distinctly from each other in the spectral feature [23]. This phenomenon is referred to as polarized emission of C K x–ray and attributable to the anisotropic character of the electronic orbitals of graphite [23]. Since h– and t–BN are a similar hexagonal structure to that of graphite [11], it is expected that the polarized B K x–ray emission spectra are observed from these BNs. The samples used for B K x–ray emission measurements are the single crystal of h–BN with a size of about 5 μm and the t–BN plate with a size of 5 x 5 x 1.3 mm. Although t–BN consists of a random stacking of the planar hexagonal networks, as with the disordered form of graphite, its c–axis is oriented perpendicular to the basal plane of the plate [38].

Figure 3–8 shows the B K x–ray emission spectra obtained from these samples, and the characteristics of the spectra are summarized in Table 3–4. The spectra denoted by t–BN (a) and h–BN (a) in Fig. 3–8 were excited parallel to the basal plane, and the spectra denoted by t–BN (c) and h–BN (c) perpendicular to the basal plane. However, as the single crystal of h–BN was very small, the focused electron beam could not be exactly impinged on this sample perpendicular or parallel to its basal plane.

On h– and t–BN, there are slight differences in both the A.I. of the main band and the relative

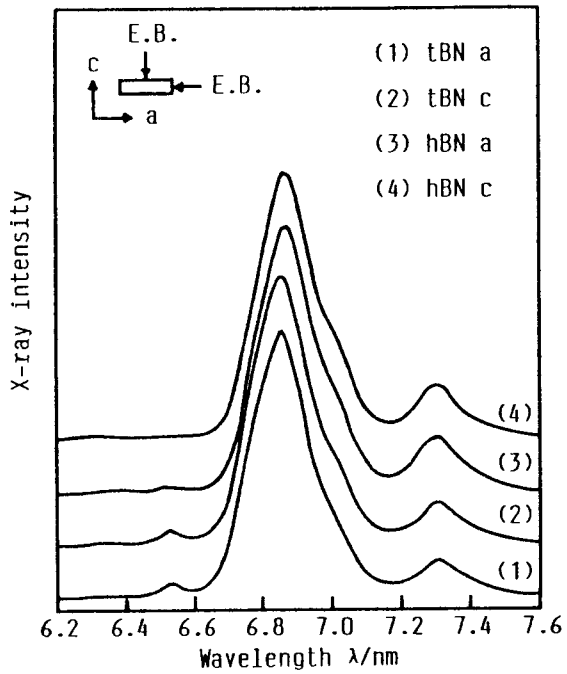

Fig. 3-8. B K x-ray spectra measured by parallel (1) and perpendicular (2) excitations to the basal plane of t-BN, and by parallel (3) and perpendicular (4) excitations to the basal plane of h-BN, using an EPMA.

Table 3-4. Characteristics of B K x-ray emission spectra measured by parallel and perpendicular excitations to the basal planes of t-BN and h-BN, using an EPMA.

Samples	Main peak			Satellite peak					
	Position (nm)	FWHM (nm)	Asymmetric index	Position (nm)			Relative intensity (%)		
tBN a	6.86	0.20	0.87	6.34	6.53	7.31	0.5	5.7	14.1
tBN c	6.86	0.20	0.98	6.34	6.53	7.31	0.7	5.1	15.5
hBN a	6.86	0.20	1.16	6.34	6.52	7.31	0.5	1.9	18.9
hBN c	6.86	0.19	1.09	6.34	6.56	7.32	0.7	1.1	18.1

intensities of the satellite bands near 6.5 and 7.3 nm between the B K x-ray emission spectra excited parallel and perpendicular to the basal plane. With respect to the A.I. of the main band and the relative intensity of the satellite band near 7.3 nm, the values of t-BN become slightly larger with the perpendicular excitation than with the parallel excitation, while those of h-BN show the reverse tendency. It is, therefore, unlikely that the differences in the values of the A.I. and the relative intensity of the satellite band near 7.3 nm between with the parallel and perpendicular excitations are due to the polarized emission of B K x-ray. On the other hand, with respect to the relative intensity of the satellite band near 6.5 nm, the values of both h- and t-BN become slightly stronger with the parallel excitation than with the perpendicular excitation. A.Mansour *et al.* [29] have also reported that this satellite band exhibits a tendency to be stronger with the parallel excitation than with the perpendicular excitation. However, it is likely in this experiment that the difference in the relative intensity of this satellite band may arise from the errors of the measurements because its difference is very small. It is, therefore, hardly declared that the polarized B K x-ray emission spectra could be clearly observed from t- and h-BN.

In summary, it was clarified that B K x-ray emission spectrum of BN changes in the spectral features, such as the peak position and A.I. of the main band, the relative intensities of the satellite bands at both sides of the main band depending on its crystal structure. Therefore, the crystal structure of BN can be distinguished by the B K x-ray emission spectral feature. In particular, this spectral feature can be used to distinguish between c- and w-BN phases, or among h-, r-, t- and a-BN phases, whereas these BN phases can not be distinguished by the IR absorption spectra. Although the polarized emission of B K x-ray was investigated using the h-BN single crystal and t-BN plate with the comparison between the B K x-ray emission spectra excited parallel and perpendicular to the basal plane by an EPMA, the polarized emission could not be clearly recognized from these samples.

3-4. B K X-Ray Emission Spectra of Cubic BN Films Deposited by Different Reactive Ion-Plating Methods

B K x-ray emission spectra were measured by an EPMA on the ion-plated c-BN thin films which had been reported to be a c-BN film, and were discussed in comparison with those of BN powders. It was found that the B K x-ray emission spectra of the c-BN films differ from that of the c-BN powder synthesized at high temperature and pressure in both values of the A.I. of the main band and the relative intensity of the satellite band near 6.5 nm. Thus, in order to elucidate the origin of the difference between the B K x-ray emission spectra of the c-BN film and the c-BN powder in these values, assuming that the c-BN film composed of the mixture of c-BN and hexagonal-like BN phases like an a-BN, it was attempted to reproduce the measured spectrum of the c-BN film with the synthesis of the measured spectra of the c-BN and a-BN powders. However, the values of the measured B K x-ray emission spectrum of the c-BN film are larger than those of the synthesized spectrum using the measured spectra of the c-BN and a-BN powders, it was found that the measured B K x-ray emission spectral feature of the c-BN film can be hardly explained by the simple assumption that the c-BN film composes of the mixture of c-BN and hexagonal-like BN phases such as an a-BN phase.

Experimental Procedure

Cubic BN was deposited on a silicon substrate at a self-bias voltage of -55 V, an Ar/N_2 gas flow ratio of 2.0, an electron-beam power (for boron evaporation) of 1.8 kW and an ionization current of 14 A by the reactive ion-plating method with a hot cathode plasma discharge in a parallel magnetic field. Details the ion-plating system and deposition procedures have been described in sections 2-2 and 2-3. Furthermore, two c-BN films deposited on silicon substrates were used for B K x-ray emission measurements. Two c-BN films, which were provided by Dr. T.Ikeda of Materials Research Laboratory, Kobe Steel, Ltd. and by Dr. S.Watanabe of Nippon Institute of Technology, were prepared by the arc-like plasma and magnetically enhanced plasma ion-plating methods [13, 39]. The c-BN film provided by Dr. T.Ikeda has been considered from results of the infrared absorption and electron diffraction analyses to be a c-BN

film with a small amount of h-BN phase [13], and hereafter, is termed as "c-BN film (1)". The c-BN film provided by Dr. S.Watanabe has also been considered from results of the infrared absorption and x-ray diffraction analyses to be a c-BN film with a small amount of h-BN phase [39], and hereafter,is termed as "c-BN film (2)".

For the EPMA measurements, the c-BN films were coated with carbon without being peeled off from the substrate in vacuum of the order of 10^{-3} Pa. The B K x-ray emission spectra were measured on the c-BN films at an accelerative voltage of 15 kV and at a sample current of 0.15 μA by an EPMA. Details of the measurement procedures have been described in section 3-3.

Results and Discussion

The c-BN films (1) and (2) were deposited on silicon substrates by different ion-plating methods. In the case of the c-BN film (1), the film had the strong IR absorption peak near 1050 cm^{-1} due to the reststrahlen band of a c-BN phase and two weak IR absorption peaks near 1380 and 800 cm^{-1} due to the B-N stretching and B-N-B bending vibrations of an h-BN phase,respectively. The diffraction rings were observed from this film by selected area electron diffractometry (SAED), and the *d*-spacings calculated from these rings agreed approximately with those of the (0002) plane of an h-BN phase and of the (111), (220), (311), (331) and (422) planes of a c-BN phase. Therefore, the c-BN film (1) has been reported to be a c-BN film with a small amount of hexagonal-like BN phase which was a general name for h-, r-, t- and a-BN phases because these phases cannot be distinguished by the IR absorption spectra [13]. On the other hand, the c-BN film (2) had also the strong IR absorption peak near 1050 cm^{-1} and two weak IR absorption peaks near 1380 and 800 cm^{-1}. By x-ray diffractometry, two diffraction peaks were observed from this film at the diffraction angles 2θ of about 43 and 74 degrees corresponding to the (111) and (220) planes of a c-BN phase, respectively. Therefore, the c-BN film (2) has been also reported to be a c-BN film with a small amount of hexagonal-like BN phase [39].

Figure 3-9 shows the B K x-ray emission spectra obtained from the c-BN films (1) and (2). The characteristics of these spectra are summarized in Table 3-5.

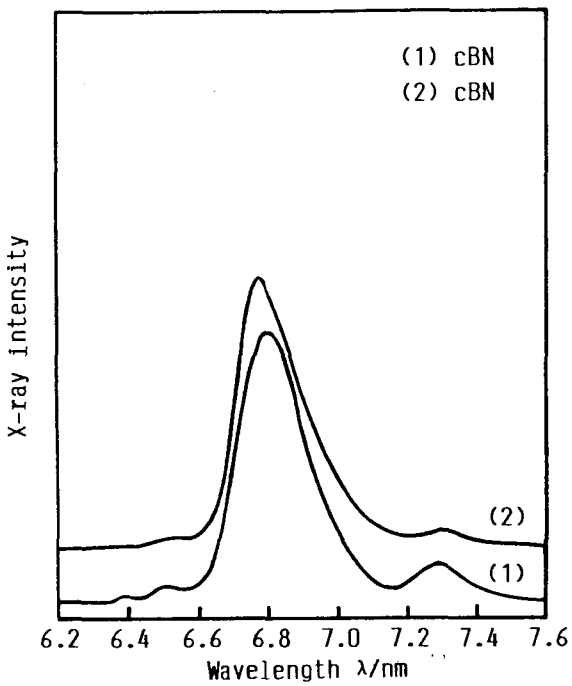

Fig. 3-9. B K x-ray emission spectra of the c-BN films deposited by the arc-like plasma ion-plating method (1) and the magnetically enhanced plasma ion-plating method (2), measured by an EPMA.

Table 3-5. Characteristics of B K x-ray emission spectra of the c-BN films deposited by the different ion-plating methods, measured by an EPMA.

Samples	Main peak			Satellite peak					
	Position (nm)	FWHM (nm)	Asymmetric index	Position (nm)			Relative intensity (%)		
cBN(1)	6.81	0.23	1.21	6.39	6.51	7.30	2.0	6.0	14.7
cBN(2)	6.78	0.22	1.99	6.34	6.53	7.31	0.9	3.8	7.0

In the case of the B K x-ray emission spectrum of the c-BN film (1), the A.I. of the main band and the relative intensity of the satellite band near 6.5 nm are larger than those of the c-BN powder synthesized at high temperature and pressure, although the other characteristics of the spectrum of this film are almost consistent with those of the c-BN powder. On the other hand, the characteristics of the B K x-ray emission spectrum of the c-BN film (2) are almost inconsistent with those of the c-BN powder. The peak position of the main band shifts to shorter wavelength side than that of the c-BN powder, and the A.I. of the main band and the relative intensity of the satellite band near 6.5 nm are larger than those of the c-BN powder. In contrast, the relative intensity of the satellite band near 7.3 nm is about one-half of that of the c-BN powder. The presence of the satellite band near 7.3 nm is considered to show that boron combines with nitrogen, and its relative intensity is considered to be a indicator of the amount of the combined boron with nitrogen. The peak position the main band of the c-BN film (2) is, furthermore, intermediate between those of M.B and the c-BN powder. Therefore, the c-BN film (2) is presumed to contain considerably the uncombined boron with nitrogen, *i.e.*, M.B. Since any x-ray diffraction peaks corresponding to M.B were not observed from this film, the M.B in the film is presumed to be an amorphous structure.

It was found that the B K x-ray emission spectra of the c-BN films (1) and (2) exhibit larger values in the A.I. of the main band and the relative intensity of the satellite band near 6.5 nm than those of the c-BN powder. The differences in these values are assumed to arise from overlapping the B K x-ray emission spectrum of the hexagonal-like BN phase with that of the c-BN phase in the films. Thus, it was attempted to elucidate the origin of the difference in these values, using the B K x-ray emission spectrum of the c-BN film deposited by the reactive ion-plating method with a hot cathode plasma discharge in a parallel magnetic field.

Figure 3-10 shows the IR absorption spectrum of this c-BN film together with those of the w-, c- and h-BN powders. The c-BN film is found from the IR absorption spectrum to contain a small amount of hexagonal-like BN phase such as h-, r-, t- and a-BN phases. The c-BN and hexagonal-like BN phase contents in the c-BN film is calculated from the IR absorption spectrum to be about 75 % and 25 %, respectively, using the calculation procedure described in

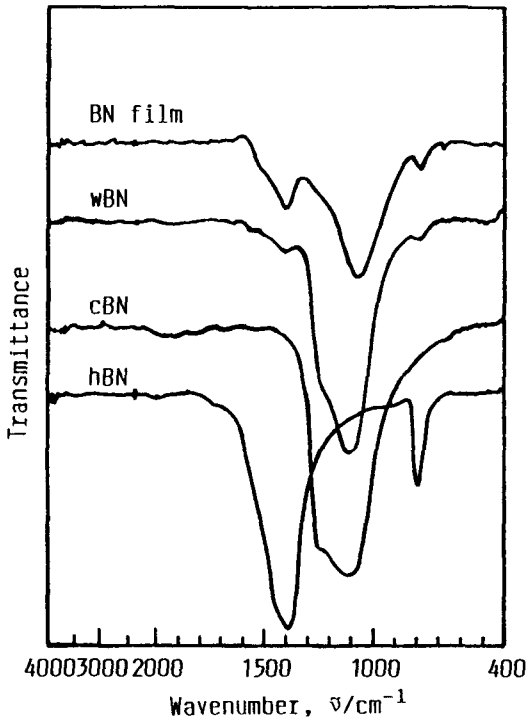

Fig. 3-10. Infrared absorption spectra of h-BN, c-BN and w-BN powders, and the BN film deposited by the ion-plating method.

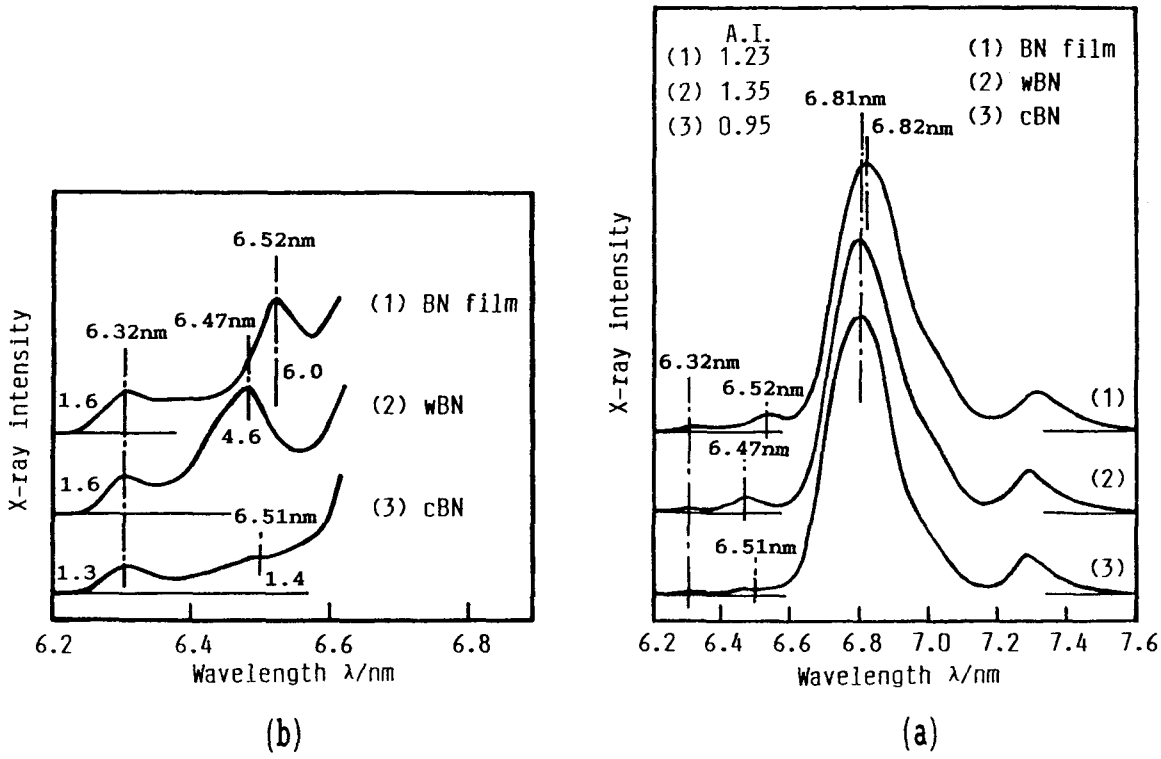

Fig. 3-11. B K x-ray emission spectra measured by an EPMA on c-BN and w-BN powders, and the BN film deposited by the ion-plating method.

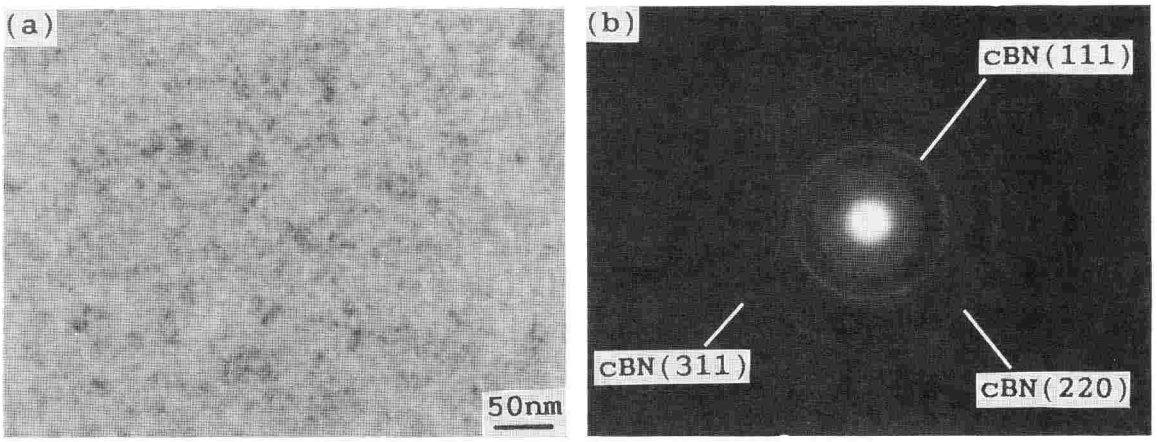

Fig. 3-12. TEM micrograph and selected area electron diffraction pattern of the BN film deposited by the ion-plating method.

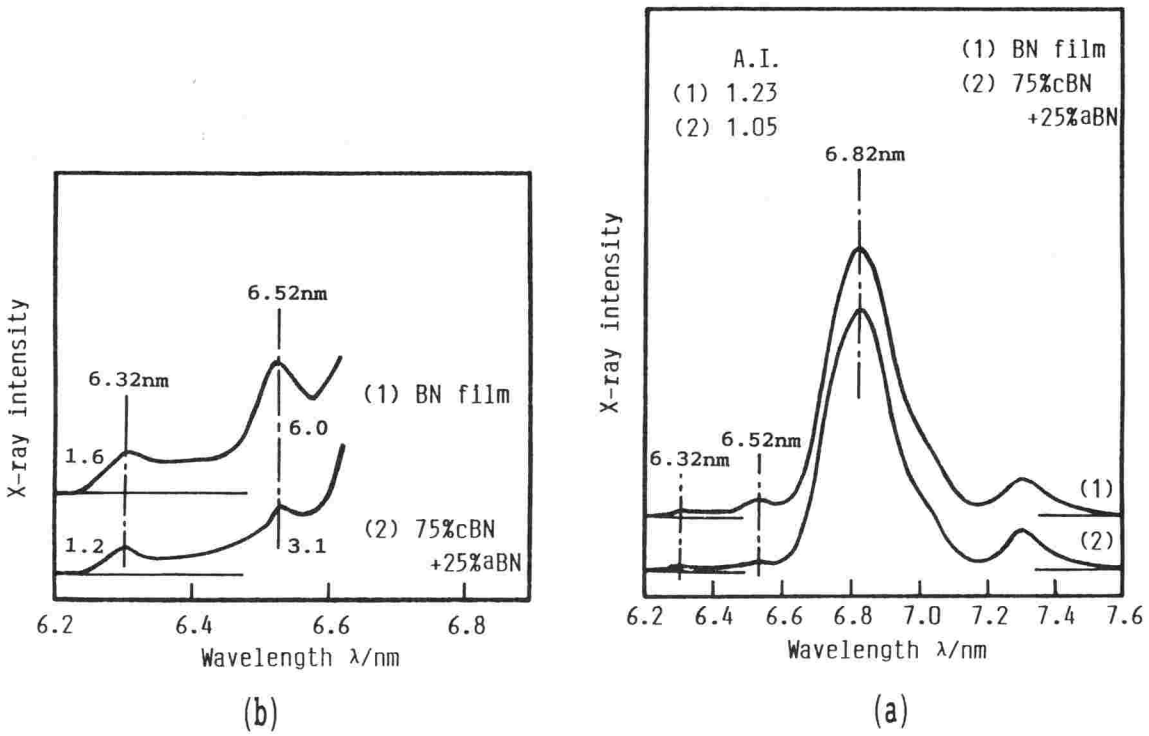

Fig. 3-13. B K x-ray spectra measured on the BN film by an EPMA (1), and synthesized from the measured spectra of c-BN and a-BN powders (2) by an EPMA.

section 2–2. Figure 3–11 shows the B K x–ray emission spectrum of the c–BN film together with those of the c–BN powder synthesized at high temperature and pressure and the w–BN powder synthesized by shock compression, and moreover, Fig. 3–12 shows the SAED pattern taken from the c–BN film. In the SAED pattern, there are diffraction rings corresponding to the (0002) plane of an h–BN phase and to the (111), (220) and (311) planes of a c–BN phase [40, 41]. The c–BN film was also confirmed from the SAED pattern to contain a small amount of hexagonal–like BN phase. As shown in Fig. 3–11, the B K x–ray emission spectrum of the c–BN film differs distinctly from that of the w–BN powder in the peak position of the satellite band near 6.5 nm, and moreover, differs from that of the c–BN powder in the values of both the A.I. of the main band and the relative intensity of the satellite band near 6.5 nm.

In order to investigate the origin of the difference in these values, it was attempted to reproduce the measured B K x–ray emission spectrum of the c–BN film with the synthesis of the measured spectra of the c–BN and hexagonal–like BN powders. It was assumed that the hexagonal–like BN phase in the c–BN film was an a–BN phase, because the B K x–ray emission spectrum of the a–BN powder had the largest values in both the A.I. of the main band and the relative intensity of the satellite band near 6.5 nm among the hexagonal–like BN powders (see Tables 3–3 and 3–4). The intensity of synthesized spectrum $I_{syn.}$ was calculated by the following relation;

$$I_{syn.} = \alpha I_{c-BN} + \beta I_{a-BN} \qquad (3-1)$$

where I_{c-BN} and I_{a-BN} are the intensities of the spectra measured on the c–BN and a–BN powders, respectively, α and β are the c–BN and a–BN phase contents in the c–BN film which were estimated from the IR absorption spectrum of the c–BN film to be 75 and 25 %, respectively, as mentioned above. The synthesized spectrum was normalized by setting the calculated peak intensity of the main band to 100. Figure 3–13 shows the synthesized spectrum, compared with the measured spectrum of the c–BN film. The characteristics of the synthesized spectrum were approximately in agreement with those of the c–BN film. However, the A.I of the main band and the relative intensity of the satellite band near 6.5 nm of the synthesized spectrum are 1.05 and 3.1, respectively, and smaller than those of the c–BN film. These values of the synthesized

spectrum would not become large if the hexagonal-like BN phase in the c-BN film is assumed not to be an a-BN phase but to be the other hexagonal-like BN phases such as h-, r- or t-BN, because these values of the B K x-ray emission spectra of the h-, r- and t-BN powders are smaller than those of the a-BN powder. Therefore, the B K x-ray emission spectral feature of the c-BN film can be hardly explained by the simple assumption that the c-BN film composes of the mixture of c-BN and hexagonal-like BN phases such as an a-BN phase. The origin of difference between the B K x-ray emission spectra of the c-BN film and the c-BN powder in the relative intensity of the satellite band near 6.5 nm will be further described later in chapters 5 and 6.

References

[1] F.Fujimoto, in *Synthesis and Properties of Boron Nitride*, edited by J.J.Pouch and S.A.Alterovitz (Trans Tech, Aedermannsdorf, 1990), p.45.

[2] A.K.Ballal, L.Salamanca-Riba, C.A.Taylor and G.L.Doll, Thin Solid Films, **224**, 46(1993).

[3] C.Weissmantel, K.Bewilogua, K.Breuer, D.Dietrich, U.Ebersbach, H.-J. Erler, B.Rau and G.Reisse, Thin Solid Films, **96**, 31(1982).

[4] H.Miyamoto, M.Hirose and Y.Osaka, Jpn. J. Appl. Phys., **22**, L216(1983).

[5] M.Murakawa, S.Watanabe and S.Miyake, Diamond Films Technol., **1**, 1(1991).

[6] D.R.McKenzie, D.J.H.Cockayne, D.A.Muller, M.Murakawa, S.Miyake, S.Watanabe and P.Fallon, J. Appl. Phys., **70**, 3007(1991).

[7] G.L.Doll, J.A.Sell, C.A.Taylor and R.Clarke, Phys. Rev., **B43**, 6816(1991).

[8] M.Okamoto, Y.Utsumi and Y.Osaka, Jpn. J. Appl. Phys., **31**, 3455(1992).

[9] K.Kaneda and K.Shibata, Jpn. J. Appl. Phys., **32**, 5652(1993).

[10] H.Saitoh, H.Morino and Y.Ichinose, Jpn. J. Appl. Phys., **32**, L1684(1993).

[11] T.A.Friedmann, P.B.Mirkarimi, D.L.Medlin, K.F.McCarty, E.J.Klaus, D.R.Boehme, H.A.Johnsen, M.J.Mills, D.K.Ottesen and J.C.Barbour, J. Appl. Phys., **76**, 3088(1994).

[12] M.Murakawa and S.Watanabe, Surf. Coat. Technol., **43/44**, 145(1990).

[13] T.Ikeda, Y.Kawate and Y.Hirai, J. Vac. Sci. Technol., **A8**, 3168(1990).

[14] T.Ichiki, T.Momose and T.Yoshida, J. Appl. Phys., **75**, 1330(1994).

[15] C.Weissmantel, K.Bewilogua, D.Dietrich, H.-J.Erler, H.-J.Hinneberg, S.Klose, W.Nowick and G.Reisse, Thin Solid Films, **72**, 19(1980).

[16] D.L.Medlin, T.A.Friedmann, P.B.Mirkarimi, P.Rez, M.J.Mills and K.F.McCarty, J. Appl. Phys., **76**, 295(1994).

[17] K.L.Chopra, V.Agarwal, V.D.Vankar, C.V.Deshpandey and R.F.Bunshah, Thin Solid Films, **126**, 307(1985).

[18] D.J.Fabian, L.M.Watson and C.A.W.Marshall, Rep. Progr. Phys., **34**, 601(1972).

[19] D.J.Nagel, Advan. X-Ray Anal., **13**, 182(1970).

[20] Y.Gohshi, J. Spectrosc. Soc. Jpn., **18**, 235(1969).

[21} W.L.Baun, Appl. Spectry. Rev., **1**, 379(1968).

[22] D.W.Fischer, Advan. X-Ray Anal., **13**, 159(1969).

[23] M.Motoyama and G.Hashizume, J. Spectrosc. Soc. Jpn., **29**, 92(1980).

[24] D.J.Joyner and D.M.Hercules, J. Chem. Phys., **72**, 1095(1980).

[25] M.Okusawa, K.Ichikawa, T.Matsumoto and K.Tsutsumi, J. Phys. Soc. Jpn., **51**, 1921(1982).

[26] S.Luck and D.S.Urch, Physica Scripta, **41**, 970(1990).

[27] R.D.Carson and S.E.Schnatterly, Phys. Rev. Lett., **59**, 319(1987).

[28] B.M.Davies, F.Bassani, F.C.Brown and C.G.Olson, Phys. Rev., **B24**, 3537(1981).

[29] A.Mansour and S.E.Schnatterly, Phys. Rev., **B36**, 9234(1987).

[30] T.L.Aselage and R.G.Tissot, J. Am. Ceram. Soc., **75**, 2207(1992).

[31] Y.Kubota, Boundary, **3**, 38(1986).

[32] A.K.Lam, R.M.Wentzcovitch and M.L.Cohen, in *Synthesis and Properties of Boron Nitride*, edited by J.J.Pouch and S.A.Alterovitz (Trans Tech, Aedermannsdorf, 1990), p.165.

[33] T.Sato, Proc. Jpn. Acad., **61, Ser. B**, 459(1985).

[34] A.Onodera, N.Takahashi, H.Yoshihara, H.Nakae, Y.Matsunami and T.Hirai, J. Mater. Sci., **25**, 4157(1990).

[35] F.S.Galasso, *Structure and Properties of Inorganic Solids* (Pergamon, Oxford, 1970), p.96.

[36] F.S.Galasso, *Structure and Properties of Inorganic Solids* (Pergamon, Oxford, 1970), p.140.

[37] K.Sugiyama and H.Itoh, Mater. Sci. Forum, **54&55**, 141(1990).

[38] H.Tanji and M.Hara, Boundary, **3**, 46(1986).

[39] M.Murakawa and S.Watanabe, Surf. Coat. Technol., **43/44**, 128(1990).

[40] Joint Committee on Powder Diffraction Standards (JCPDS, Swarthmore, PA), pattern 25-1033.

[41] Joint Committee on Powder Diffraction Standards (JCPDS, Swarthmore, PA), pattern 34-421.

Chapter 4

Adhesion of Cubic BN Film to Silicon Substrate and Atmospheric Degradation of BN Film

4-1. Introduction

There have been many previous attempts to deposit a cubic boron nitride (c-BN) film using chemical or physical vapor deposition methods [1 - 6]. The author has investigated the preparation of c-BN film using the reactive ion-plating method with a hot cathode plasma discharge in a parallel magnetic field. The BN film deposited by the reactive ion-plating method has been identified as c-BN from infrared absorption spectrum, electron diffraction pattern and B K x-ray emission spectrum *etc.*.

One of the most serious problems for the c-BN film is low adhesion strength to a substrate [1, 4, 7]. Therefore, the c-BN film peels off from the substrate in a little while after deposition and occasionally even during deposition. Several techniques for the adhesion improvement of c-BN film to the substrate have been presented [8 - 16]. The author has attempted the following three techniques in combination to improve the adhesion of the ion-plated c-BN film to a silicon substrate: (1) a buffer interlayer with gradually increasing nitrogen concentration was formed between the silicon substrate and c-BN film; (2) the c-BN film was annealed in vacuum to reduce internal stress; (3) the c-BN film with the buffer interlayer was deposited on the silicon substrate which had been implanted with nitrogen and/or boron ions.

Another problem of the c-BN film is the atmospheric degradation. It is reported that c-BN films deposited by various PVD and CVD processes degrade quickly in appearance after a few days' exposure to atmospheric humidity, and that this degradation takes place especially readily on the c-BN films which contain a large amount of amorphous BN phase, metallic boron or oxygen [3, 17, 18]. However, there are few investigations on the concrete degradation of c-BN film in air, although amorphous BN film deposited by an RF sputtering process has been reported to change into ammonium borate in air [19, 20]. Using several BN films with different struc-

tures deposited under various deposition conditions by the reactive ion-plating method, the atmospheric degradations of these films were investigated by SEM observations and EPMA measurements after exposing these films to air for a long time to about 3000 hours.

In this chapter, the adhesion of the c-BN film to the silicon substrate and its atmospheric degradations are described.

4-2. Adhesion Improvement of Cubic BN Film on Silicon Substrate

The adhesion improvement of the c-BN film deposited on a silicon substrate by the reactive ion-plating method has been investigated using techniques such as the formation of the buffer interlayer between the c-BN film and the substrate, the annealing of the c-BN film and the ion implantation of nitrogen and/or boron into the substrate. It was found that the formation of the buffer interlayer and the ion implantation of nitrogen and/or boron increased the adhesion of the c-BN film to the silicon substrate, and that the c-BN film with the buffer interlayer deposited on the silicon substrate implanted with both nitrogen and boron ions showed the best adhesion. However, the annealing of the c-BN film did not bring about any improvement in the adhesion to the substrate.

Experimental Procedure

The c-BN film was prepared by reactive ion plating. Details of the ion-plating system and deposition procedures have been described in chapter 2, so a brief discussion is presented here. The c-BN film was deposited on a silicon substrate by reaction of the evaporated boron (purity 99.9%) with the nitrogen ion generated in the plasma. Radio-frequency power was applied to the silicon substrate to generate a negative self-bias voltage. Conditions for the deposition of c-BN film are given in Table 4-1.

The buffer interlayer was formed by first depositing a pure boron layer on the silicon substrate at a self-bias voltage of -10 V, followed by a BN_x ($0<x<1$) layer with gradually increasing nitrogen concentration at a self-bias voltage of -30 V until the stoichiometric BN layer was

Table 4-1. Experimental conditions for the deposition of c-BN film by the ion-plating method.

Evaporant	99.9 % boron
Electron beam power	1.6 kW
Ionization voltage	66 V
Ionization current	14 A
Self-bias voltage	-60 V (R.F. 13.56 MHz)
Ar/N_2 gas flow ratio	2.0
Total gas pressure	7×10^{-2} Pa
Deposition rate	0.25 nm/s

attained. Nitrogen concentration of the buffer interlayer was controlled by varying the flow rate of nitrogen gas. Finally, the c-BN film was deposited under the conditions given in Table 4-1.

The N/B ratio of the buffer interlayer was measured by an electron probe microanalyzer (EPMA). The c-BN film with the buffer interlayer was analyzed by infrared absorption spectroscopy and x-ray emission spectroscopy. B K x-ray emission spectrum was measured at an excitation voltage of 15 kV and a sample current of about 0.1 μA by an EPMA, using a multilayer pseudo-crystal of lead stearate as an analyzing element. The depth profile of the c-BN film with the buffer interlayer was measured by a glow discharge spectrometer (GDS). A GDS measurement was carried out at a radio-frequency power of 40 W, while sputtering with argon ion at the analytical area of 4 mm diameter. The detection limits of nitrogen and boron are on the order of 0.1% and 1 ppm, respectively, and the depth resolution of a GDS is on the order of 10 nm [21].

The c-BN films with the buffer interlayer were deposited on unimplanted silicon substrates and on silicon substrates which had been implanted with nitrogen and/or boron ions. The ion implantations into the silicon substrates were carried out at an energy of 200 keV which was suitable for the near surface implantation of these ions. Nitrogen and boron fluences were 5×10^{17} and 1.5×10^{17} ions/cm^2, respectively. It was expected that some surface properties of the

silicon substrate were changed by these fluences which were generally used for surface modification of the metal [22]. Annealing of the c-BN film to reduce internal stress was performed by heating at 1073 K for 75.6 ks in vacuum (pressure 4×10^{-3} Pa).

Adhesion measurements of the c-BN films to the silicon substrate were carried out using a microtribometer [23].

Results and Discussion

Buffer interlayer and c-BN film

The buffer interlayer was deposited on the silicon substrate for 0.6 ks and its thickness was about 0.2 μm. Nitrogen concentration of the buffer interlayer was controlled by varying the flow rate of nitrogen gas. Figure 4-1 shows the N/B ratio of the BN film deposited at a self-bias voltage of -30 V on the silicon substrate at various flow rates of nitrogen gas. The N/B ratio increases approximately linearly with increasing the flow rate of nitrogen gas.

The c-BN film was subsequently deposited on the buffer interlayer for 1.2 ks and its thickness was about 0.3 μm. Figure 4-2 shows infrared absorption spectra of the c-BN film with the buffer interlayer. These infrared absorption spectra were measured on the BN film without being peeled off from the substrate in transmittance mode by FTIRS. Three absorption peaks are observed in the spectrum of the as-deposited film, namely, the peak at 1087 cm^{-1} (reststrahlen band) which originates from the c-BN structure, and peaks at 1390 (B-N-B stretching mode) and 781 cm^{-1} (B-N-B bending mode) absorbed by the buffer interlayer. The peak position of the c-BN film shifted slightly from 1087 cm^{-1} to 1080 cm^{-1} after annealing. This shift is considered to be due to the reduction of internal stress in the c-BN film [16]. The reduction of internal stress was estimated to be about 20 % from this shift, since the peak position of the c-BN film peeled off from a substrate was 1050 cm^{-1}.

The crystal structure of BN can be determined from the features of the B K x-ray emission spectrum, because the B K x-ray emission spectrum of BN changes depending on the crystal structure, in the spectral features such as the peak position and asymmetric index of the main band or the peak position and relative intensity of the satellite band. Figure 4-3 shows B K x-

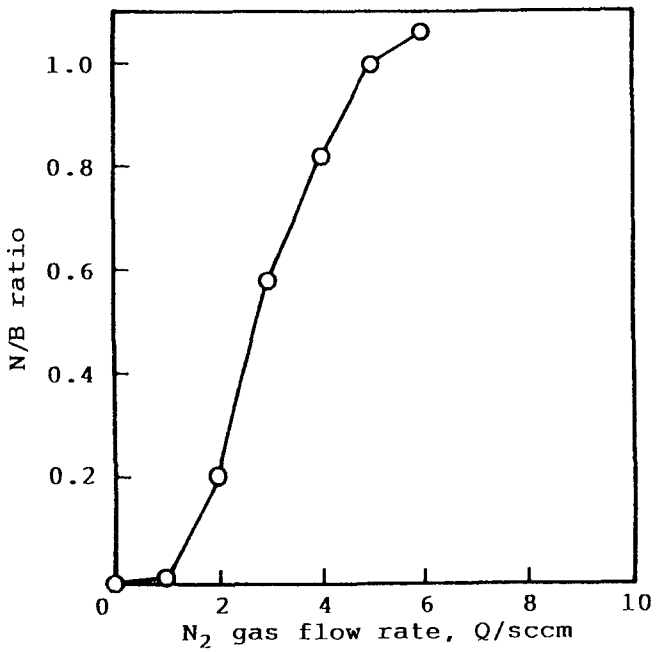

Fig. 4-1. Change in the N/B ratio of BN film with nitrogen gas flow rate.

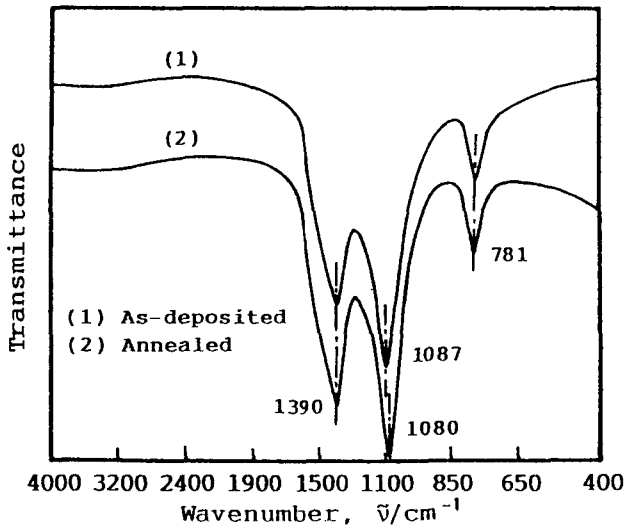

Fig. 4-2. Change in infrared absorption spectrum of c-BN film with buffer interlayer, before and after annealing.

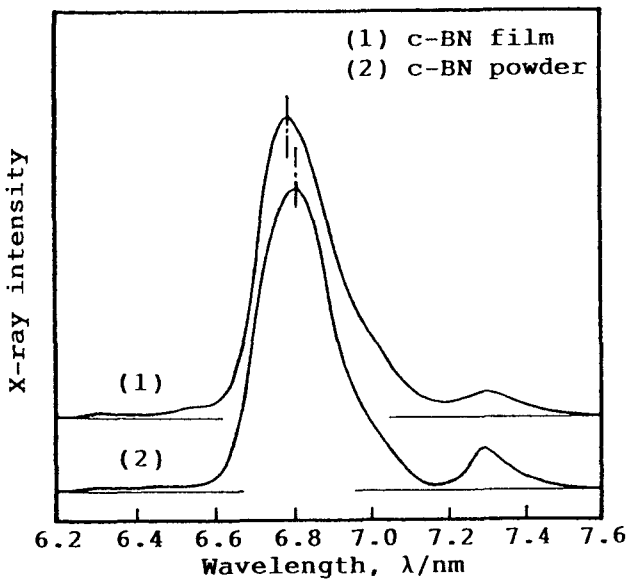

Fig. 4-3. B K x-ray emission spectra measured by an EPMA on c-BN film with buffer interlayer and c-BN powder synthesized at high temperature and pressure.

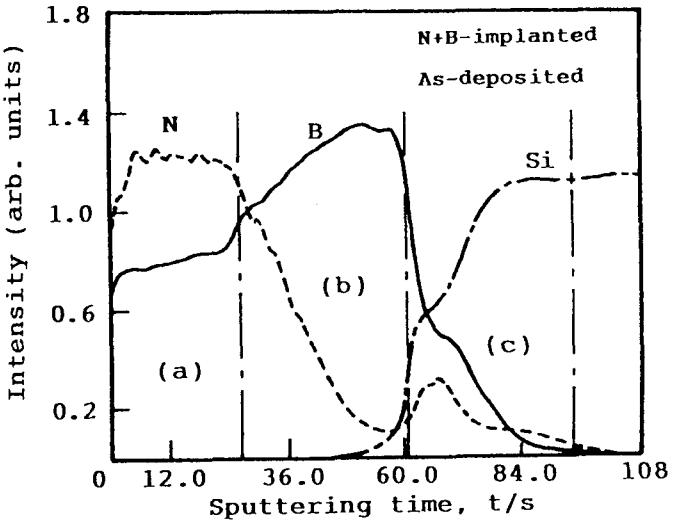

Fig. 4-4. Depth profile of c-BN film with buffer interlayer deposited on the silicon substrate implanted with both nitrogen and boron ions, measured by a glow discharge spectrometer (GDS).

Table 4-2. Characteristics of B K x-ray emission spectra measured on c-BN film with buffer interlayer and c-BN powder.

	Main peak			Satellite peak	
	Position (nm)	FWHM* (nm)	A.I.**	Position (nm)	R.I.*** (%)
c-BN powder	6.81	0.21	0.95	6.34 6.51 7.29	0.6 1.4 14.4
c-BN film	6.79	0.22	1.57	6.32 6.54 7.30	1.3 3.2 8.3

* Full width at half maximum

** Asymmetric index

*** Relative intensity

ray emission spectra obtained from the c–BN film with the buffer interlayer and c–BN powder synthesized at high pressure and high temperature, and characteristics of these spectra are given in Table 4–2. The B K x–ray emission spectral feature of the c–BN film with the buffer interlayer differs from that of c–BN powder in the peak position and the asymmetric index of the main band, and in the relative intensity of the satellite band at 7.30 nm. These differences are considered to be due to the overlap of the B K x–ray emission spectrum of the buffer interlayer with that of the c–BN film, reflecting the difference of the crystal structure as described in section 3–3.

Figure 4–4 shows the depth profile of the c–BN film with the buffer interlayer deposited on a silicon substrate which was implanted with both nitrogen and boron ions. Three regions are observed, namely, a near–surface region (a) corresponding to the c–BN film, an intermediate region (b) corresponding to the buffer interlayer with gradual changing nitrogen concentration and a region (c) corresponding to the layer implanted with both nitrogen and boron ions. Judging from this depth profile, the buffer interlayer is thicker than the c–BN film. However, this is considered to be caused by slight etching of the c–BN film by pre–sputtering before analysis. No change in the depth profile was observed upon annealing of the c–BN film.

Adhesion strength of c–BN film to silicon substrate

Figure 4–5 shows the schematic diagram of the microtribometer used for adhesion measurements. This microtribometer is essentially a scratch tester. During the measurement, the cartridge is vibrated at a frequency of 30 Hz normal to the scratching direction, and a diamond stylus (radius 10 μm) scratches the surface of the c–BN film at a constant speed of 20 μm/s with gradual increase of load applied vertically to the stylus. The motion of the diamond stylus is detected as the cartridge signal by a pair of coils inside the cartridge. Figure 4–6 shows the curves of cartridge signal *v.s.* load applied to the diamond stylus for the c–BN films. The cartridge signal increases linearly with increasing load applied to the diamond stylus, but becomes abrupt as soon as the c–BN film begins to peel off from the substrate. Figure 4–7 shows a micrograph of the scratched surface of the c–BN film with the buffer interlayer. The adhesion of

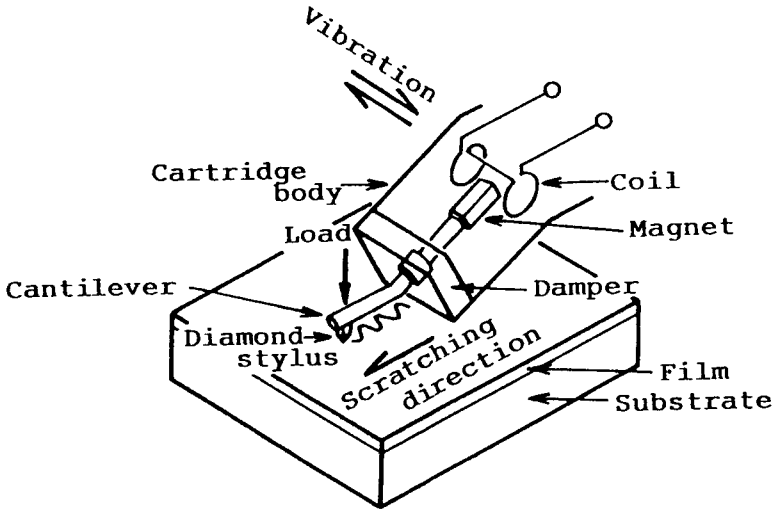

Fig. 4-5. Schematic diagram of the microtribometer.

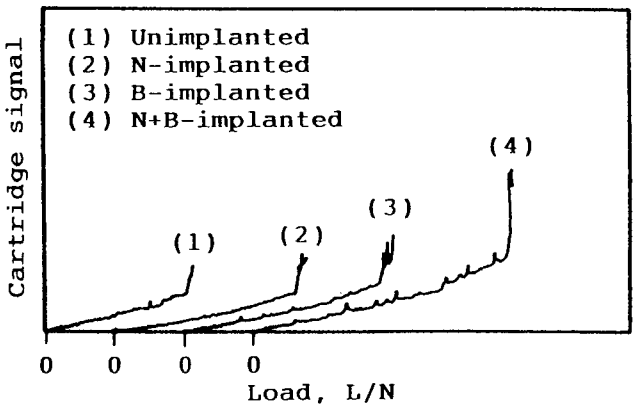

Fig. 4-6. Load *v.s.* cartridge signal curves for c-BN films.

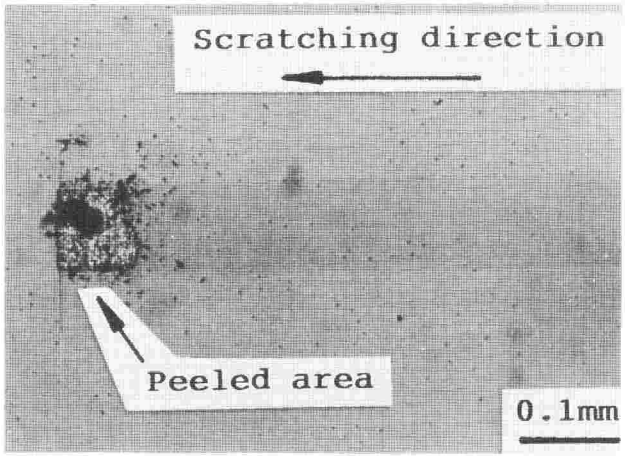

Fig. 4-7. Scratched surface of c-BN film with buffer interlayer.

Table 4-3. Peeling loads (units in N) for c-BN films, measured by the microtribometer.

Implanted species	As-deposited	Annealed
-	0.136 ± 0.007	0.134 ± 0.007
N	0.179 ± 0.004	0.186 ± 0.006
B	0.183 ± 0.030	0.181 ± 0.010
N + B	0.224 ± 0.007	0.239 ± 0.005

the c–BN films on the silicon substrates was evaluated from the applied load (peeling load) at which the cartridge signal showed an abrupt increase. Table 4–3 shows the peeling loads for the c–BN films. These values of the peeling load are obtained from the average of five measurements.

The c–BN film without the buffer interlayer peeled off from the silicon substrate shortly after deposition (Fig. 4–8), but the c–BN film with the buffer interlayer did not peel off from the silicon substrate after deposition (Fig. 4–9), and its peeling load measured with a microtribometer was about 0.14 N. On the other hand, the peeling load was about 0.18 N for the c–BN films with the buffer interlayer deposited on silicon substrates which had been implanted with either nitrogen or boron ions. In contrast, the peeling load of the c–BN film with the buffer interlayer deposited on the silicon substrate implanted with both nitrogen and boron ions was greater than those of the former two. It was obvious that ion implantation of nitrogen and/or boron into the silicon substrate improved the adhesion of the c–BN film with the buffer interlayer to the substrate. However, in spite of the reduction of the internal stress in the c–BN films with annealing, there was no significant difference in the peeling load between as–deposited and annealed c–BN films. No effect of the annealing of the c–BN film on the adhesion improvement to the substrate was observed. It is assumed that the reason why the ion implantation improved the adhesion is that the implantation of nitrogen and boron ions created a favorable gradient of chemical composition near the substrate surface.

In summary, the adhesion improvement of the c–BN film deposited on the silicon substrate by the reactive ion–plating method has been investigated using techniques such as the formation of the buffer interlayer between the c–BN film and the substrate, the annealing of the c–BN film and the ion implantation of nitrogen and/or boron into the substrate. It was found that the formation of the buffer interlayer and the ion implantation of nitrogen and/or boron increased the adhesion of the c–BN film to the silicon substrate, and that the c–BN film with the buffer interlayer deposited on the silicon substrate implanted with both nitrogen and boron ions showed the best adhesion. However, the annealing of the c–BN film did not bring about any improvement in the adhesion to the substrate.

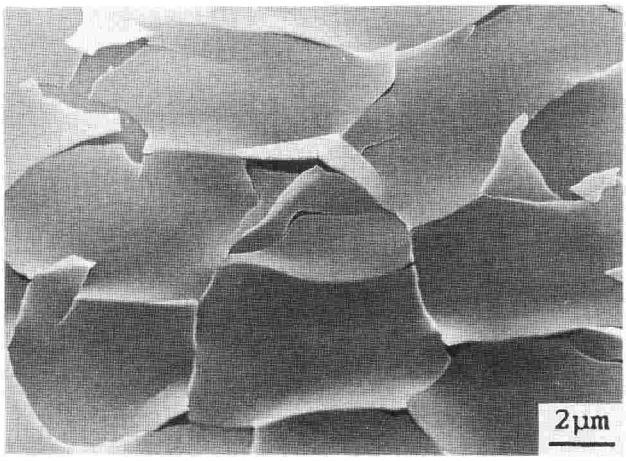

Fig. 4-8. SEM image of c-BN film peeled off from silicon substrate.

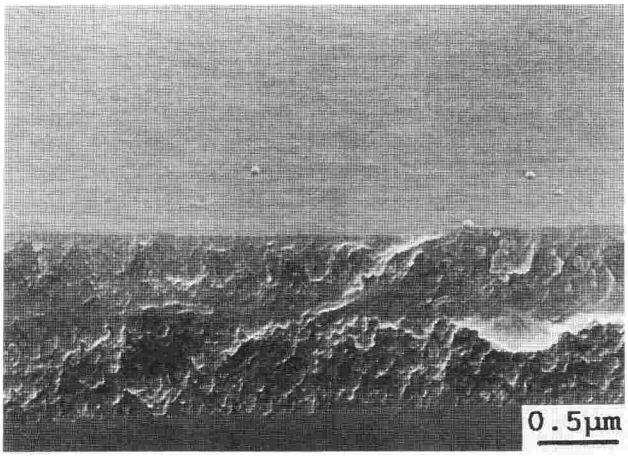

Fig. 4-9. SEM image of fractured section of c-BN film with buffer interlayer.

4-3. Atmospheric Degradation of BN Films Deposited by Reactive Ion-Plating Method

Several BN films were deposited on silicon substrates under different deposition conditions by the reactive ion-plating method with a hot cathode plasma discharge in a parallel magnetic field. Their crystalline phases were considered to be amorphous, cubic, and either turbostratic or rhombohedral. These BN films were exposed to air with relative humidities of about 30 %, 65 ~ 85 % and 100 % for a long time to about 3000 hours, and their atmospheric degradations were investigated by SEM observations and EPMA measurements.

Small particles which were considered to be one of boron oxide, boric acid or ammonium borate were observed to form on the surface of amorphous BN film after a short-period exposure to air, whereas no reaction product could be observed even on the surfaces of the other BN films exposed to air for about 3000 hours. However, all BN films were cracked or peeled off from the substrate on exposure to air. Since the cracking was brought about after shorter time's exposure to air with increasing the relative humidity of air, it is assumed that the cracking is induced by atmospheric moisture. However, the c-BN film is hard to be cracked with atmospheric moisture and is stable in air, compared with the other films.

Experimental Procedure

Details of the ion-plating system and deposition procedures have been described in chapter 2. The deposition conditions for BN films are summarized in Table 4-4. The soft BN films (A) and (B) shown in Table 4-4 were deposited on silicon substrates under the deposition conditions without forming a c-BN phase in the films. These films had the same IR absorption spectra as shown in Fig. 4-10. These BN films have two IR absorption peaks at 1390 and 775 cm^{-1} corresponding to those of an sp^2-bonded BN phase and a broad IR absorption peak at around 3200 cm^{-1} which are considered to be due to the B-H stretching (~2500 cm^{-1}), N-H stretching (~3200 cm^{-1}) and O-H stretching (~3400 cm^{-1}) [24, 25]. Thus, these BN films are sp^2-bonded BN phases such as h-, t-, r- and a-BN, and a small amount of water vapor would be adsorbed on their surfaces or incorporated into the films during the depositions. The soft BN films (A) and (B) are considered from their B K x-ray emission spectra to be a-BN and either t- or r-BN,

Table 4-4. Experimental conditions for the depositions of BN films by the ion-plating method.

	Soft BN film		Hard BN film	
	(A)	(B)	(A)	(B)
E.B. power	2.0 kW	2.0 kW	1.7 kW	1.7 kW
Ionization current	2 A	14 A	14 A	14 A
Self-bias voltage	-10 V	-30 V	-60 V	-60 V
Annealing	—	—	—	1072 K 75.6 ks 4×10^{-3} Pa
Substrate	Si wafer			
E.B. evaporant	99.9% boron			
Ionization voltage	66 V			
Ar/N_2 gas flow ratio	2.0			
Pressure	7×10^{-2} Pa			

respectively, as described later. These BN films have a thickness of about 0.5 μm.

The hard BN film (A) shown in Table 4–4 was deposited on a silicon substrate under the deposition condition with predominant forming a c–BN phase in the film. This film has the same buffer interlayer with about 0.2 μm thickness as described in section 4–2 and the c–BN layer with about 0.3 μm thickness on the buffer interlayer. Figure 4–11 (1) shows the IR absorption spectrum obtained from this film. An IR absorption peak at 1096 cm^{-1} corresponding to that of an sp^3–bonded BN phase can be observed in this spectrum. The presence of c–BN phase in this film was confirmed from electron diffractometry, as described later. Although the c–BN phase content in the c–BN layer cannot be calculated from the IR absorption spectrum shown in Fig. 4–11 (1) because the sp^2–bonded BN phase is contained not only in the c–BN layer but also in the buffer interlayer, the c–BN phase content is assumed from the deposition condition to be more than 70%. The hard BN film (B) shown in Table 4–4 was deposited under the identical deposition condition with that of the hard BN film (A), and annealed at 1073 K for 75.6 ks in vacuum of 4×10^{-3} Pa. Figure 4–11 (2) shows the IR absorption spectrum of the hard BN film (B). In the case of the hard BN film (B), the IR absorption peak corresponding to that

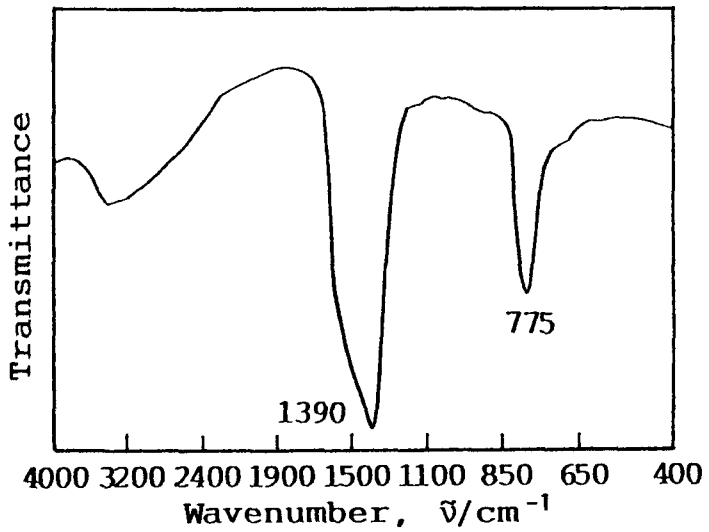

Fig. 4-10. Infrared absorption spectrum of soft BN film.

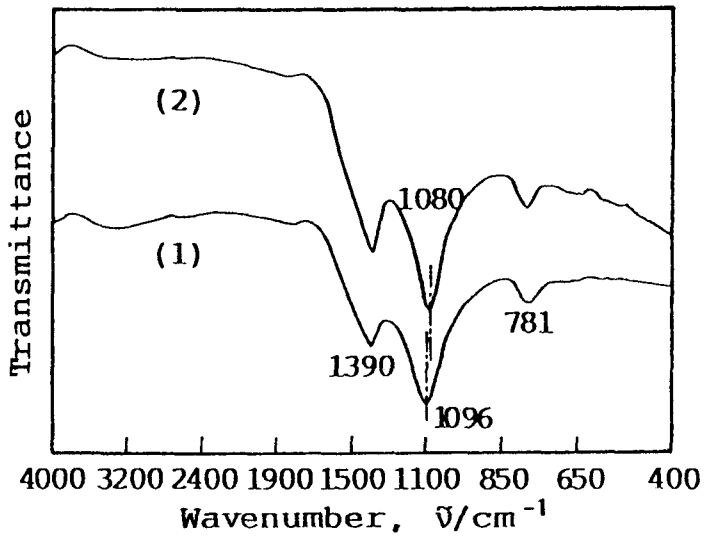

Fig. 4-11. Infrared absorption spectra of (1) hard BN film (A) and (2) hard BN film (B).

of a c-BN phase shifts shorter wavenumber side than that of the hard BN film (A). This shift is considered to be due to the decrease of internal stress.

The 10 specimens were cut from each BN film on the silicon substrate into the square shapes of 10 x 10 mm immediately after the deposition, and then were exposed to air with relative humidities of about 30 %, 65 ~ 85 % and 100 % for a long time to about 3000 hours. Using the specimens exposed to air for different times, the atmospheric degradations were investigated by SEM observations and EPMA measurements.

Results and Discussion

Most of the BN films exposed to air were observed to begin to get apparently cloudy after some times' exposure, and then to extend the cloudy area with proceeding of the time (see Fig. 4-12). The times required for the BN films to begin to get cloudy from the onset of exposure to air varied with the differences in the BN film and relative humidity, as shown in Fig. 4-13. All the BN films began to get cloudy after shorter time's exposure to air with higher relative humidity, and the soft BN films got cloudy more readily than the hard BN films, However, the BN films except the soft BN film (A) could be observed not to get cloudy in air with a relative humidity of about 30 % even after 3000 hours' exposure to air. In the cases of the hard BN films, since the hard BN film (B) began to get cloudy after longer time's exposure to air than the hard BN film (A), it is considered that the annealing of BN film exhibits inhibitory action against the cloud of the film on exposure to air. This inhibitory action is considered to be mainly due to the reduction of internal stress, as described later.

Figure 4-14 shows SEM micrographs taken from the cloudy areas of the BN films. On exposure to air, all the BN films were observed to crack or peel off from the substrates, especially, only the soft BN film (A) was observed to form small particles on the surface. However, there were no changes on exposure to air in the configurations of all the BN films at the areas without getting cloudy. The hard BN film (A) was broken to pieces and peeled off almost perfectly from the substrate. The hard BN film (B) was not almost peeled off from the substrate, though it was cracked. On the other hand, the soft BN film (B) was cracked and peeled off

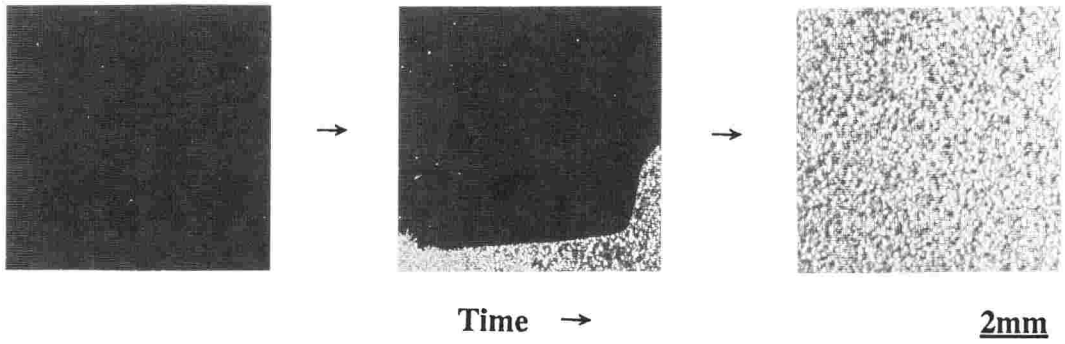

Fig. 4-12. Macroscopic change in appearance of BN film on exposure to air.

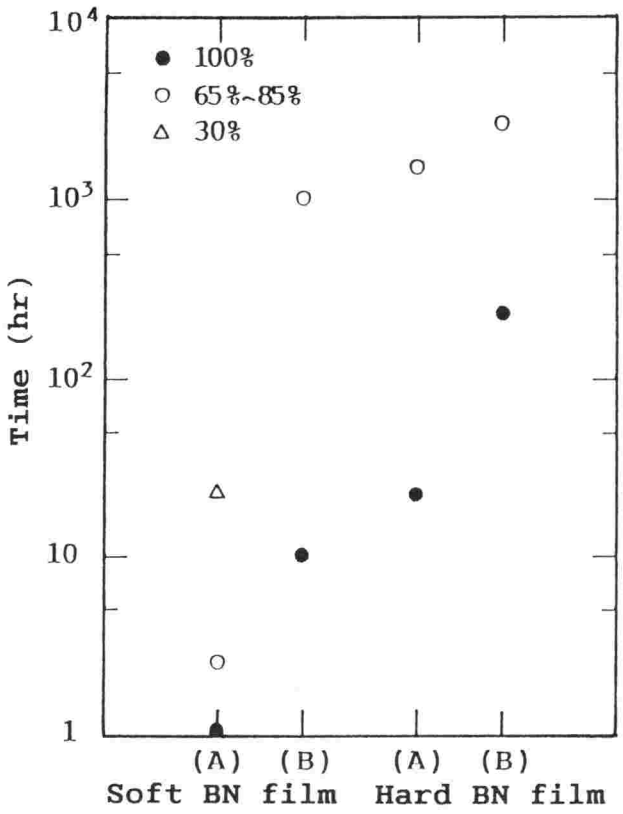

Fig. 4-13. Time-dependence of atmospheric degradation of soft and hard BN films exposed to air with relative humidity of 30 % to 100 %.

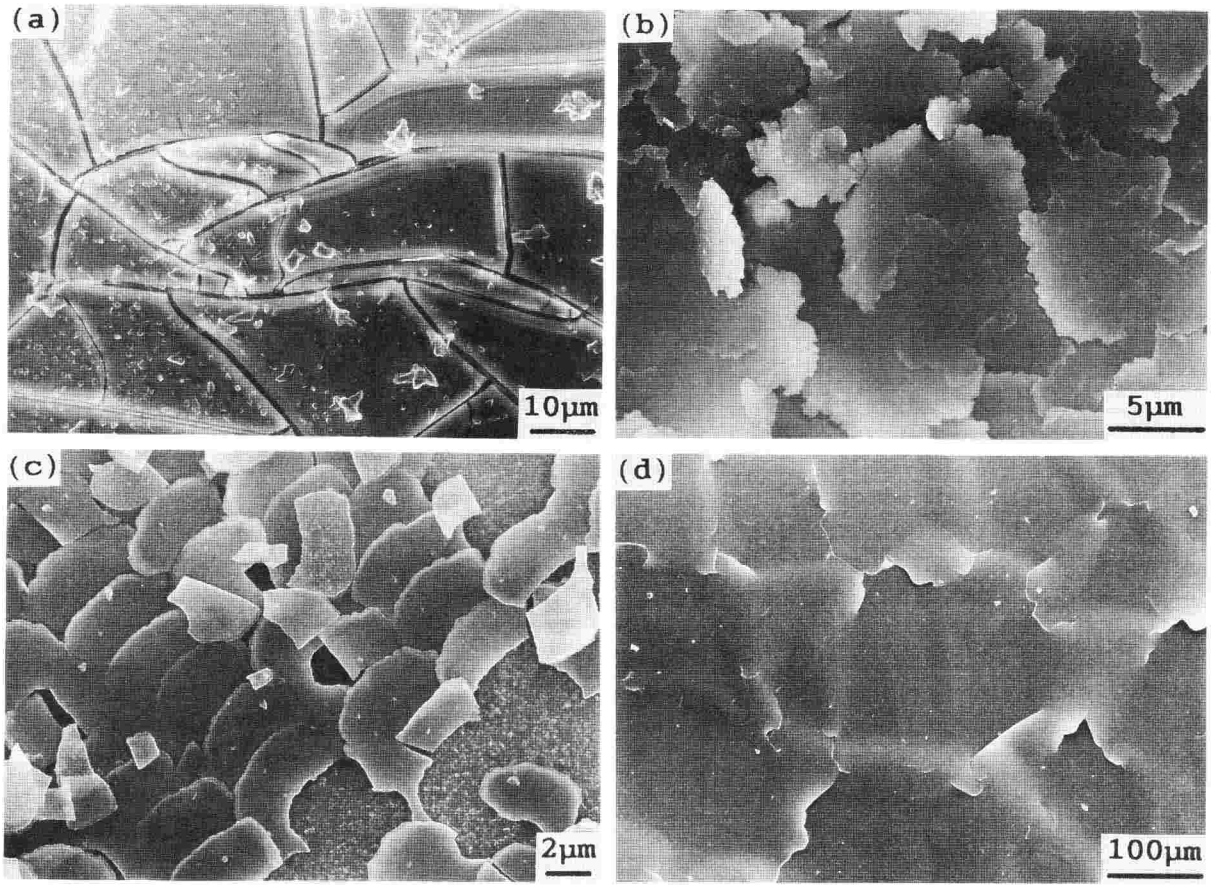

Fig. 4-14. SEM images of cloudy areas of soft and hard BN films exposed to air with 100 % relative humidity : (a) soft BN film (A), (b) soft BN film (B), (c) hard BN film (A) and (d) hard BN film (B).

partially from the substrate, whereas the soft BN film (A) was only cracked. T.Ikeda and co-workers [26] have reported that the c-BN film deposited by an ion-plating method had a high compressive stress of about 4.0 GPa, while BN film without a c-BN phase had a compressive stress of about 1.6 GPa. The compressive stress in BN film is considered to be caused by ions bombarding the growing film [27 - 33]. Thus, the intensity of internal stress in the BN film is considered to become higher in this order: the soft BN film (A), (B) and the hard BN film (A), judging from the self-bias voltage applied to the substrate. The hard BN film (B) may have compressive stress of about 30 % lower than the hard BN film (A) because of annealing after the deposition, judging from the shift of the IR absorption peak corresponding to that of c-BN (see Fig. 4-11). Therefore, the differences in the morphology of cracks of the BN films are considered to be due to the differences in the intensities of internal stress in the films

Figure 4-15 shows the B K x-ray emission spectra of the soft BN film (A) measured before and after exposure to air with a relative humidity of 65 ~ 85% together with that of B_2O_3. In the spectrum measured after exposure to air, the satellite bands are observed at 6.48 and 7.47 nm, although these satellite bands cannot be observed in the spectrum measured immediately after the deposition. Therefore, these satellite bands are considered to origin from the small particles formed on the surface after exposure to air. The peak positions of these satellite bands are consistent with those of B_2O_3 However, boron oxide has the same B K x-ray emission spectrum as boron acid and ammonium borate, as shown in Fig. 4-16. Thus, the small particles are considered to be one of these boron compounds.

Figure 4-17 shows the B K x-ray emission spectra of the hard BN film (A) measured before and after exposure to air. In the cases of the spectra measured after exposure to air (see spectra (2) and (3) in Fig. 4-17), the main peak positions shifted to shorter wavelength side than that of the spectrum measured immediately after the deposition, and the relative intensities of satellite bands were weaker than those of the spectrum measured immediately after the deposition. In the spectrum (4) in Fig. 4-17 measured on the peeled area of this film marked by the circle in Fig. 4-18, the relative intensities of satellite bands were very weak, and the main band features such as the peak position, FWHM and asymmetric index were very close to those of metallic

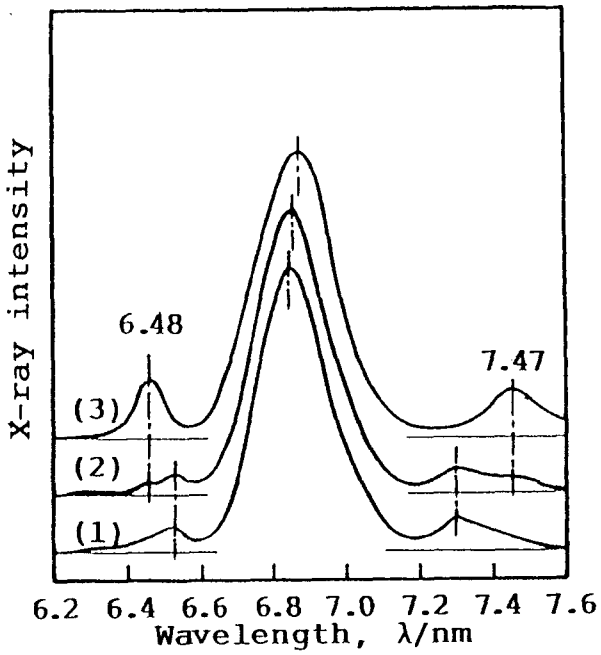

Fig. 4-15. B K x-ray emission spectra measured by an EPMA on soft BN films (A) as-deposited (1), exposed to air with relative humidity of 65 % to 85 % (2) and B_2O_3 (3).

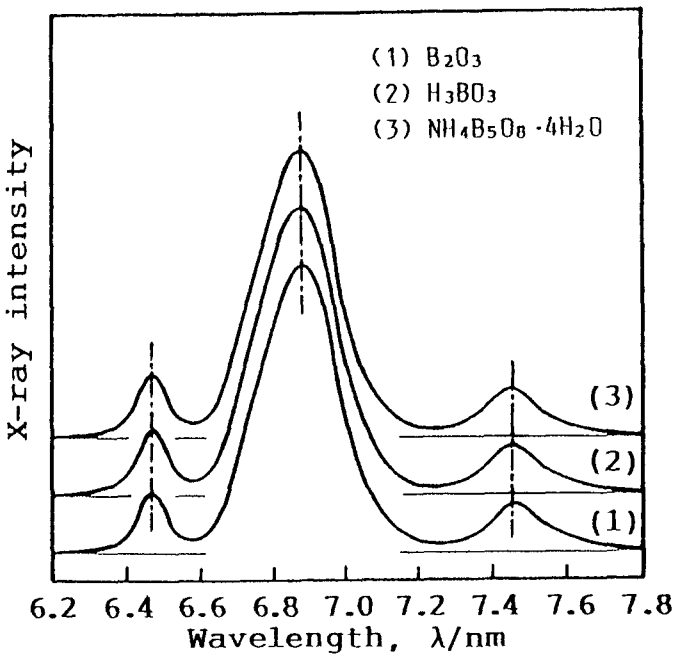

Fig. 4-16. B K x-ray emission spectra measured by an EPMA on B_2O_3 (1), H_3BO_3 (2) and $NH_4B_5O_8 \cdot 4H_2O$ (3).

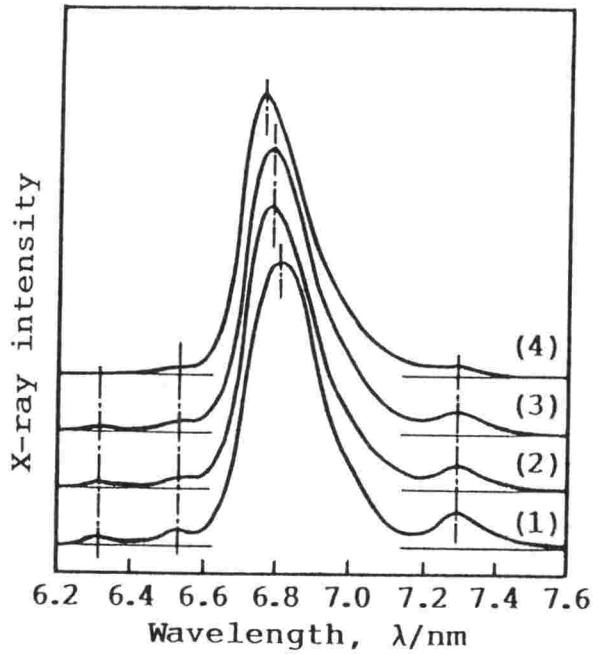

Fig. 4-17. B K x-ray emission spectra measured on hard BN films (A) as-deposited (1), exposed to air with 100 % (2) and with 65 ~ 85% relative humidity (3), and peeled area marked by the circle in Fig. 4-18 (4).

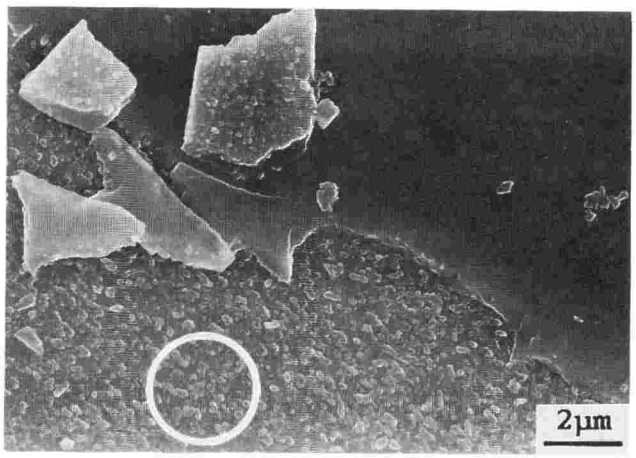

Fig. 4-18. SEM image of peeled area of hard BN film (A) on exposure to air.

boron. Therefore, the hard BN film (A) is considered to peel off from the buffer interlayer with a small N/B ratio, and the changes in the spectral features on exposure to air are considered to be due to the overlap of the spectrum of the film without peeling off from the substrate with that of the buffer interlayer (the peeled area). On the other hand, there were no changes on exposure to air in the spectral features of the soft BN film (B) and the hard BN film (B) which were observed not to peel off from the substrate and to form no reactive products on the surfaces after exposure to air.

Figure 4–19 shows the B K x–ray emission spectra of the BN films measured immediately after the depositions, and the characteristics of these spectra are summarized in Table 4–5. Regarding the soft BN film (A), the peak position and asymmetric index of the main band are almost consistent with those of a–BN or h–BN. The relative intensities of the satellite band near 6.5 nm of this film, a–BN and h–BN are 9.1, 7.3 and 2.9, respectively. Since the relative intensity of this film is close to that of a–BN rather than of h–BN, the soft BN film (A) is considered to be a–BN. The soft BN film (B) is considered to be either t–BN or r–BN, because its peak position and asymmetric index of the main band are almost consistent with those of t–BN or r–BN. However, these soft BN films may contain uncombined boron with nitrogen, because only BN film with substoichiometric with respect to nitrogen (an N/B ratio of about 0.5) can be deposited under their deposition conditions, as described in section 2–3. In the cases of the B K x–ray emission spectra of the hard BN films, although their main peak positions are almost consistent with that of c–BN, their asymmetric indices are close to that of w–BN rather than of c–BN. However, the hard BN films are actually confirmed from the electron diffraction pattern shown in Fig. 4–20 to be c–BN films with a small amount of sp^2–bonded BN phase.

On exposure to air, the soft BN film (A), which was considered to be a–BN, got cloudy after the shortest time's exposure to air among the BN films and small particles formed on the surface of this film, such as boron oxide, boron acid or ammonium borate which were considered to be produced by the reaction of this film with atmospheric moisture. It has been reported that a–BN film deposited by an RF sputtering process changed into ammonium borate in air [20], and that a–BN had many dangling bonds [34]. Therefore, the a–BN film is considered to react readily

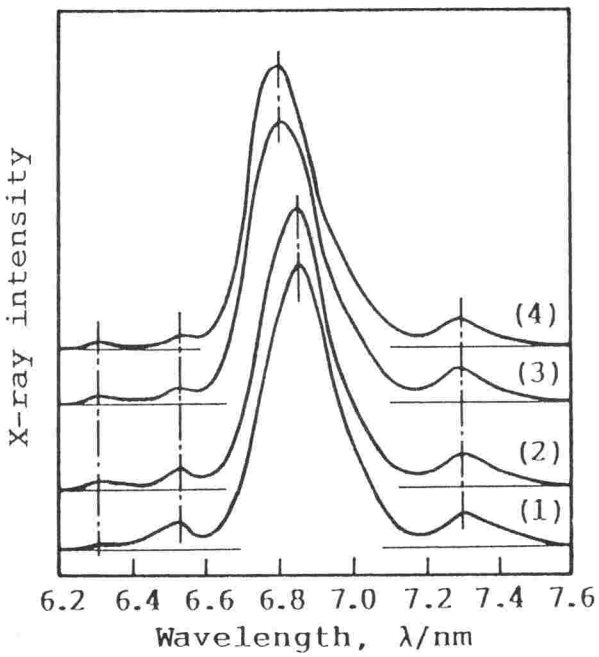

Fig. 4-19. B K x-ray emission spectra of (1) soft BN film (A), (2) soft BN film (B), (3) hard BN film (A) and (4) hard BN film (B), measured by an EPMA before exposure to air.

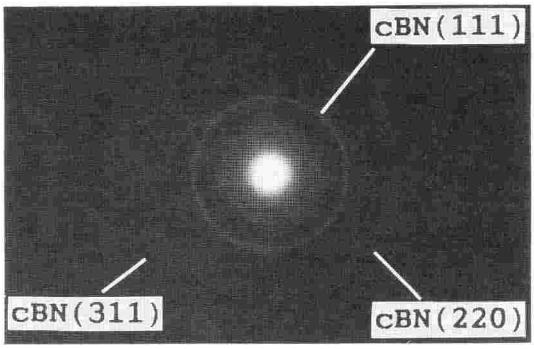

Fig. 4-20. Selected area electron diffraction pattern of hard BN film (A).

Table 4-5. Characteristics of B K x-ray emission spectra of BN powders with different crystalline phases, and as-deposited soft and hard BN films.

Samples	Main peak		
	Position (nm)	FWHM (nm)	Asymmetric index (A.I.)
c-BN powder	6.81	0.21	0.95
w-BN powder	6.80	0.22	1.35
h-BN powder	6.86	0.20	1.12
t-BN powder	6.86	0.20	0.87
r-BN powder	6.86	0.21	0.85
a-BN powder	6.86	0.21	1.20
Soft BN film (A)	6.85	0.22	1.10
Soft BN film (B)	6.85	0.21	0.82
Hard BN film (A)	6.81	0.23	1.29
Hard BN film (B)	6.80	0.22	1.39

with atmospheric moisture due to the dangling bonds. On the other hand, the BN films except the soft BN film (A) were only cracked on exposure to air, and could be observed to form no reaction products with atmospheric moisture. The cracking were brought about after shorter time's exposure to air as the relative humidity was higher. Therefore, the cracking is considered to be induced by atmospheric moisture. It is considered that the reason why the hard BN film (B) cracked after longer time's exposure to air than the hard BN film (A) is that the internal stress in the former film was reduced by annealing after the deposition. However, the soft BN film (B) cracked after shorter time's exposure to air than the hard BN film (A), although the former film was considered to have lower internal stress than the latter film. It has been reported that the cracking of c-BN film deposited by an RF sputtering process was brought about from the a-BN phase in the film on exposure to air [19]. Since the BN films used in this experiment may contain some amounts of a-BN phase, it is likely that the cracking was also brought about due to the a-BN phase in the films. The soft BN film (B), which is either t-BN or r-BN film, may contain some amounts of uncombined boron with nitrogen, whereas the hard BN film (A), which is a c-BN film, does not contain such boron. S.V.Nguyen *et al.* [18] have reported that boron-rich BN film was highly hygroscopic. Therefore, it is likely that the t-BN or r-BN film may be cracked on exposure to air more readily than the c-BN film. And it is assumed that the reason why the c-BN film peels off from the buffer interlayer is that the buffer interlayer is boron-rich.

In summary, the atmospheric degradation of BN film is that the a-BN film reacts with atmospheric moisture into boron compound such as boron oxide, boron acid or ammonium borate, and that BN films except the a-BN film are only cracked on exposure to air. It was found that the a-BN film reacts very readily with atmospheric moisture, and that the c-BN film is hard to be cracked with atmospheric moisture and is stable in air, compared with the other BN films.

References

[1] C.Weissmantel, J. Vac. Sci. Technol., **18**, 179(1981).

[2] C.Weissmantel, J. Vac. Sci. Technol., **A3**, 2384(1985).

[3] S.P.S.Arya and A.D'Amico, Thin Solid Films, **157**, 267(1988).

[4] H.Saitoh and Y.Ichinose, Bull. Jpn. Inst. Met., **27**, 720(1988).

[5] J.J.Pouch and S.A.Alterovitz, *Synthesis and Properties of Boron Nitride* (Trans Tech, Aedermannsdorf, 1990).

[6] Y.Ichinose, H.Saitoh and Y.Hirotsu, Surf. Coat. Technol., **43/44**, 116(1990).

[7] S.S.Dana, Mater. Sci. Forum, **54&55**, 229(1990).

[8] K.Miyoshi, D.H.Buckley and T.Spalvins, J. Vac. Sci. Technol., **A3**, 2340(1985).

[9] K.Miyoshi, D.H.Buckley, J.J.Pouch, S.A.Alterovitz and H.E.Sliney, Surf. Coat. Technol., **33**, 221(1987).

[10] K.Watanabe, K.Saitoh, Y.Yuchi, K.Sekino, K.Inagawa and A.Itoh, Proc. 11th Symp. on ISIAT '87, Tokyo, (1987), p.347.

[11] K.Inagawa, K.Watanabe, K.Saitoh, Y.Yuchi and A.Itoh, Surf. Coat. Technol., **39/40**, 253(1989).

[12] M.Okamoto, H.Yokoyama and Y.Osaka, Jpn. J. Appl. Phys., **29**, 930(1990).

[13] M.Murakawa and S.Watanabe, Surf. Coat. Technol., **43/44**, 145(1990).

[14] K.Miyoshi, Mater. Sci. Forum, **54&55**, 375(1990).

[15] H.Kuwano, Mater. Sci. Forum, **54&55**, 399(1990).

[16] M.Murakawa, S.Watanabe and S.Miyake, Diamond Films Technol., **1**, 55(1991).

[17] W.D.Halverson, T.G.Tetreault and J.K.Hirvonen, Mater. Sci. Forum, **54&55**, 71(1990).

[18] S.V.Nguyen, T.Nguyen, H.Treichel and O.Spindler, J. Electrochem. Soc., **141**, 1633(1994).

[19] M.Mieno and T.Yoshida, Pro. Symp. on Synthesis of Cubic Boron Nitride, Tokyo, (1991), p.1.

[20] M.Sakakibara, J.Satoh and Y.Ichinose, Abstracts Jpn. Inst. Met., Hiroshima, (1991), p.232.

[21] Y.Furunushi, J. Jpn. Soc. Surf. Fin., **41**, 502(1990).

[22] T.Hirao, T.Nitta, M.Mikoda and S.Hayakawa, *Ion Kougaku Gijutsu no Kiso to Oyo* (means basis and applications of ionic technology), (Kogyo-Chosa-Kai, Tokyo, 1992), p.99.

[23] A.Kinbara, S.Baba and A.Kikuchi, J. Adhesion Sci. Technol., **2**, 1(1988).

[24] K.Nakamura, Mater. Sci. Forum, **54&55**, 111(1990).

[25] K.Sugiyama and H.Itoh, Mater. Sci. Forum, **54&55**, 141(1990).

[26] T.Ikeda, Y.Kawate and Y.Hirai, J. Vac. Sci. Technol., **A8**, 3168(1990).

[27] C.A.Davis, Thin Solid Films, **226**, 30(1993).

[28] H.Windischmann, J. Appl. Phys., **62**, 1800(1987).

[29] P.M.Fabis, R.A.Cooke and S.McDonough, J. Vac. Sci. Technol., **A8**, 3809(1990).

[30] H.Windischmann, J. Vac. Sci. Technol., **A9**, 2431(1991).

[31] D.R.McKenzie, D.Muller and B.A.Pailthorpe, Phys. Rev. Lett., **67**, 773(1990).

[32] D.R.McKenzie, W.D.McFall, W.G.Sainty, C.A.Davis and R.E.Collins, Diamond Relat. Mater., **2**, 970(1993).

[33] R.D.Bland, G.J.Kominiak and D.M.Mattox, J. Vac. Sci. Technol., **11**, 671(1974).

[34] B.Rother, H.D.Zscheile, C.Weissmantel, C.Heiser, G.Holzhüter, G.Leonhardt and P.Reich, Thin Solid Films, **142**, 83(1986).

Chapter 5

Analysis of Formation Process and Microstructure of Cubic Boron Nitride Film by Soft X-Ray Spectroscopy

5-1. Introduction

It has been suggested by C.Weissmental *et al.* [1, 2] or D.J.Kester *et al.* [3] that thermal spikes caused or momentum transferred into the BN film by ions impinging on the growing film play a significant role for the formation of c-BN film. Further, D.R.McKenzie *et al.* [4, 5] have suggested that its formation is induced by compressive stress caused by ions bombarding the film. Although the growth mechanism of c-BN film has not been made clear yet, it is considered that the favorable ion bombardment is required for the formation of c-BN film. It has been actually reported that bombarding the growing film with argon ion *etc.* is always necessary to deposit successfully a c-BN film with both PVD and CVD techniques [7 - 16]. In the case of a reactive ion-plating method, it is considered that the important factor in determining an amount of bombardment is a substrate bias voltage. On the other hand, it has been recently reported in some PVD processes that the film composed of a non-cubic BN such as turbostratic or amorphous BN exists in the interface between a c-BN film and a substrate [17 - 22]. It is likely that c-BN film deposited by an ion-plating method has the same non-cubic BN film, and that the non-cubic BN film plays a role as a precursor of c-BN film.

In order to investigate the formation process and the microstructure of c-BN film deposited by the reactive ion-plating method, BN films were deposited on silicon substrates by varying a substrate bias voltage and deposition time. These BN films were characterized using soft x-ray spectroscopy, infrared spectroscopy, selected area electron diffractometry and transmission electron microscopy (TEM). In this work, especially, the characterization of BN film formed at the initial stage of deposition was mainly carried out using B K x-ray emission spectrum, and its spectral feature analysis was performed by the discrete variational Hartree-Fock-Slater (DV-Xα) method [23, 24]. Further, in order to investigate the microstructure of c-BN film, B K x-

ray emission spectra were measured on the c-BN film with synchrotron radiation by varying the take-off angle, since the lower take-off angle measurement is more surface-sensitive.

5-2. Effect of Self-Bias Voltage on Formation of Cubic BN Film

In order to investigate the effect of a self-bias voltage applied to a substrate on the formation of c-BN film, BN films were deposited on silicon substrates by varying the self-bias voltage with keeping other ion-plating factors constant. Further, in order to investigate the formation process of c-BN film, BN films were deposited by varying deposition time. Their crystalline phases were probed by soft x-ray spectroscopy and infrared absorption spectroscopy.

Consequently, there is a minimum value of self-bias voltage applied to the substrate for the formation of c-BN film. In this experimental condition, its value of the voltage is -15 V. The self-bias voltage required for the formation of c-BN film is needed to be applied to the substrate for several minutes after the onset of deposition, not throughout the deposition. The c-BN film does not form on the substrate immediately after the onset of deposition, and there is the dependence upon deposition time for its formation. In other words, the non-cubic BN film forms on the substrate at the initial stage of deposition, and follows with the growth of c-BN film on the non-cubic BN film.

Experimental Procedure

Details of the ion-plating apparatus used and deposition procedures have been described in chapter 2. Deposition chamber was pre-evacuated to the order of 10^{-4} Pa by a oil diffusion pump with a liquid nitrogen trap and rotary pump system. A mirror-polished silicon wafer was used as a substrate, and cleaned for 5 minutes by argon ion sputtering before deposition. Deposition conditions are summarized in Table 5-1.

A self-bias voltage (V_{DC}) was generated by applying radio-frequency (RF) power to the substrate, and controlled by varying RF power. In order to investigate the effect of V_{DC} on the formation of c-BN film, BN films were deposited on the silicon substrates by following proce-

Table 5-1. Experimental conditions for the depositions of BN films by the ion-plating method.

Substrate	Si wafer (50 mm$^{\phi}$)
E.B. power	1.8 (10 kV, 180 mA)
E.B. evaporant	99.9 % boron
Ionization voltage	60 ~ 70 V
Ionization current	14 ~ 15 A
Self-bias voltage	0 ~ -65 V (R.F. 13.56 MHz)
Ar/N_2 gas flow ratio	2.0
Total gas pressure	~ 1 X 10^{-1} Pa

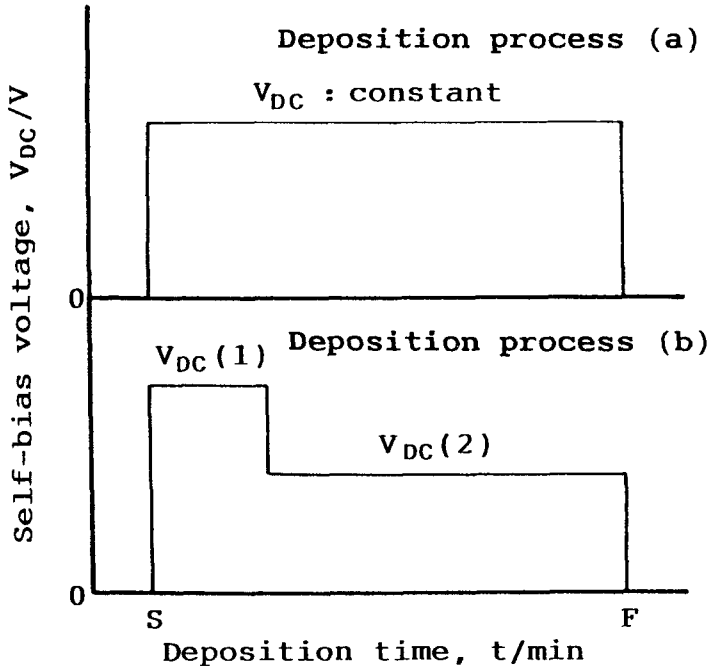

Fig. 5-1. Schematic illustration of how to apply self-bias voltage to a silicon substrate during deposition of BN film. Deposition process (a) : self-bias voltage was kept constant at a given value during deposition, deposition process (b) : self-bias voltage was dropped to V_{DC} (2) after first deposition at V_{DC} (1) for several minutes.

dures (see Fig. 5–1) : (a) V_{DC} was kept constant at a given potential throughout deposition; (b) V_{DC} was dropped to low potential of V_{DC} (2) after first deposition at high potential of V_{DC} (1) for several minutes. The procedures (a) and (b) are, hereafter, referred to as deposition processes (a) and (b), respectively. The deposited BN films were characterized by soft x–ray and infrared absorption spectroscopic analysis. B K x–ray emission spectra were measured on BN films using an EPMA by the procedure described in chapter 3. Infrared (IR) absorption spectra were measured on BN films without being peeled off from the substrates in transmittance mode by a Fourier transform infrared spectrometer.

Results and Discussion

As described in section 3–4, it has been confirmed that a BN film composes predominantly of a c–BN phase if its B K x–ray emission spectrum has the main peak position near 6.81 nm, although the asymmetric index of the main band and the relative intensity of the satellite band near 6.5 nm are close to those of a w–BN phase. The BN film having the main peak position near 6.86 nm composes of an sp^2–bonded BN phase, and the BN film having the main peak position between 6.81 and 6.86 nm composes of the mixture of c–BN and sp^2–bonded BN phases. There are h–, t–, r– and a–BN phases in sp^2–bonded BN phases, so an sp^2–bonded BN phase is hereafter termed "h–BN phase" as a general name for h–, t–, r– and a–BN phases.

Figure 5–2 shows the changes with V_{DC} applied to the substrate in the main peak positions of B K x–ray emission spectra measured on BN films prepared by the deposition processes (a) and (b). By the deposition process (a), the BN films (denoted by (a) in Fig. 5–2) were deposited for 10 minutes at various V_{DC} values of −65 V or less. In the case of the deposition process (b), the BN films (denoted by (b) in Fig. 5–2) were prepared by first depositing for 5 minutes at V_{DC} (1) of −65 V, and by subsequent depositing for 8 minutes at various values of V_{DC} (2) of less than that of V_{DC} (1).

On the BN films prepared by the deposition process (a), the main peak position changes abruptly at V_{DC} of −15 V, and the positions of the BN films deposited at V_{DC} of −15 V or more are almost consistent with that of a c–BN phase. Therefore, the c–BN film can be deposited at

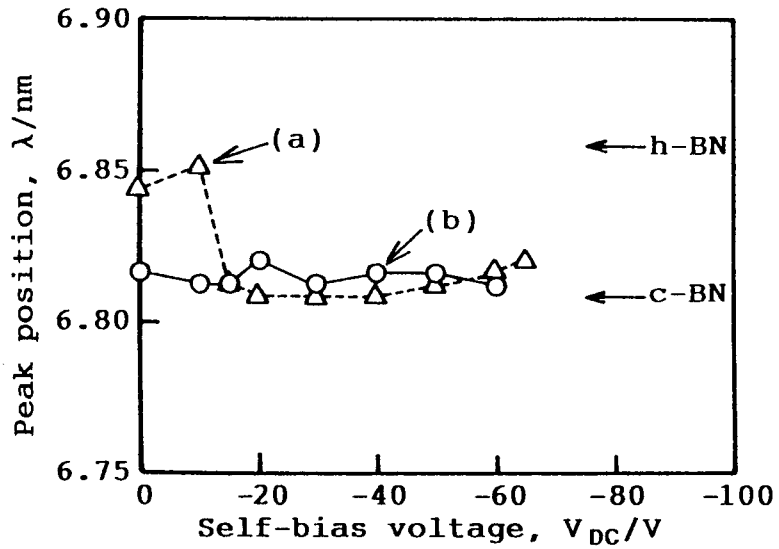

Fig. 5-2. Effects of self-bias voltage (V_{DC}) on the main peak positions of B K x-ray emission spectra measured on the BN films deposited for 10 minutes at constant V_{DC} (a) and deposited for 8 minutes at various V_{DC} (2) dropped after first deposition at V_{DC} (1) of -65 V for 5 minutes (b).

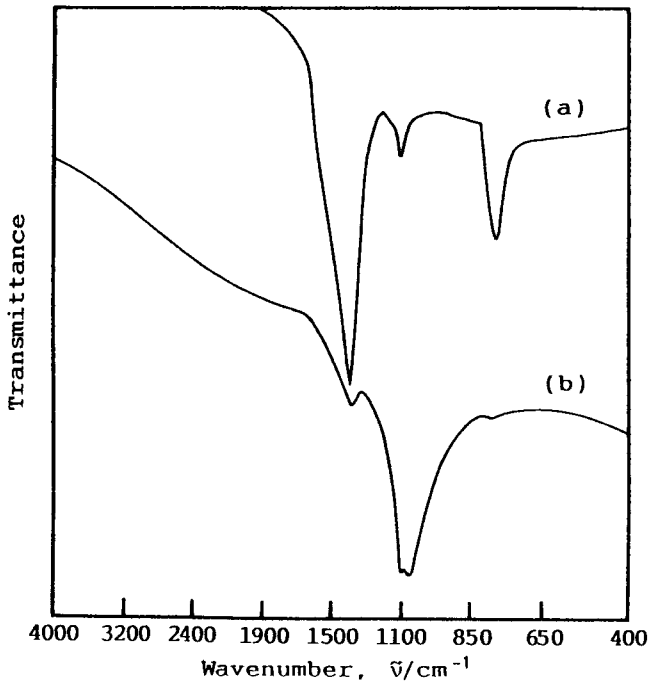

Fig. 5-3. Infrared absorption spectra of the BN films deposited for 10 minutes at V_{DC} of 0 V (a) and deposited for 8 minutes at V_{DC} (2) of 0 V after first deposition at V_{DC} (1) of -65 V for 5 minutes (b).

V_{DC} of −15 V or more in this experimental conditions. C.Weissmental *et al.* [1, 2] or D.J.Kester *et al.* [3] have suggested that thermal spikes caused or momentum transferred into the BN film by ions impinging on the growing film play a significant role for the formation of c−BN film. Further, D.R.McKenzie *et al.* [4, 5] have suggested that its formation is induced by compressive stress caused by ions bombarding the film. In any event, it is considered for the formation of c−BN film that the favorable ion bombardment is required and that there would be a minimum amount of ion bombardment. In this experiment, it is assumed that a minimum amount of ion bombardment required for its formation is attained when nitrogen and argon ions generated in a plasma are accelerated toward the substrate with V_{DC} of −15 V.

On the other hand, with respect to BN films prepared by the deposition process (b), there are almost no changes in the main peak positions with the values of V_{DC} (2), and their positions are almost consistent with that of a c−BN phase. That is, after depositing for 5 minutes at V_{DC} (1) of −65 V, the c−BN film can grow independently of the value of V_{DC} (2) and even at V_{DC} (2) of 0 V. Figure 5−3 (b) shows the example of IR absorption spectrum measured on the BN film deposited for 5 minutes at V_{DC} (1) of −65 V and subsequently for 8 minutes at V_{DC} (2) of 0 V, compared with IR absorption spectrum (denoted by (a) in Fig. 5−3) of the BN film for 10 minutes at V_{DC} of 0 V by the deposition process (a). It is confirmed from these IR absorption spectra that the former film has a strong IR absorption peak near 1100 cm^{-1} corresponding to that of a c−BN phase and composes predominantly of a c−BN phase, whereas the latter film has strong IR absorption peaks near 1390 and 800 cm^{-1} corresponding to those of an h−BN phase and is predominantly an h−BN phase. Consequently, it is assumed that although favorable ion bombardment is required for the formation of c−BN film, such ion bombardment is not always required for its growth after it has formed.

In order to investigate the effect of V_{DC} (1) on the formation of c−BN film, BN films were prepared by first depositing for 5 minutes at various V_{DC} (1) values of −65 V or less and by subsequent depositing for 8 minutes at V_{DC} (2) of −10 V. The results are shown in Fig. 5−4. Furthermore, in order to investigate the effect of the deposition time at V_{DC} (1) on the formation of c−BN film, BN films were prepared by first depositing at V_{DC} (1) of −65 V for 3 minutes and

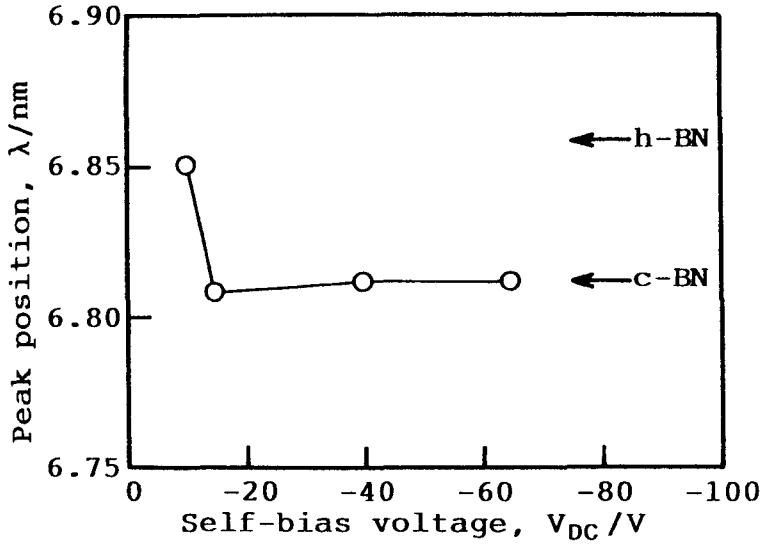

Fig. 5-4. Change in the main peak positions of B K x-ray emission spectra measured on the BN films deposited for 8 minutes at V_{DC} (2) of -10 V after first deposition at various V_{DC} (1) for 5 minutes.

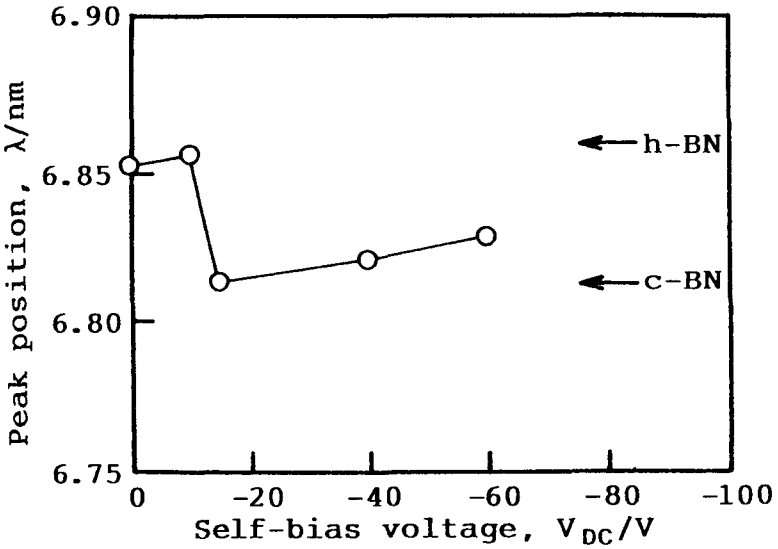

Fig. 5-5. Effect of V_{DC} on the main peak positions of B K x-ray emission spectra measured on the BN films deposited for 8 minutes at various V_{DC} (2) dropped after first deposition at V_{DC} (1) of -65 V for 3 minutes.

by subsequent depositing at various V_{DC} (2) values for 8 minutes. The results are shown in Fig. 5–5. It is seen in Fig.5–4 that V_{DC} (1) of –15 V or more is required for the formation of c–BN film. This result is similar to that of the deposition process (1), and shows that it is necessary to apply V_{DC} of –15 V or more to the substrate in order to form the c–BN film. On the other hand, it is seen in Fig. 5–5 that BN films deposited for 3 minutes at V_{DC} (1) of –65 V change in their crystalline phases with the difference in the value of V_{DC} (2). This result differs from that obtained from the BN films deposited for 5 minutes at V_{DC} (1) of –65 V. Therefore, it is assumed that the deposition time of 3 minutes at V_{DC} (1) of –65 V is too short to form the c–BN film, and that there is the dependence upon the deposition time for its formation.

Thus, BN films were deposited at V_{DC} of –65 V by varying the deposition time. The results are shown in Fig. 5–6. It is seen in Fig. 5–6 that the BN films deposited for 7 minutes or less are predominantly an h–BN phase, and that the crystalline phases of BN films are transformed to a c–BN phase by depositing for 8 minutes or more. Figure 5–7 shows the examples of IR absorption spectra measured on the BN films deposited at V_{DC} of –65 V for 3, 5 and 8 minutes. It is also confirmed from these spectra that BN films formed at the initial stage of deposition compose of the mixture of c–BN and h–BN phases, and that the c–BN film is at last formed by depositing for 8 minutes. Therefore, it is considered that the BN film composed predominantly of an h–BN phase forms on the substrate at the initial stage of deposition and follows with the growth of c–BN film on the h–BN film. The same formation process of c–BN film has been observed by K.Inagawa *et al.* [25] and T.Ikeda *et al.* [12], with respect to the c–BN films deposited by the hollow cathode plasma discharge and arc–like plasma discharge ion–plating methods. Further, it has been recently reported that the film composed of a non–cubic BN such as t– or a–BN is actually present in the interface between the substrate and c–BN film [19 – 21].

As mentioned earlier, after depositing for 5 minutes at V_{DC} (1) of –65 V, the c–BN film can grow independently of the value of V_{DC} (2), whereas the crystalline phase of BN film depends on the value of V_{DC} (2) after depositing for 3 minutes at V_{DC} (1) of –65 V. This difference is attributable to the formation process of c–BN film described above. In other words, it is assumed that the surface of BN film is at last covered with a c–BN phase after depositing for 5 minutes at

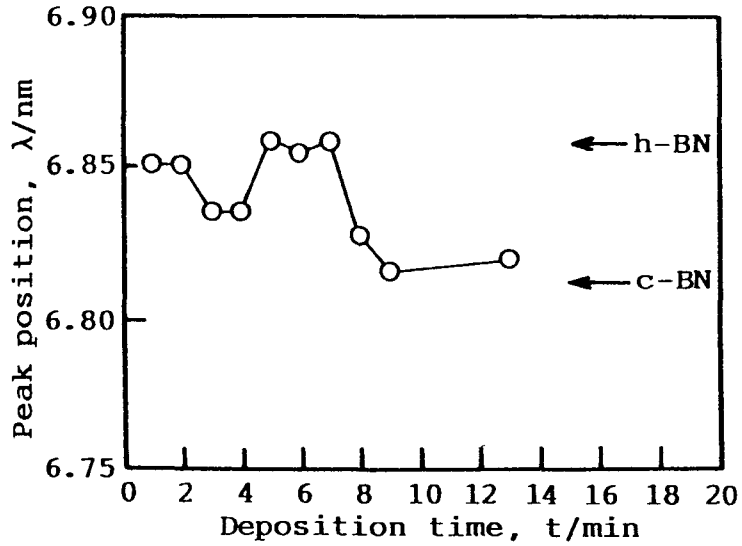

Fig. 5-6. Change with deposition time in the main peak positions of B K x-ray emission spectra measured on the BN films deposited at V_{DC} of -65 V.

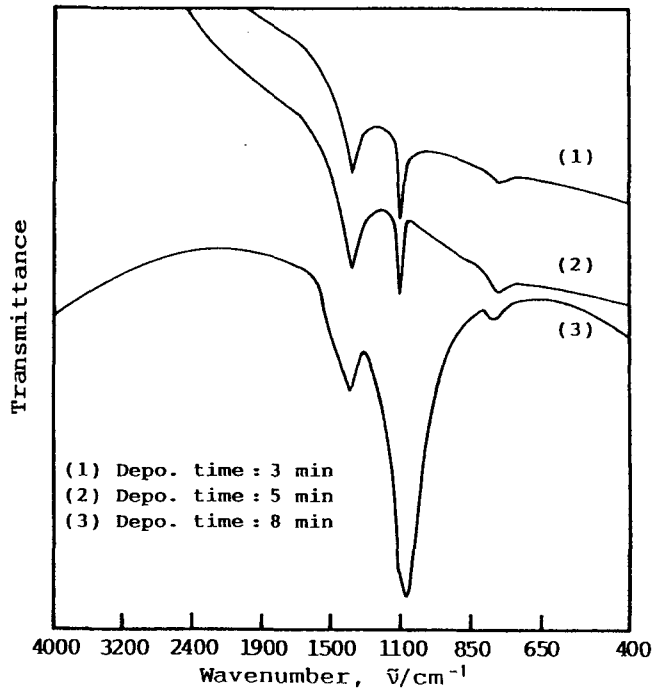

Fig. 5-7. Infrared absorption spectra of the BN films deposited at V_{DC} of -65 V for several minutes.

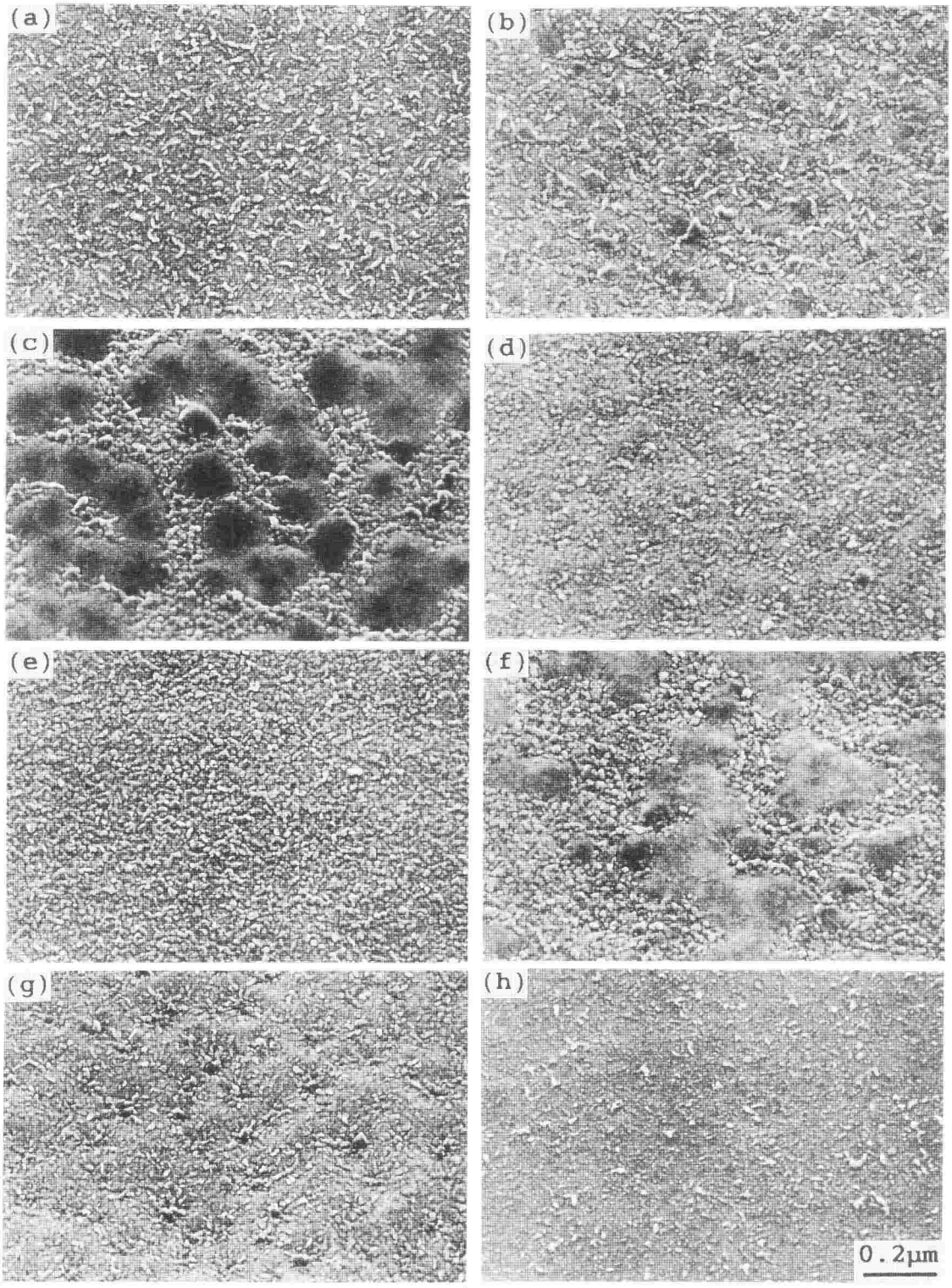

Fig. 5-8. SEM images of surfaces of the BN films deposited for various deposition times of 1 min (a), 2min (b), 3 min (c), 4 min (d), 5 min (e), 6 min (f), 7 min (g) and 8 min (h).

V_{DC} of −65 V, and hereafter, the c−BN film can grow independently of the value of V_{DC}. In order to confirm this assumption, high−resolution SEM observations were performed for the surfaces of BN films deposited for 1 ~ 8 minutes at V_{DC} of −65 V. Their SEM micrographs are shown in Fig. 5−8. The surface morphology of BN film was changed with the difference in deposition time. However, it was unknown whether the surface of BN film has been covered with a c−BN phase by 5 minutes' deposition.

In summary, there is a minimum value of self−bias voltage applied to the substrate for the formation of c−BN film. In this experimental condition, its value of the voltage is −15 V. The self−bias voltage required for the formation of c−BN film is needed to be applied to the substrate for several minutes after the onset of deposition, not throughout the deposition. The c−BN film does not form on the substrate immediately after the onset of deposition, and there is the dependence upon deposition time for its formation. In other words, the non−cubic BN film forms on the substrate at the initial stage of deposition, and follows with the growth of c−BN film on the non−cubic BN film. And it is assumed that the c−BN film can grow independently of the self−bias voltage after it has covered the film surface.

5−3. Soft X−Ray Spectroscopic Analysis of Cubic BN Thin Film Microstructure

In the case of the c−BN thin film deposited on a silicon substrate by the reactive ion−plating method, it was assumed that the non−cubic BN film formed on the substrate at the initial stage of deposition before the c−BN film began to grow, that is, the c−BN film had a depth−dependent structure. In order to confirm this assumption, B K x−ray emission spectra of the c−BN film were measured with synchrotron radiation by varying the take−off angle, since the lower take−off angle measurement is more surface−sensitive. Consequently, the crystalline phase distribution of the BN thin film with sub−micron thickness could be analyzed by fluorescent x−ray spectrometry, and it was confirmed that the c−BN film had the depth−dependent structure, that is, the non−cubic BN film with about 30 nm thickness was present in the lower region of the film and the c−BN film of about 80 nm thickness in the upper region, and that the c−BN film began to

grow after deposition for about 2 minutes.

Experimental Procedure

Details of deposition procedures have been described previously in section 5-2. BN films were deposited on silicon substrates at a self-bias voltage of -65 V by varying deposition time from 1 to 13 minutes. In order to obtain the deposition rate of BN film, the film thickness was measured using the cross-sectional SEM micrograph of the BN film deposited for 13 minutes, and divided by its deposition time. The deposition rate was about 16 nm/min.

B K x-ray emission spectra of the BN film deposited for 7 minutes were measured with synchrotron radiation by varying the incidence and exit angles, using a monochromatic undulator beam at the National Laboratory for High Energy Physics. The excitation x-ray source was used from the undulator beam lines BL2B, BL16u and BL19B installed at PF ring. In these beam lines, photon flux at the sample was $10^{11} \sim 10^{12}$ photons per second. A high resolution soft x-ray emission spectrometer was designed using the Rowland circle geometry in which an input slit, spherical grating, and multichannel detector lay on the focal circle. The Rowland circle radii of the blazed holographic grating was 7 m and its line density was 1200 lines/mm. The angle of incidence was 2.87 degrees from the grating surface. The resolution obtained by the 100 μm input-slit width was 0.2 eV for the photon energy about 180 eV.

In addition to these SR measurements, laboratory spectra were measured at a voltage of 15 kV and at a sample current of 0.2 μA by an EPMA, using a multilayer pseudo-crystal of lead stearate as an analyzing element. The specimens for EPMA measurements were coated with carbon. The x-ray take-off angle was 52.5 degrees.

Results and Discussion

BN forms both cubic and non-cubic phases [26]. There are c- and w-BN in cubic phases, and h-, t- r- and a-BN in non-cubic phases. The B K x-ray emission spectra of cubic and non-cubic BN phases differ in the main peak position, and also from that of metallic boron (M.B). The main peak positions of M.B, c-BN and h-BN are 6.76, 6.81 and 6.86 nm in wave-

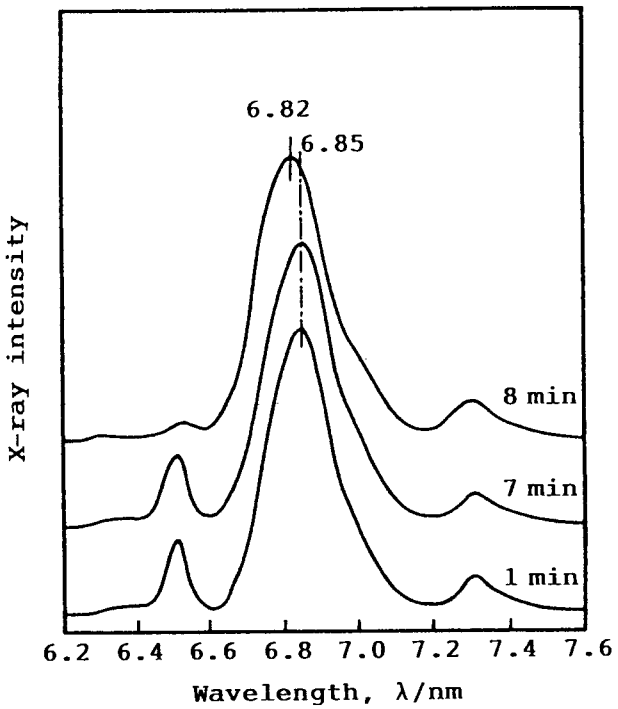

Fig. 5-9. B K x-ray emission spectra of the BN films deposited on silicon substrates for 1, 7 and 8 minutes, measured by an EPMA at a take-off angle of 52.5 degrees.

length, respectively.

Figure 5-9 shows B K x-ray emission spectra measured by an EPMA, obtained from the BN films deposited for 1, 7 and 8 minutes by the ion-plating method. The main peak position changes apparently after deposition time of 8 minutes. The main peak positions of the BN films deposited for 7 minutes or less are consistent nearly with that of a non-cubic BN phase, and that of the BN films deposited for 8 minutes or more are consistent nearly with that of a cubic BN phase. Therefore, it is assumed that the non-cubic BN film forms on the substrate at the initial stage of deposition, and the growth of c-BN film follows. In other words, the ion-plated c-BN thin film is considered to have the depth-dependent structure.

To confirm this matter, B K x-ray emission spectra were measured with synchrotron radiation by varying the take-off angle, namely, by varying x-ray detection depth, using the BN film deposited for 7 minutes of which the crystalline phase was seemed from its B K x-ray emission spectrum to be a non-cubic phase. The results are shown in Fig. 5-10. When the take-off

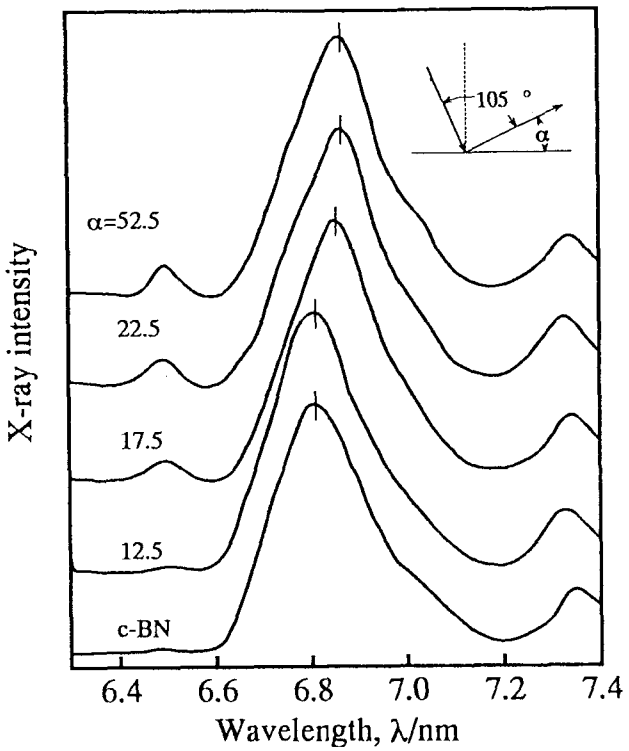

Fig. 5-10. B K x-ray emission spectra of the BN film deposited on a silicon substrate for 7 minutes and c-BN powder synthesized at high temperature and pressure. Upper four spectra were measured on the BN film with synchrotron radiation by varying the take-off angle (α), and the lowest spectrum on c-BN powder at a take-off angle of 52.5 degrees.

Table 5-2. Take-off angle *v.s.* x-ray detection depth.

Take-off angle	Detection depth
52.5°	300 nm
22.5°	150 nm
17.5°	120 nm
12.5°	83 nm

angle α is large, the main peak position is consistent with that of a non-cubic BN phase, and shifts to that of a cubic BN phase with lowering the take-off angle. When the take-off angle is 12.5 degrees or less, the main peak position is consistent exactly with that of c-BN synthesized at high temperature and high pressure. Thus, it was confirmed that the c-BN film formed in the upper region of the film, and the non-cubic BN film in the lower region. The fact tells us that the c-BN film formed already at deposition time prior to 8 minutes.

Table 5-2 shows the relationship between the take-off angle and x-ray detection depth. X-ray detection depth is estimated to be about 83 nm at a take-off angle of 12.5 degrees, and the thickness of the BN film deposited for 7 minutes is estimated from the deposition rate of 16 nm/min to be about 110 nm. Therefore, it is considered that the BN film has the microstructure shown in Fig. 5-11, that is, the non-cubic BN film with about 30 nm thickness forms on a silicon substrate, and subsequently the c-BN film with about 80 nm thickness forms on that film, and that the c-BN film begins to grow after deposition for about 2 minutes.

D.L.Medlin *et al.* [21] have demonstrated from a cross-sectional high-resolution TEM observation that the c-BN film formed after a-BN and t-BN films formed, using an ion-assisted pulsed laser deposition process. The c-BN film deposited by the ion-plating method is considered to grow with the same process as their demonstration. As mentioned earlier in section 2-3, it is considered that the reason why the BN film composed only of a c-BN phase cannot be deposited by the reactive ion-plating method is due to the formation process of c-BN film

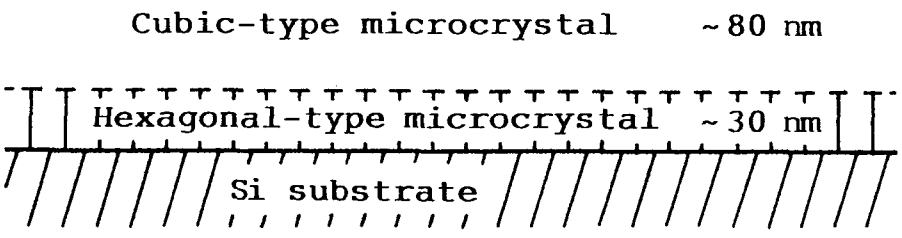

Fig. 5-11. Schematic diagram of the microstructure of c-BN film assumed from the results of the measurements of the B K x-ray emission spectra with synchrotron radiation by varying the take-off angle.

as mentioned above.

The BN film deposited for 1 minutes is considered to be the pure non-cubic BN film. As shown in Fig. 5-9, its B K x-ray emission spectrum has the very strong satellite band at the short wavelength side (near 6.5 nm). The relative intensity is stronger than those of any other non-cubic BN phases. This is considered to be attributable to the BN crystallite size. The detailed discussion will be described in section 5-4.

On the B K x-ray emission spectra of the BN film deposited for 7 minutes, shown in Fig. 5-10, the intensity of the satellite band near 6.5 nm is very strong when the take-off angle is large, and decreases with lowering the take-off angle. And when the take-off angle is less than 12.5 degrees, its intensity is consistent exactly with that of c-BN synthesized at high temperature and high pressure. On the other hand, B K x-ray emission spectrum of the BN film deposited for 8 minutes, measured by an EPMA of which the take-off angle is 52.5 degrees, has the stronger satellite band near 6.5 nm than that of c-BN synthesized at high temperature and high pressure. It is considered that the reason why its intensity becomes stronger in the case of a large take-off angle measurement is due to the contribution of the non-cubic BN phase in the lower region of the film to the spectrum. Further, as mentioned earlier in section 3-4, the B K x-ray emission spectrum of the BN film with 75 % c-BN phase content, which were measured at a take-off angle of 52.5 degrees by an EPMA, has the stronger satellite band than the spectrum synthesized using equation (3-1) from those of a-BN and c-BN. This is also considered to be due to the same reason.

In summary, using the ion-plating method, BN films were deposited on silicon substrates at the condition of c-BN film formation by varying deposition time, and were characterized by soft x-ray spectroscopic analysis. It was found that the non-cubic BN film with about 30 nm thickness was present in the lower region of the film and the c-BN film with about 80 nm thickness in the upper region, and that the ion-plated c-BN film had the same depth-dependent structure as the c-BN film deposited by an ion-assisted pulsed laser deposition process. It is worthy to mention that the crystalline phase distribution of the BN thin film with sub-micron thickness can be analyzed by x-ray spectrometry in addition to ordinary state analysis.

5-4. Soft X-Ray Spectroscopic Analysis of BN Film Formed at Initial Stage of Deposition

In the case of c-BN film deposited on a silicon substrate by the reactive ion-plating method, it was shown in sections 5-2 and 5-3 that the BN film with sp^2-bonding formed initially on the substrate and subsequently the c-BN film formed. In the B K x-ray emission spectrum obtained from the BN film with sp^2-bonding, the intensity of the satellite band near 6.5 nm was extremely stronger than that of sp^2-bonded BN like h-, t-, r- and a-BN. In order to elucidate this origin, B K x-ray emission spectra were calculated by the discrete variational Hartree-Fock-Slater (DV-Xα) method, assuming a cluster model of sp^2-bonded BN film. Consequently, it was found that this satellite band was brought about by the transition from the *2p* σ* to the *1s* orbitals after the excitation of an electron to the *2p* σ* from the inner occupied orbitals with electron-beam irradiation, and that its intensity of the 2-coordinated boron with a dangling bond on a crystalline surface became stronger than that of the 3-coordinated boron inside crystallite, and it was expected that its intensity should become stronger as the BN crystallite became smaller. As was expected, it was confirmed that its intensity became stronger as h-BN crystallites were become smaller by mechanical grinding. Therefore, the initially deposited BN film with sp^2-bonding was considered to compose of very fine BN crystallite having 2-coordinated borons with dangling bonds, and to play a role as the precursor of c-BN film. However, it is cannot be explained only from the crystallite size why the sp^2-bonded BN film exhibits the extremely strong satellite band near 6.5 nm. It is, therefore, assumed as another factor in the microstructure of film that its basal plane is preferentially oriented perpendicular to the substrate surface.

Experimental Procedure

Details of the ion-plating system and deposition procedures have been described previously in section 5-2. BN films were deposited on silicon substrates at a negative self-bias voltage of 65 V by varying deposition time from 1 to 13 minutes. Figure 5-6 in section 5-2 has shown the change with deposition time in the main peak positions of B K x-ray spectra obtained from these BN films, measured by an EPMA.

Infrared absorption spectra were measured on the BN films without being peeled off from the substrates in transmittance mode by Fourier transform infrared spectroscopy. TEM specimens were dimpled from the back side of the substrate by argon ion thinning. A TEM observation and selected area electron diffraction (SAED) were performed at regions of free-standing film suspended over hole in the substrate, using conventional TEM operated at 200 kV. On all BN films, B K x-ray emission spectra were measured at a voltage of 15 kV and at a sample current of 0.2 μA by an EPMA, using a multilayer pseudo-crystal of lead stearate as an analyzing element. The specimens for EPMA measurements were coated with carbon. Assuming a cluster model of BN film, B K x-ray emission spectra were calculated by the DV-Xα method, and were compared with the spectra of BN films measured by an EPMA.

Results and Discussion

As described in section 5-2, It is judged from Fig. 5-6 that the BN films deposited for 7 minutes or less have mainly sp^2-bonding, and that the BN films deposited for 8 minutes or more have dominantly sp^3-bonding. Figure 5-12 shows the examples of infrared absorption spectra of the BN films. Three absorption peaks are observed in the infrared spectra, *i.e.*, the peak at 1087 cm^{-1} (reststrahlen band) which originates from sp^3-bonded BN [27], and peaks at 1390 (B-N-B stretching) and at 781 cm^{-1} (B-N-B bending) absorbed by sp^2-bonded BN [27]. It is also found from Fig. 5-12 that the BN film deposited for 8 minutes composes mainly of sp^3-bonded BN, and that the BN films deposited for 7 minutes or less compose of a mixture of sp^2- and sp^3-bonded BNs. Figure 5-13 shows SAED pattern and dark field image using the (111) reflection of c-BN shown in Fig. 5-13, obtained from the BN film deposited for 8 minutes. Four diffraction rings are observed in the SAED pattern. These d-spacings were calculated to be 0.328, 0.207, 0.127 and 0.109 nm, respectively. The latter three rings were indexed as the (111), (220) and (311) reflections of c-BN with d-spacings of 0.2087, 0.1278 and 0.1090 nm,respectively [28]. The first ring is more diffuse than the latter three rings, and its d-spacing is close to that of the (0002) plane of h-BN (having d=0.332813 nm) [29]. The size of c-BN crystallites in the films was measured using the dark field image to be about 30 nm, and their

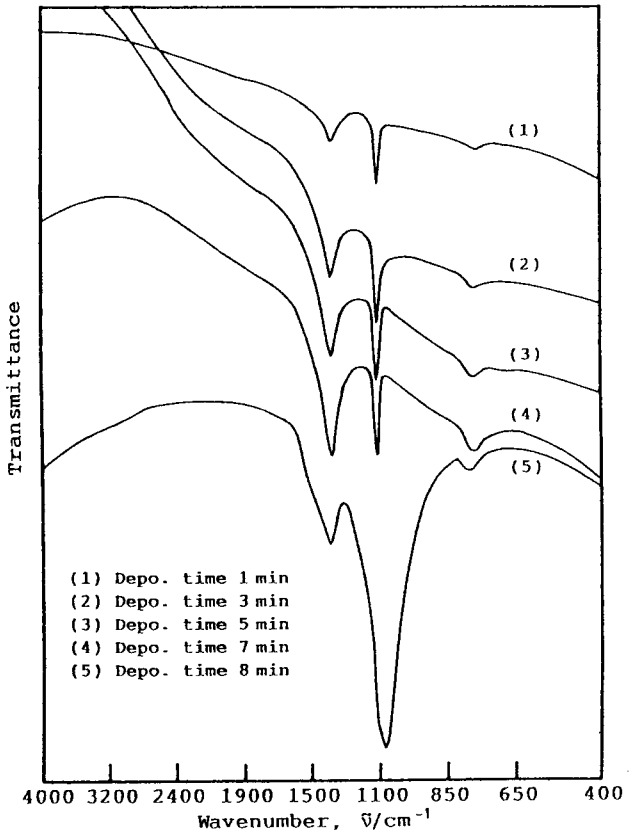

Fig. 5-12. Infrared absorption spectra of the BN films deposited on silicon substrates for various deposition times of 1 min (1), 3 min (2), 5 min (3), 7 min (4) and 8 min (5).

orientation was random. The BN film deposited for 8 minutes is also considered from SAED pattern to be a c-BN film. On the other hand, the sharp diffraction rings were not observed from the BN films deposited for 7 minutes or less, and the observable diffraction rings were two diffuse diffraction rings and one weak diffraction ring. Figure 5-14 shows the SAED pattern and bright field image from the BN film deposited for 1 minute. The *d*-spacings of two diffuse diffraction rings were calculated to be about 0.315 and 0.141 nm, and that of weak diffraction ring to be about 0.212 nm. The latter *d*-spacing is not so much in agreement with that of the (111) plane of c-BN. It is, however, presumed that the weak diffraction ring is indexable as the (111) reflection of c-BN, because infrared absorption spectrum (1), shown in Fig. 5-12, of the BN film deposited for 1 minute has an infrared absorption peak corresponding to that of sp^3-bonded BN, *i.e.*, c-BN. The diffuse diffraction rings are considered to be reflection from an

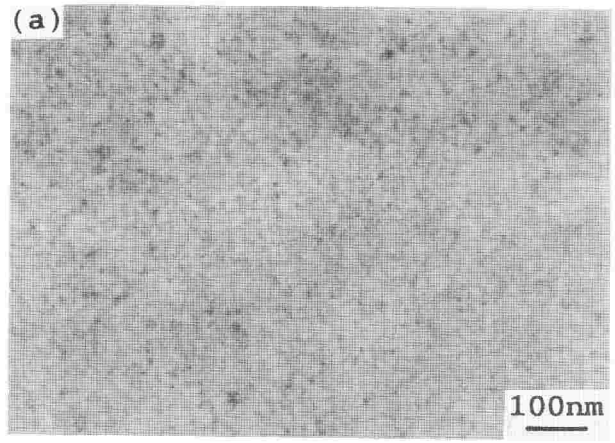

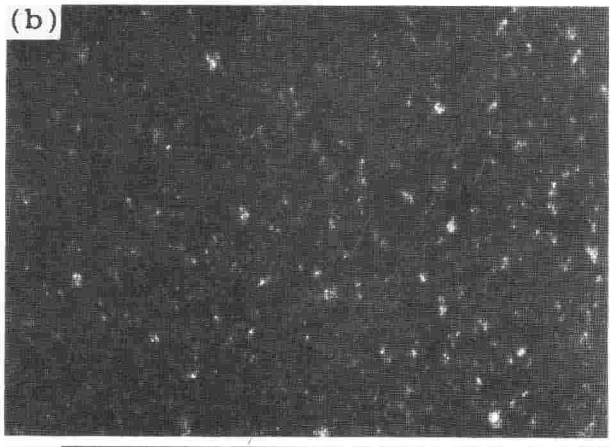

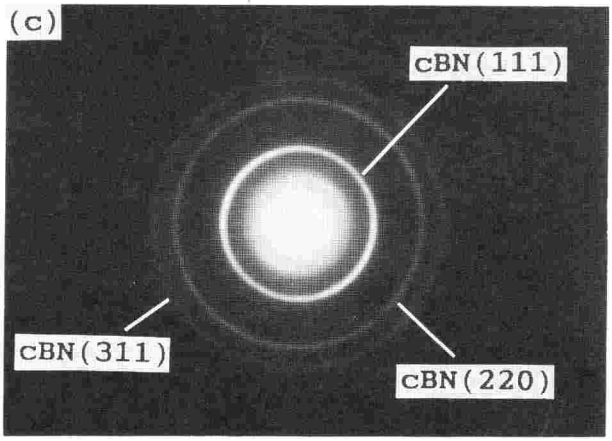

Fig. 5-13. Bright field image (a), dark field image (b) formed with a segment of the ring indexed as the (111) reflection of c-BN, and selected area electron diffraction pattern (c), taken from the BN film deposited on a silicon substrate for 8 minutes.

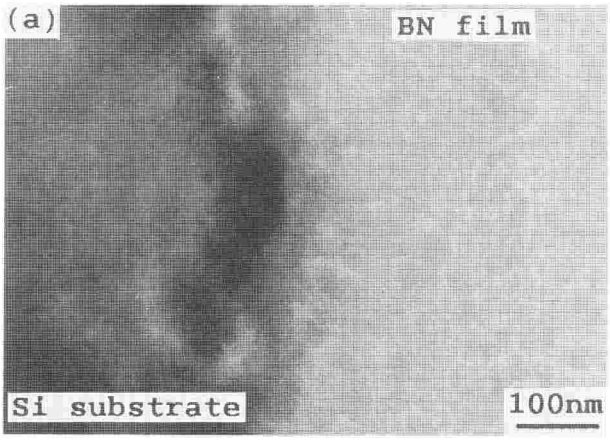

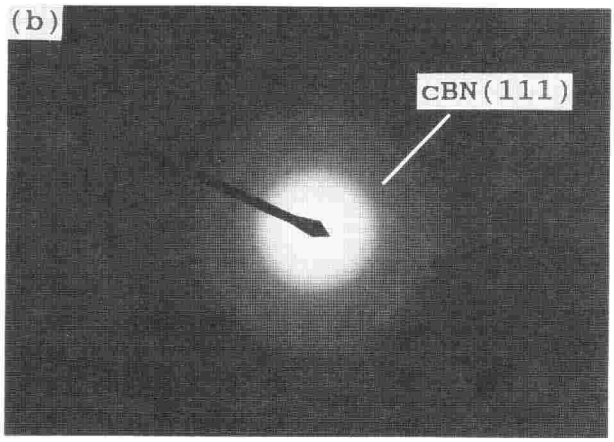

Fig. 5-14. Bright field image (a) and selected area electron diffraction pattern (b) taken from the BN film deposited on a silicon substrate for 1 minute.

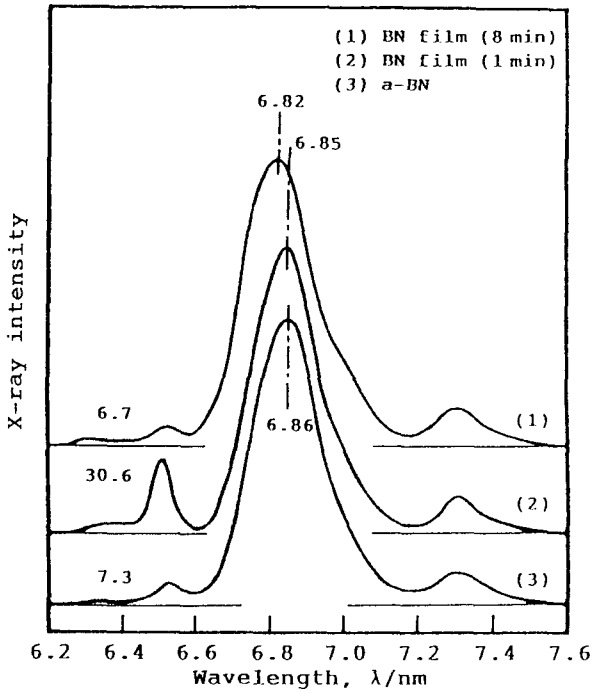

Fig. 5-15. B K x-ray emission spectra measured by an EPMA on the BN films deposited on silicon substrates for 8 min (1) and 1 min (2), and a-BN powder (3).

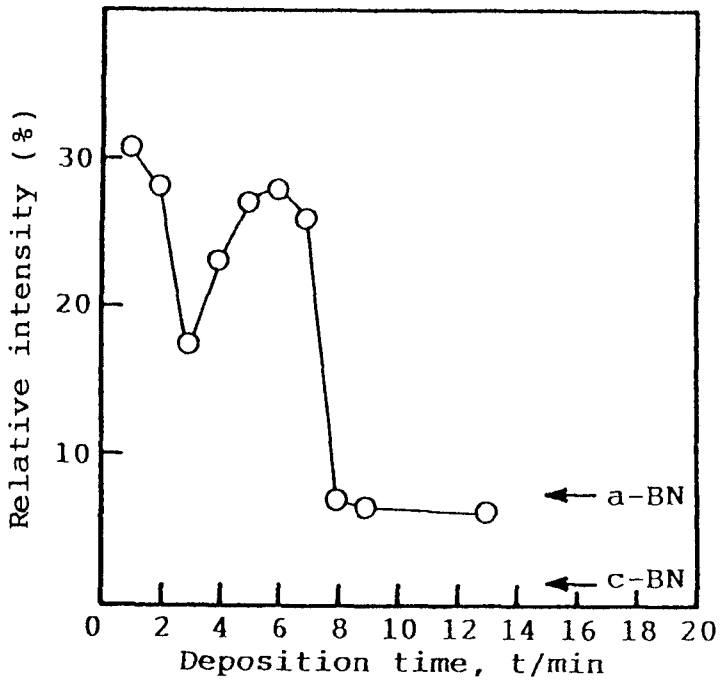

Fig. 5-16. Change in the intensity of the satellite band near 6.5 nm in B K x-ray emission spectra measured by an EPMA on BN films deposited on silicon substrates for several times, as a function of deposition time.

sp^2–bonded BN phase which is seemed to be very fine crystalline or amorphous BN. It has been suggested from a high–resolution TEM observation by D. J. Kester *et al.* [20] that a–BN and h–BN formed on a substrate at the initial stage of deposition, and by D. L. Medlin *et al.* [21] that a–BN and t–BN formed. In this experiment, it was clearly unknown from SAED pattern whether this sp^2–bonded BN film was classified into any BN phases of h–BN, t–BN, r–BN and a–BN. It is possible for this sp^2–bonded BN film to play a role as the precursor of c–BN film, because this film forms before the growth of c–BN film.

Figure 5–15 shows B K x–ray emission spectra from a–BN and the BN films deposited for 1 and 8 minutes. In the case of the BN film deposited for 1 minute, the intensity of the satellite band at the short wavelength side (near 6.5 nm) is extremely stronger than those of a–BN and the BN film deposited for 8 minutes. Figure 5–16 shows the change in the intensity of the satellite band of the BN films, as a function of deposition time. The intensity fluctuates until deposition time of 7 minutes, and decreases abruptly between deposition times of 7 and 8 minutes, and then is consistent nearly with that of a–BN at deposition time of 8 minutes or more. The relative intensity of the satellite band of the BN films deposited for 8 minutes or more is stronger than that of c–BN. As described in section 5–3, the c–BN film has a depth–dependent structure, that is to say, a c–BN phase exists in the upper region of the film and an sp^2–bonded BN phase in the lower region. This is, therefore, considered to be due to the contribution of the lower region of the film to the spectrum, because the x–ray take–off angle of the EPMA used is as large as 52.5 degrees.

In order to elucidate the reason why the BN films deposited for 7 minutes or less exhibit the extremely strong satellite band near 6.5 nm, the density of states (DOS) of boron *2p* orbital in BN was calculated by the DV–Xα method, using the cluster model of BN shown in Fig. 5–17, because B K x–ray is emitted by the transition of an electron from *2p* to *1s* orbitals. In Fig. 5–17, a boron atom (a) on a crystalline surface has 2–coordinated bonding to neighboring nitrogen atoms and a dangling bond, while a boron atom (b) inside crystallite has 3–coordinated bonding to neighboring nitrogen atoms. Figure 5–18 shows the calculated DOS of the π, σ and σ* components in boron *2p* orbitals of BN. The abscissa of Fig. 5–18 is represented by wave–

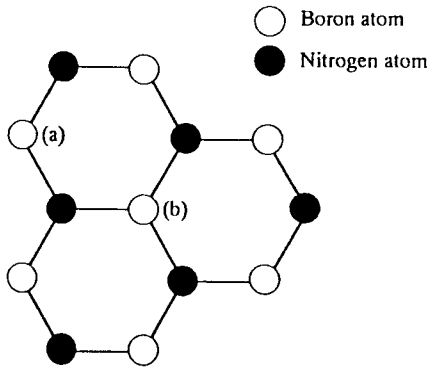

Fig. 5-17. Schematic diagram of the h-BN cluster model used for calculation of the density of states (DOS) of boron *2p* orbital with the discrete variational Hartree-Fock-Slater (DV-Xα) method. A boron atom (a) on a crystalline surface has 2-coordinated bonding to neighboring nitrogen atoms and a dangling bond, and a boron atom (b) inside crystallite has 3-coordinated bonding to neighboring nitrogen atoms.

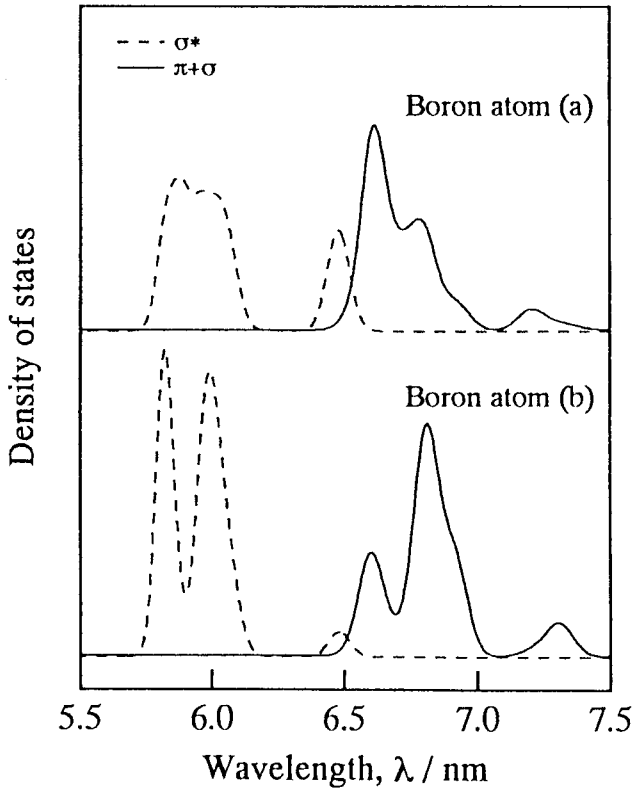

Fig. 5-18. The density of states (DOS) of π, σ and σ* components in boron *2p* orbital of h-BN, calculated for boron atoms (a) and (b) shown in Fig. 5-17 by the discrete variational Hartree-Fock-Slater (DV-Xα) method.

length, not by energy, in order to compare easily the DOS of boron *2p* orbitals with the measured B K x-ray emission spectra. The DOS of both π and σ components corresponds to the main band and the satellite band at the long wavelength side (near 7.3 nm) of B K x-ray emission spectrum. The DOS of π^* component exists in near 6.5 to 6.2 nm (not shown in Fig. 5-18), and corresponds to the weak satellite band near 6.3 nm (see Table 3-3 shown in section 3-3). The DOS of σ^* component corresponds to the satellite band near 6.5 nm. As the *2p* σ^* is empty orbital, this satellite band is considered to be brought about by the transition from the *2p* σ^* to the *1s* orbitals after the excitation of an electron to the *2p* σ^* from the inner occupied orbitals with electron-beam irradiation. Its part of the DOS of a boron atom (a) is considerably higher than that of a boron atom (b). Therefore, it is expected that if BN crystallite has many 2-coordinated boron atoms like a boron atom (a) on a crystalline surface, the intensity of this satellite band will become stronger. In other words, the intensity of this satellite band should become stronger as BN crystallites become smaller, because the number of boron atoms on a crystalline surface increases as BN crystallites become smaller. As shown in Fig. 5-19, it was actually confirmed that the intensity of this satellite band increased as h-BN crystallites were become smaller by mechanical grinding. The maximum intensity of the satellite band from ground h-BN crystals was 8.4 in percentage to the main peak intensity when the mean size of h-BN crystallite was about 1.1 nm (see Fig. 5-20). The intensities of the satellite band of c-BN, w-BN, h-BN, r-BN, t-BN and a-BN are 1.4, 5.2, 2.9, 4.8, 5.4 and 7.3 in percentage to the main peak intensity, respectively. The intensity of the satellite band of the BN film deposited for 1 minute is 30.6 in percentage to the main peak intensity, and extremely stronger than the maximum value of ground h-BN crystals. In addition, the intensities of the satellite band of all BN films deposited for 7 minutes or less are very stronger than those of any BNs. Therefore, the sp^2-bonded BN film formed at the initial stage of deposition is considered to compose of much finer BN crystallites having 2-coordinated borons than that shown in Fig. 5-20. However, by extrapolating the curve shown in Fig. 5-19 to the minimum crystallite size of about 0.3 nm composed of the only six-membered ring, the maximum relative intensity of this satellite band is estimated to be about 11.0 in percentage to the main peak intensity. Consequently, it is cannot

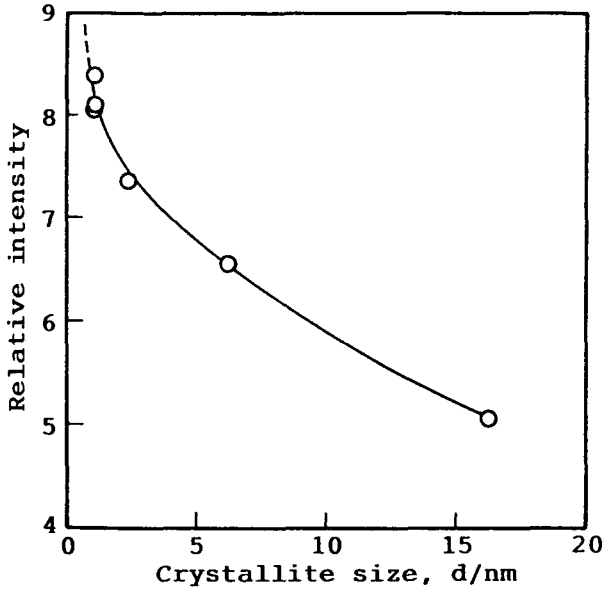

Fig. 5-19. Relation between the intensity of the satellite band near 6.5 nm in B K x-ray emission spectrum and the mean crystallite size of mechanically ground h-BN.

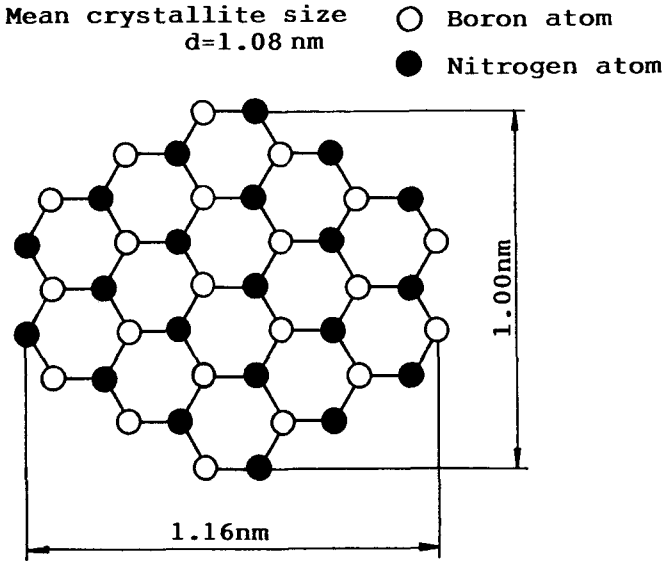

Fig. 5-20. Schematic diagram of mechanically ground h-BN crystallite with the minimum size.

be explained only from the crystallite size why the sp^2–bonded BN film exhibits the extremely strong satellite band. A.Mansour *et al.* [30] have reported that this satellite band became stronger with the parallel excitation to the basal plane of h–BN than with the perpendicular excitation. Thus, it is assumed that the basal plane of sp^2–bonded BN film is preferentially oriented perpendicular to the substrate surface. It is further required to investigate in details the relationship between B K x–ray emission spectral feature and crystal structure of BN using the DV–Xα method.

In summary, using the reactive ion–plating method, BN films were deposited on silicon substrates at the condition of c–BN film formation by varying deposition time, and were characterized by soft x–ray spectroscopic analysis, TEM analysis and infrared spectroscopic analysis. It was found that the sp^2–bonded BN film formed on the substrate at the initial stage of deposition, and the growth of c–BN film followed. The initially deposited BN film with sp^2–bonding exhibits the extremely strong satellite band near 6.5 nm in B K x–ray emission spectrum. As a result of calculation of the DOS of boron *2p* orbital in BN using the DV–Xα method, it was found that this satellite band was brought about by the transition from the *2p* σ* to the *1s* orbitals after the excitation of an electron to the *2p* σ* from the inner occupied orbitals with electron–beam irradiation, and that its intensity of the 2–coordinated boron with a dangling bond on a crystalline surface became stronger than that of the 3–coordinated boron inside crystallite, and it was expected that its intensity should become stronger as an h–BN crystallite size became smaller. As was expected, it was confirmed that its intensity became stronger as an h–BN crystallite size was become smaller by mechanical grinding. Therefore, the initially deposited BN film with sp^2–bonding was considered to compose of very fine BN crystallite having 2–coordinated borons with dangling bonds, and to play a role as the precursor of c–BN film. However, it cannot be explained only from the crystallite size why the sp^2–bonded BN film exhibits the extremely strong satellite band near 6.5 nm. It is, therefore, assumed as another factor in the microstructure of film that its basal plane is preferentially oriented perpendicular to the substrate surface.

References

[1] C.Weissmantel, K.Bewilogua, D.Dietrich, H.-J.Erler, H.-J.Hinneberg, S.Klose, W.Nowick and G.Reisse, Thin Solid Films, **72**, 19(1980).

[2] C.Weissmantel, Thin Solid Films, **92**, 55(1982).

[3] D.J.Kester and R.Messier, J. Appl. Phys., **72**, 504(1992).

[4] D.R.McKenzie, D.Muller and B.A.Pailthorpe, Phys. Rev. Lett., **67**, 773(1991).

[5] D.R.McKenzie, W.D.McFall, W.G.Sainty, C.A.Davis and R.E.Collins, Diamond Relat. Mater., **2**, 970(1993).

[6] M.Satou and F.Fujimoto, Jpn. J. Appl. Phys., **22**, L171(1983).

[7] C.Weissmantel, J. Vac. Sci. Technol., **A3**, 2384(1985).

[8] B.Rother, H.D.Zscheile, C.Weissmantel, C.Heiser, G.Holzhüter, G.Leonhardt and P.Reich, Thin Solid Films, **142**, 83(1986).

[9] A.Chayahara, H.Yokoyama, T.Imura and Y.Osaka, Jpn. J. Appl. Phys., **26**, L1435(1987).

[10] K.Inagawa, K.Watanabe, H.Ohsone, K.Saitoh and A.Itoh, J. Vac. Sci. Technol., **A5**, 2696(1987).

[11] Y.Ichinose, H.Saitoh and Y.Hirotsu, Surf. Coat. Technol., **43/44**, 116(1990).

[12] T.Ikeda, Y.Kawate and Y.Hirai, J. Vac. Sci. Technol., **A8**, 3168(1990).

[13] M.Murakawa and S.Watanabe, Surf. Coat. Technol., **43/44**, 128(1990).

[14] H.Yokoyama, M.Okamoto and Y.Osaka, Jpn. J. Appl. Phys., **30**, 344(1991).

[15] A.Weber, U.Bringmann, R.Nikulski and C.-P.Klages, Surf. Coat. Technol., **60**, 493(1993).

[16] T.Ichiki, T.Momose and T.Yoshida, J. Appl. Phys., **75**, 1330(1994).

[17] G.L.Doll, J.A.Sell, C.A.Taylor and R.Clarke, Phys. Rev., **B43**, 6816(1991).

[18] D.R.McKenzie, D.J.H.Cockayne, D.A.Muller, M.Murakawa, S.Miyake, S.Watanabe and P.Fallon, J. Appl. Phys., **70**, 3007(1991).

[19] A.K.Ballal, L.Salamanca-Riba, C.A.Taylor and G.L.Doll, Thin Solid Films, **224**, 46(1993).

[20] D.J.Kester, K.S.Ailey, R.F.Davis and K.L.More, J. Mater. Res., **8**, 1213(1993).

[21] D.L.Medlin, T.A.Friedmann, P.B.Mirkarimi, P.Rez, M.J.Mills and K.F.McCarty,

J. Appl. Phys., **76**, 295(1994).

[22] T.A.Friedmann, P.B.Mirkarimi, D.L.Medlin, K.F.McCarty, E.J.Klaus, D.R.Boehme, H.A.Johnsen, M.J.Mills, D.K.Ottesen and J.C.Barbour, J. Appl. Phys., **76**, 3088(1994).

[23] C.Satoko, M.Tsukada and H.Adachi, J. Phys. Soc. Jpn., **45**, 1333(1978).

[24] H.Adachi, *Ryoshi-Zairyo-Kagaku-Nyumon* (means an introduction to quantum chemistry for materials), (Kyoritsu-Shuppan, Tokyo, 1991).

[25] K.Inagawa, K.Watanabe, K.Saitoh, Y.Yuchi and A.Itoh, Surf. Coat. Technol., **39/40**, 253(1989).

[26] L.Vel, G.Demazeau and J.Etourneau, Mater. Sci. Eng., **B10**, 149(1991).

[27] K.L.Chopra, V.Agarwal, V.D.Vankar, C.V.Deshpandy and R.F.Bunshah, Thin Solid Films, **126**, 307(1985).

[28] Joint Committee on Powder Diffraction Standards (JCPDS, Swarthmore, PA), pattern 25-1033.

[29] Joint Committee on Powder Diffraction Standards (JCPDS, Swarthmore, PA), pattern 34-421.

[30] A.Mansour and S.E.Schnatterly, Phys. Rev., **B36**, 9234(1987).

Chapter 6

Reproduction of Measured B K X-Ray Emission Spectra by DV-Xα Method

6-1. Introduction

As described in section 5-4, the initially deposited BN film with sp^2-bonding exhibits an extremely strong satellite band near 6.5 nm. The one reason for this matter is considered that this film composes of very fine BN crystallite. However, another reason should be further required for this matter, since the origin of the strong satellite band cannot be explained only from the crystallite size of BN. A.Mansour *et al.* [1] have reported that this satellite band becomes stronger with the parallel x-ray detection to the basal plane of h-BN than with the perpendicular x-ray detection. Therefore, it is assumed that the basal plane of the sp^2-bonded BN film is preferentially oriented perpendicular to the substrate surface. In order to confirm this assumption, it was attempted to calculate the B K x-ray emission spectra of h-BN detected at different take-off angles for the basal plane, *i.e.*, the polarized B K x-ray emission spectra, using the discrete variational Hartree-Fock-Slater (DV-Xα) method developed by H.Adachi *et al.* [2, 3] which is one of molecular orbital calculation methods.

Many measured x-ray emission spectra, such as the C K x-ray emission spectra of graphite, diamond, C_{60} and C_{70} [4 - 6], the B K x-ray emission spectra of several boron compounds (B_{12}, B_2O_3, BF_3) [7], the S Kβ x-ray emission spectra of SO_4^{2-} and S_8 [8, 9], and the Cr and Mn Kβ x-ray emission spectra of chromium and manganese compounds [10], have been successfully reproduced by the DV-Xα calculation of the partial density of states (DOS) of these compounds. In the case of the DV-Xα method, an x-ray emission spectrum is generally calculated using a cluster model, and more precisely with using a larger one [11]. However, an appropriate cluster model must be assumed for each purpose, since the time required for the calculation becomes rapidly longer with using a larger cluster model and the number of the total electrons in a cluster model is limited to less than 400 for the calculation by the DV-Xα program used [11].

First, in order to test the reproducibility of a B K x-ray emission spectrum with the DV-Xα method, those of h-BN were calculated by varying the size of its cluster model. The B K x-ray emission spectra of c- and w-BN were also calculated, using the cluster models with the total electrons of about 230. Second, using the h-BN cluster model which has made it possible to approximately reproduce the measured B K x-ray emission spectrum, the polarized B K x-ray emission spectra were calculated and discussed in comparison with the measured spectrum of the initially deposited BN film with sp^2-bonding.

6-2. DV-Xα Calculation of B K X-Ray Emission Spectra of Boron Nitrides with Different Crystalline Phases

It was attempted to reproduce the B K x-ray emission spectra measured on h-BN, c-BN and w-BN by an EPMA with the DV-Xα calculations of the *2p* DOS of boron in these nitrides. Consequently, it was found that the B K x-ray emission spectrum of h-BN can be approximately reproduced by the DV-Xα calculation using the 2-dimensional cluster model constructed of the 1-layer of the planar hexagonal network which composes of 21-boron and 21-nitrogen atoms and of the total electrons of 252, and that the interlayer B-N bonds due to the van der Waals' force in this BN do not have so much effect on the spectral feature. Furthermore, the B K x-ray emission spectra of c-BN and w-BN could be successfully calculated by the DV-Xα method using the 3-dimensional cluster models composed of about 19-boron and 19-nitrogen atoms and of the total electrons of about 230. The DV-Xα calculations of the *2p* DOS of boron in these nitrides also revealed the origins of these B K x-ray emission spectra. The main band is the fundamental B K-emission band due to the electron transition to the *1s* from the *2p* σ and π (in the case of h-BN) or from the *2p* σ (in the cases of c-BN and w-BN) orbitals of boron, the low-energy satellite band near 170 eV due to the electron transition to the *1s* from the *2p* σ orbitals near 170 eV of boron formed as a result of the hybridization of the boron *2p* orbital with the nitrogen *2s* orbital, and the high-energy satellite band near 190 to 195 eV due to the electron transition to the *1s* from the *2p* π* orbitals of boron in h-BN or from the *2p* σ* orbitals near 190

eV of borons in c–BN and w–BN after the excitation of the electrons in the inner occupied orbital to the *2p* π^* and σ^* antibonding orbitals. Although the measured B K x–ray emission spectra of c–BN and w–BN differ from each other in the relative intensity of the high–energy satellite band near 190 eV, this difference could not be unfortunately verified by the DV–Xα calculations. It is considered that the transition probability between the σ^* near 190 eV and *1s* orbitals of boron should be taken into account for these DV–Xα calculations in order to verify this difference.

Calculational Procedure

The B K x–ray is emitted by the electric dipole transition of an electron from the *2p* to *1s* atomic orbitals of boron after the photoionization of one of the *1s* electrons. The *2p* orbital of boron forms a valence molecular orbital in BN. Therefore, because the B K x–ray emission spectral feature of BN reflects the *2p* DOS of boron and its wavelength is determined by the energy difference between the *2p* and *1s* orbitals of boron, the measured B K x–ray emission spectrum of BN can be reproduced by the DV–Xα calculation of the *2p* DOS of boron.

In the molecular orbital calculation with the DV–Xα method, a molecular orbital is usually approximated by the linear combination of atomic orbitals of the atoms which form the molecule, and expressed by

$$\phi_k(r_1) = \Sigma(i)\, c_{ik}\, \chi_i(r_1)$$

where $\phi_k(r_1)$ is the wave function of molecular orbital, $\chi_i(r_1)$ is the wave function of atomic orbital and c_{ik} is a coefficient [3]. Hence the schrödinger's equation of the molecular orbital is given in the one–electron approximation by

$$h(r_1)\, \Sigma(j)\, c_{jk}\, \chi_j(r_1) = \varepsilon_k\, \Sigma(j)\, c_{jk}\, \chi_j(r_1)$$

where $h(r_1)$ is the Hamiltonian operator and ε_k is the electronic energy [3]. The molecular orbital can be obtained by solving this schrödinger's equation. In the DV–Xα method, this equation is solved by numerical integration using the known wave functions of atomic orbitals [3]. The calculated value of ε_k represents the electronic energy level, the square of the calculated absolute value of c_{jk} represents the probability of finding the electron at a given point and is considered to

be proportional to the x-ray intensity I [8], that is,

$$I \propto | c_{jk} |^2 .$$

Therefore, the sum of the square of the calculated absolute value of c_{jk} in each calculated energy level was used as the x-ray intensity at its energy level, and the calculated B K x-ray emission spectra were obtained by plotting the x-ray intensity against each energy level over the energy range of the *2p* DOS of boron. The energy levels were broadened by a Gaussian function of 1 eV FWHM so that the calculated spectra may approach to the measured ones in the spectral feature.

Using h-, c- and w-BN cluster models, the electronic structures were calculated by the DV-Xα program on a DEC 3000 300LX UNIX work station. Each B-N bond length of the BN cluster models was determined from the lattice constants of the BNs [12 - 14]. The number of sampling points used for each atom in the cluster models was 200 to 300 points which are considered to be appropriate for the molecular orbital calculation with the DV-Xα method [3]. These sampling points were used for the numerical integration, as mentioned above. The atomic orbitals used as basis set were *1s*, *2s*, $2p_x$, $2p_y$ and $2p_z$ for each atom in the cluster models.

Results and Discussion

Calculation of B K x-ray emission spectrum of h-BN by DV-Xα method

Hexagonal BN has a layered structure similar to that of graphite [15]. The interlayer B-N bond due to the van der Waals' force is very weaker than the intralayer B-N bond, and the former B-N bond length (0.3331 nm) is more than twice that of the latter B-N bond (0.1445 nm) [16]. Therefore, it seems that the interlayer B-N bond does not have so much effect on the *2p* DOS of boron in BN, *i.e.*, the B K x-ray emission spectral feature. To verify this assumption, B K x-ray emission spectra were calculated by the DV-Xα method using the h-BN cluster models constructed of the 1-layer and 3-layers of the planar hexagonal networks, as shown in Fig. 6-1. Figure 6-2 shows the calculated B K x-ray emission spectra. The solid curves in Fig. 6-2 denote the B K x-ray emission spectra obtained by the sum of the σ and π subbands denoted by the fine chain and broken curves, respectively. In Fig. 6-2, the π* and σ* subbands are also

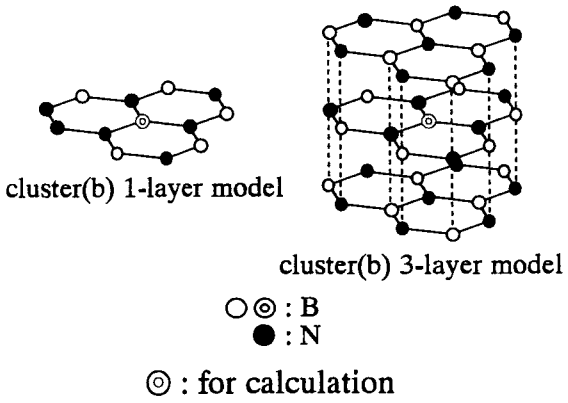

Fig. 6-1. Hexagonal BN cluster models constructed of 1- and 3-layers of planar hexagonal networks, used for DV-Xα calculations.

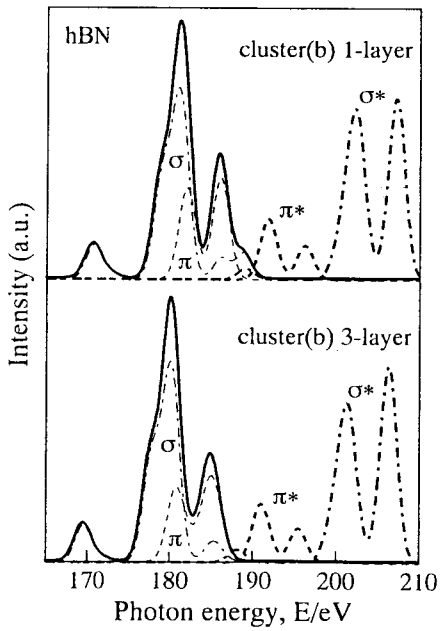

Fig. 6-2. B K x-ray emission spectra (solid curves) obtained by the sum of σ and π subbands, and σ (fine chain curves), π (fine broken curves), π* (broken curves) and σ* (chain curves) subbands, which were calculated by the DV-Xα method for h-BN cluster models constructed of 1- (top) and 3-layers (bottom) of planar hexagonal networks shown in Fig. 6-1.

denoted by the thick broken and chain curves, respectively. The σ, π, π* and σ* subbands were calculated using the σ, π, π* and σ* orbitals of boron in the molecular orbital of BN, respectively. The σ and π orbitals are occupied bonding ones, whereas the π* and σ* orbitals are unoccupied antibonding ones. Because the π* and σ* subbands are calculated from unoccupied orbitals in BN while the σ and π subbands are calculated from occupied orbitals in BN, the intensities of the π* and σ* subbands are not simply comparable with those of the σ and π subbands. Therefore, the π* and σ* subbands were conveniently shown in Fig. 6–2 by scaling down to one–tenth of the calculated intensities. In comparison between the B K x–ray emission spectra calculated from the cluster models with the 1–layer and 3–layers of the hexagonal networks, both spectra have approximately the same features, although there is a small difference in the intensities of the σ and π subbands near 188 eV. Therefore, it was verified that the interlayer B–N bond does not have so much effect on the B K x–ray emission spectral feature of h–BN. It is considered that the measured B K x–ray emission spectrum of h–BN can be calculated by the DV–Xα method using the cluster model constructed of a 1–layer of the planar hexagonal network.

Next, the B K x–ray emission spectra of h–BN were calculated by the DV–Xα method, using the cluster models constructed of the 1–layer of the hexagonal network as shown in Fig. 6–3. The calculated B K x–ray emission spectra were shown in Fig. 6–4 together with the spectrum measured by an EPMA. The calculated B K x–ray emission spectra were obtained by the sum of the σ and π subbands, and arranged in Fig. 6–4 so that the peak position of the main band of the spectrum calculated from the cluster (d) may correspond to that of the measured one. The photon energy of the abscissa of Fig. 6–4 was converted from the wavelength of the measured spectrum. The B K x–ray emission spectrum calculated from the cluster (a) of the minimum size differs distinctly from the measured one in the peak positions of the main band and the low–energy satellite band near 170 eV (near 7.3 nm in wavelength), and in the spectral feature of the main band. On the other hand, the peak positions of the main band and the low–energy satellite band near 170 eV of the spectra calculated from the clusters (b) and (c) are considerably close to those of the measured one. However, these calculated spectra differ from the measured one in

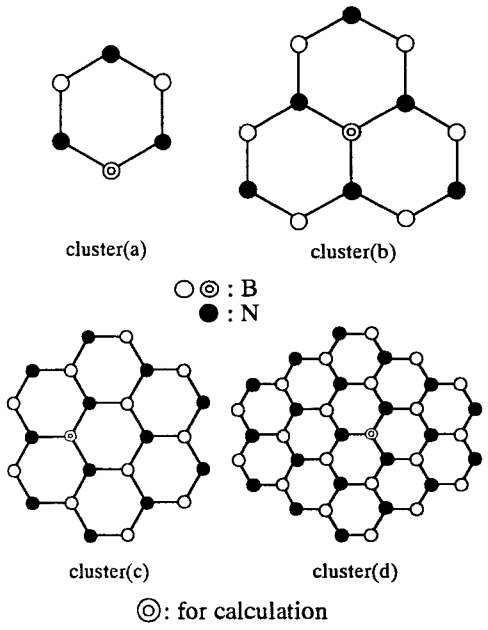

Fig. 6-3. Hexagonal BN cluster models constructed of 1-layer of planar hexagonal networks, used for DV-Xα calculations.

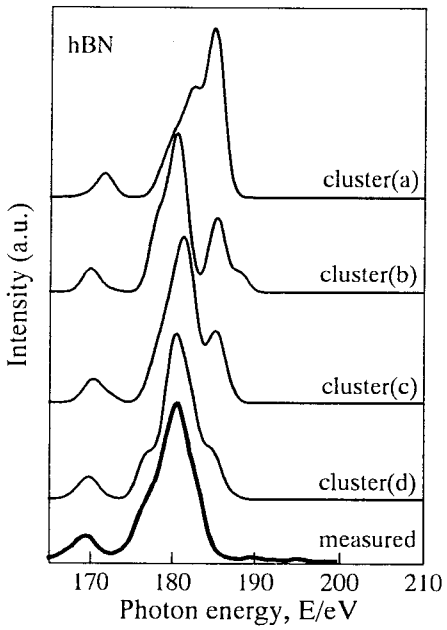

Fig. 6-4. B K x-ray emission spectra obtained by the sum of σ and π subbands which were calculated by the DV-Xα method for h-BN cluster models constructed of 1-layer of planar hexagonal networks shown in Fig. 6-3, and the measured spectrum (bottom) of h-BN powder by an EPMA.

the spectral feature of the main band, that is, the calculated spectra have a considerably strong peak near 185 eV. In the case of the spectrum calculated from the cluster (d), the peak position of the low-energy satellite band near 170 eV is in good agreement with that of the measured spectrum, and the spectral feature of the main band is considerably close to that of the measured spectrum, although the shoulders are observed near 178 and 185 eV in the calculated spectrum. Thus, the more precise B K x-ray emission spectrum can be calculated by the DV-Xα method with using the larger cluster model, and it is found that the measured B K x-ray emission spectrum of h-BN can be approximately reproduced by the DV-Xα calculation, using the cluster model (d) constructed of the 1-layer of the planar hexagonal network which compose of 21-boron and 21-nitrogen atoms, and of the total electrons of 252.

Figure 6-5 shows separately the σ, π, π* and σ* subbands, together with the B K x-ray emission spectrum calculated from the h-BN cluster (d). Since the main band of the calculated B K x-ray emission spectrum is formed from the σ and π subbands, its origin is due to the electron transition from the σ and π to *1s* orbitals of boron. The σ subband has a peak at the photon energy which corresponds to the low-energy satellite band near 170 eV (near 7.3 nm in wavelength) observed in the measured B K x-ray emission spectrum. This peak is formed mainly as a result of the effect of the nitrogen *2s* orbital on the *2p* DOS of boron, *i.e.*, as a result of the hybridization of the boron *2p* orbital with the *2s* orbital of nitrogen which is the ligand of boron in BN. Therefore, as described in section 3-2, and observed by A.Mansour *et al.* and S.Luck *et al.* [1, 17], this peak changes in its position with the ligand in boron compounds. On the other hand, although the weak satellite band is observed at the high-energy side near 190 to 195 eV (near 6.5 to 6.3 nm in wavelength) in the measured B K x-ray emission spectrum, there is no peak in the calculated σ and π subbands at the high-energy side. And the calculated π* subband lies near 190 to 195 eV and corresponds approximately to the high-energy satellite band. As mentioned above, however, the π* orbital is an unoccupied one in BN. Therefore, in order to emit the x-ray associated with this orbital, the electron transition to the π* from the inner occupied orbitals of boron must be brought about by electron-beam excitation *etc.* before its emission. In other words, the origin of the high-energy satellite band is considered to be due to the

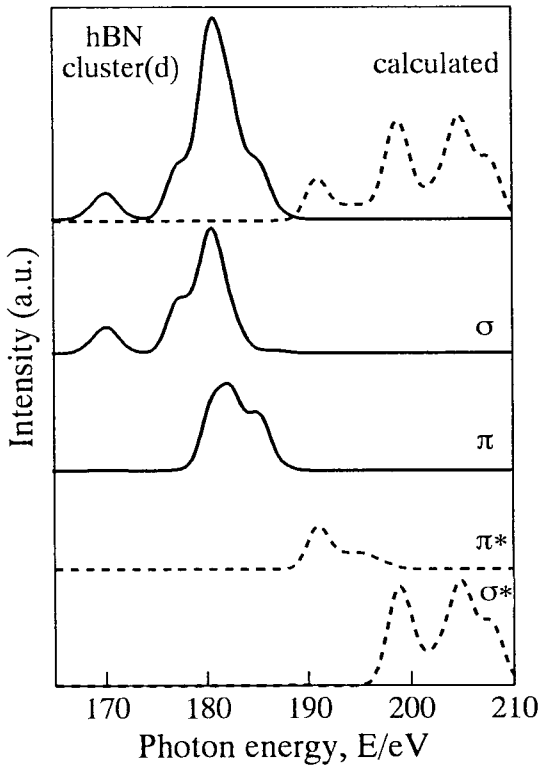

Fig. 6-5. B K x-ray emission spectrum (top) obtained by the sum of σ and π subbands (solid curve), and of π* and σ* subbands (broken curve) which were calculated by the DV-Xα method for h-BN cluster model (d) shown in Fig. 6-3. In lower sides, σ, π, π* and σ* subbands are separately shown.

electron transition to the *1s* from π* orbitals of boron after the excitation of electrons to the π* from the inner occupied orbitals of boron with electron-beam irradiation *etc.*. Consequently, the B K x-ray emission spectrum of h-BN composes of the main band, low- and high-energy satellite bands due to the electron transition to the *1s* orbital of boron from the σ and π, σ near 170 eV, and π* orbitals of boron, respectively. Although there is the σ* orbital of boron at the high-energy side according to the DV-Xα calculation, no satellite band associated with this orbital is observed in the measured B K x-ray spectrum. S.Luck *et al.* [17] have reported that the σ* orbital of boron in BN lies in the continuum beyond the ionization limit. It is, therefore, considered that there is no satellite band associated with the σ* orbital of boron in the measured spectrum because the electron transition to the σ* orbital corresponds to ionization. As described in

section 5–4, however, since the partial σ* subband lies near 190 eV and becomes stronger as the h–BN crystallite size smaller, its effect appears on the intensity of the high–energy satellite band near 190 eV when an h–BN crystallite is very small.

Calculations of B K x–ray emission spectra of c– and w–BN by DV–Xα method

Cubic and wurtzite–type BN have the crystal structures similar to those of cubic and hexagonal diamond (lonsdaleite), respectively, whereas the crystal structure of h–BN is similar to that of graphite [18]. The former two BNs are three–dimensional sp^3–bonded phases, that is, boron atoms in these BNs combine with neighboring nitrogen atoms in four–fold coordination [19]. On the other hand, h–BN is a two–dimensional sp^2–bonded phase with a layered structure, that is, boron atoms in h–BN combine with neighboring nitrogen atoms in three–fold coordination in the layer plane, and the interlayer B–N bonds are attributed to the van der Waals' force and very weaker than the intralayer B–N bonds [16]. As described in section 3–3, therefore, c–BN and w–BN differ distinctly from h–BN in the features of B K x–ray emission spectra measured by an EPMA, such as the peak position of the main band, the relative intensities of the satellite bands and so on, furthermore, there are several differences between c–BN and w–BN in the measured spectral features such as the asymmetric index of the main band and the relative intensity of the

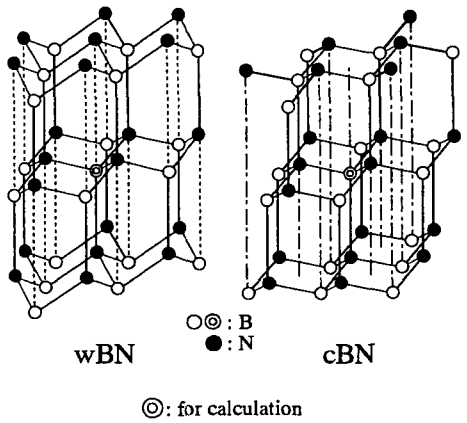

Fig. 6-6. Wurtzite-type and cubic BN cluster models used for DV-Xα calculations.

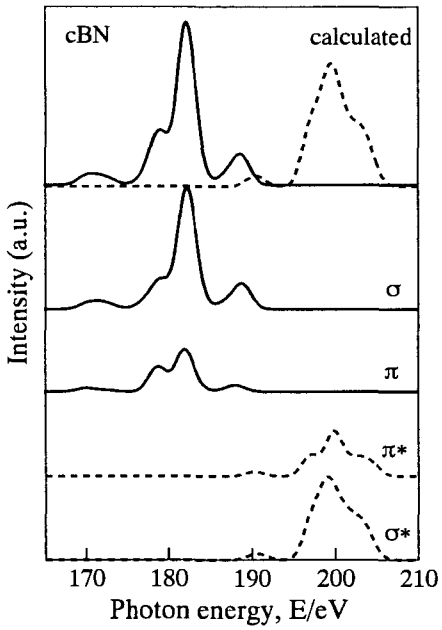

Fig. 6-7. B K x-ray emission spectrum (top) obtained by the sum of σ and π subbands (solid curve), and of π* and σ* subbands (broken curve) which were calculated by the DV-Xα method for c-BN cluster model shown in Fig. 6-6. In lower sides, σ, π, π* and σ* subbands are separately shown.

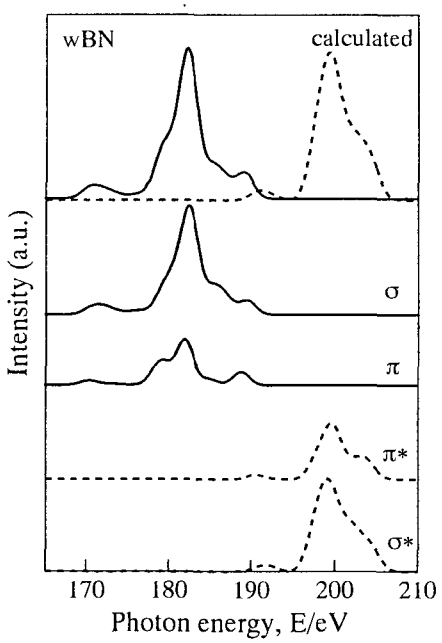

Fig. 6-8. B K x-ray emission spectrum (top) obtained by the sum of σ and π subbands (solid curve), and of π* and σ* subbands (broken curve) which were calculated by the DV-Xα method for w-BN cluster model shown in Fig. 6-6. In lower sides, σ, π, π* and σ* subbands are separately shown.

high-energy satellite band near 190 eV (near 6.5 nm in wavelength).

The B K x-ray emission spectra of c-BN and w-BN were calculated by the DV-Xα method, using the cluster models shown in Fig. 6-6. The cluster model of c-BN composes of 19-boron and 19-nitrogen atoms, and of the total electrons of 228, while that of w-BN composes of 19-boron and 20-nitrogen atoms, and of the total electrons of 235. Figures 6-7 and 6-8 show separately the σ, π, π* and σ* subbands, together with the B K x-ray emission spectra calculated from the cluster models of c-BN and w-BN. Although the σ and π, or the π* and σ* subbands are separately delineated in Figs. 6-7 and 6-8 in order to compare easily these subbands of c-BN and w-BN with those of h-BN, c-BN and w-BN are sp^3-bonded phases and have actually neither π nor π* orbitals [20]. Therefore, the σ and π, or the π* and σ* subbands of c-BN and w-BN lie in the same photon energy ranges, respectively, as shown in Figs. 6-7 and 6-8. Figures 6-9 and 6-10 show the calculated B K x-ray emission spectra of c-BN and w-BN, respectively, compared with their spectra measured by an EPMA. The peak positions of the main band of the calculated spectra are corresponded to those of the measured spectra in Figs. 6-9 and 6-10, because the real value of the x-ray photon energy cannot be precisely calculated by the DV-Xα method [8]. The features of the calculated spectra of c-BN and w-BN are considerably close to those of their observed spectra, although there is a little difference in the feature of the high-energy tail of the main band between them. Therefore, it is found that the B K x-ray emission spectra of c-BN and w-BN can be approximately reproduced by the DV-Xα calculations using the cluster models shown in Fig. 6-6. In comparison between the calculated and measured spectra of c-BN and w-BN, the main band and low-energy satellite band near 170 eV (near 7.3 nm in wavelength) are found to correspond to the *2p* σ subband. Therefore, their origins are attributed to the electron transition from the *2p* σ to *1s* orbitals. Like h-BN, the low-energy satellite band is formed as a result of the hybridization of the boron *2p* orbital with the nitrogen *2s* orbital. In the measured spectra of c-BN and w-BN, there are barely observable high-energy satellite band near 190 to 195 eV (near 6.5 to 6.3 nm in wave length). Both σ and σ* subbands have a peak near 190 eV. On both c-BN and w-BN, the peak of σ subband near 190 eV becomes weaker with using the larger cluster model for the calculation, and its position

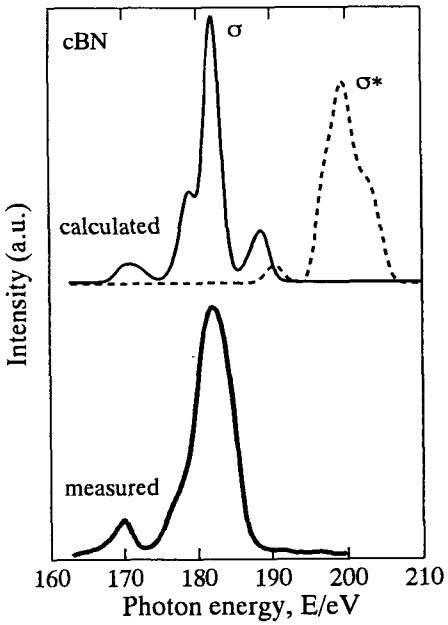

Fig. 6-9. Comparison of measured B K x-ray emission spectrum (bottom) of c-BN powder with the calculated spectrum (top) of c-BN cluster model by the DV-Xα method.

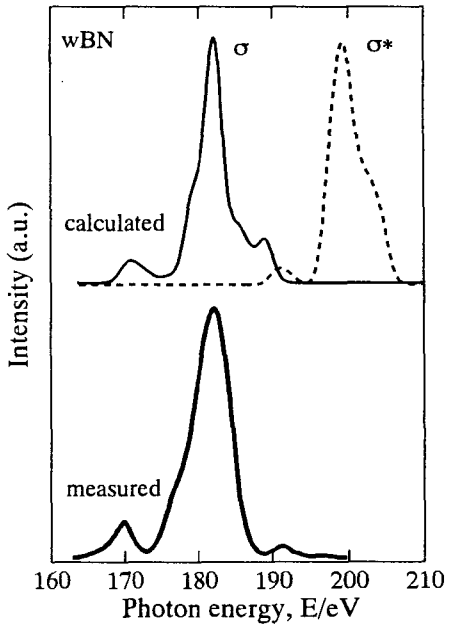

Fig. 6-10. Comparison of measured B K x-ray emission spectrum (bottom) of w-BN powder with the calculated spectrum (top) of w-BN cluster model by the DV-Xα method.

shifts slightly to the lower energy side than those of the measured satellite bands. Therefore, the high-energy satellite bands of c-BN and w-BN are considered to be formed by the emission due to the electron transition between the σ* near 190 eV and *1s* orbitals of boron. The peak of σ* subband near 190 eV is considered to correspond to the antibonding molecular orbital formed as a result of the hybridization of the boron *2p* atomic orbital with the nitrogen *2s* atomic orbital.

The measured B K x-ray emission spectra of c-BN and w-BN differ from each other in the relative intensity of the high-energy satellite band near 190 eV (near 6.5 nm in wavelength), as described in section 3-2. However, the calculated spectrum of c-BN exhibits the approximately same intensity of the σ* subband near 190 eV as that of w-BN. Therefore, it is considered that the transition probability between the σ* near 190 eV and *1s* orbitals of boron should be taken into account for the DV-Xα calculation of the B K x-ray emission spectra of c-BN and w-BN, in order to verify this difference.

In summary, in the case of h-BN, the B K x-ray emission spectrum measured by an EPMA can be approximately reproduced by the DV-Xα calculation of the *2p* DOS of boron in h-BN using the 2-dimensional cluster model constructed of the 1-layer of the planar hexagonal network which composes of 21-boron and 21-nitrogen atoms and of the total electrons of 252, because the interlayer B-N bonds due to the van der Waals' force in h-BN do not have so much effect on the spectral feature. Furthermore, the B K x-ray emission spectra of c-BN and w-BN measured by an EPMA can be also successfully reproduced by the DV-Xα calculations of the *2p* DOS of boron in these BNs, using the 3-dimensional cluster models composed of about 19-boron and 19-nitrogen atoms and of the total electrons of about 230. The DV-Xα calculations of the *2p* DOS of boron in h-, c- and w-BN, further, revealed the origins of the B K x-ray emission spectra. The main band is the fundamental B K emission band due to the electron transition to the *1s* from the *2p* σ and π orbitals (in the case of h-BN) or from the *2p* σ (in the cases of c-BN and w-BN) orbitals of boron, the low-energy satellite band near 170 eV due to the electron transition to the *1s* from the *2p* σ orbitals near 170 eV of boron formed as a result of the hybridization of the boron *2p* orbital with the nitrogen *2s* orbital. On the other hand, the high-energy satellite band near 190 to 195 eV is considered to be associated with the *2p* π* or

the *2p* σ* (near 190 eV) antibonding orbitals which are unoccupied ones, and to be due to the electron transition to the *1s* from the *2p* π* orbitals of boron in h-BN or from the *2p* σ* (near 190 eV) orbitals of borons in c-BN and w-BN after the excitation of the electrons in the inner occupied orbital to the *2p* π* and σ* antibonding orbitals. However, although the measured B K x-ray emission spectra of c-BN and w-BN differ from each other in the relative intensity of the high-energy satellite band near 190 eV, this difference could not be unfortunately verified by the DV-Xα calculations. It is considered that the transition probability between the σ* (near 190 eV) and *1s* orbitals of boron should be taken into account for these DV-Xα calculations, in order to verify this difference.

6-3. Comparison of Polarized B K X-Ray Emission Spectrum of Hexagonal BN Calculated by DV-Xα Method with Measured Spectrum of Initially Deposited BN Film

Hexagonal BN with a layered structure is expected to exhibit anisotropy of its B K x-ray emission spectrum, *i.e.*, the polarized emission spectrum. In order to verify theoretically its polarized emission spectrum, using the calculated B K x-ray emission spectrum of h-BN by the DV-Xα method, the contributions of the σ, π and π* subbands to its spectral feature were estimated at the different take-off angles from the *c* axis of h-BN crystal. In the case of the low-energy satellite band, the relative intensity can be estimated using the calculated intensities of this satellite band and the main band, and is in good agreement with the measured one. On the other hand, in the case of the high-energy satellite band, the relative intensity cannot be directly estimated using the calculated intensities of this satellite band and the main band, because of the difference in the x-ray emission mechanism between both bands. Therefore, assuming that the intensity of this satellite band calculated at a take-off angle of 45 degrees corresponds to the maximum relative intensity measured on the mechanically ground h-BN powder, the relative intensities at the take-off angles except 45 degrees were estimated by the product of the intensities which were calculated at each take-off angle from the π* subband of h-BN by Eq. (6-1) as described in the section of calculational procedure and the fraction of the

measured maximum relative intensity of the high-energy satellite band of the mechanically ground h-BN powder to the calculated intensity at a take-off angle of 45 degrees. Consequently, it is found that the calculated B K x-ray emission spectra at the different take-off angles are in considerably good agreement with the measured ones, and it is possible to estimate quantitatively the changes in the relative intensities of the low- and high-energy satellite bands with the take-off angle using the calculated spectra. The high-energy satellite band due to the contribution of the π^* subband increases remarkably its relative intensity with increasing the take-off angle, whereas the low-energy satellite band decreases its relative intensity due to the contribution of the σ subband. And the polarized emission spectrum of h-BN was verified from the theoretical calculations of the B K x-ray emission spectra at the different take-off angles.

In comparison of the measured B K x-ray emission spectrum of the initially deposited BN film with the calculated spectra, the extremely strong high-energy satellite band of this film is found to be emitted due to the size effect of h-BN crystallite and to the preferential orientation of h-BN crystal, and it is verified that this BN film composes of fine h-BN crystallites of less than 1.1 nm and that its basal plane is preferentially oriented perpendicular to the substrate surface.

Calculational Procedure

The B K x-ray emission spectrum of h-BN was calculated by the DV-Xα method, using the 2-dimensional cluster model constructed of the 1-layer of the planar hexagonal network which composed of 21-boron and 21-nitrogen atoms and of the total electrons of 252, denoted by the cluster (d) in Fig. 6-3. The DV-Xα calculation was performed by the same procedure as described in section 6-2.

A.Mansour *et al.* [1, 21] have suggested the theoretical equation for the estimate of the contribution of the σ and π valence electrons in BN to the B K x-ray emission spectrum. According to them, the σ-emission intensity in the dipole approximation can be expressed as a function of the energy E and the take-off angle θ from the c axis of h-BN as

$$I_\sigma(E, \theta) = I_\sigma(E) \{ (1 + \cos^2\theta) / 2 \}$$

where $I_\sigma(E)$ is the σ-band transition density of states. And the π-emission intensity is

$$I_{\pi}(E, \theta) = I_{\pi}(E) \sin^2\theta$$

where $I_{\pi}(E)$ is the π–band transition density of states. Therefore, the intensity of B K x–ray emission spectrum measured at the take–off angle θ is given by a linear combination of σ and π contributions, and expressed by

$$I(E, \theta) = I_{\sigma}(E) \{ (1 + \cos^2\theta) / 2 \} + I_{\pi}(E) \sin^2\theta \quad . \qquad (6–1)$$

Using Eq. (6–1), the polarized B K emission spectra of h–BN were calculated at several take–off angles from the calculated spectrum by the DV–Xα method, and compared with the measured spectrum of the initially deposited BN film with the strong satellite band near 190 eV.

Results and Discussion

Hexagonal BN is analogous to graphite, and is one of anisotropic layered compounds [15]. Extensive theoretical and experimental studies have been carried out with respect to anisotropic emission of characteristic x–rays of non–cubic crystals, because of providing useful information about electronic structure [1, 17, 22 – 38]. Although the anisotropy of the C K x–ray emission spectrum of graphite has been clarified by many studies [22 – 27], nobody has observed experimentally the anisotropy of the B K x–ray emission spectrum of h–BN, so far as the author knows. Although the author has attempted to observe the polarized B K x–ray emission spectra of h–BN and pyrolytic BN (t–BN) samples, the polarized emission spectra could not distinctly observed, as described in section 3–3. However, the BN film composed of an sp^2–bonded phase like h–BN has been found to be deposited at initial stage prior to forming the c–BN film by the ion–plating method, and to have a very strong high–energy satellite band near 190 eV in its B K x–ray emission spectrum measured by an EPMA, as described in section 5–4. The one cause of the emission of this strong satellite band was considered to be due to the x–ray emission from the boron atoms on BN crystalline surface. But, it is difficult to explain perfectly the origin of the strong satellite band only from this cause. Recently, it has been reported that c–BN films deposited by several PVD techniques have an sp^2–bonded phase between the substrate and c–BN film, of which the basal plane is preferentially oriented perpendicular to the substrate surface [39 –41]. Therefore, it is possible that the basal plane of the BN film initially deposited by the ion–plating

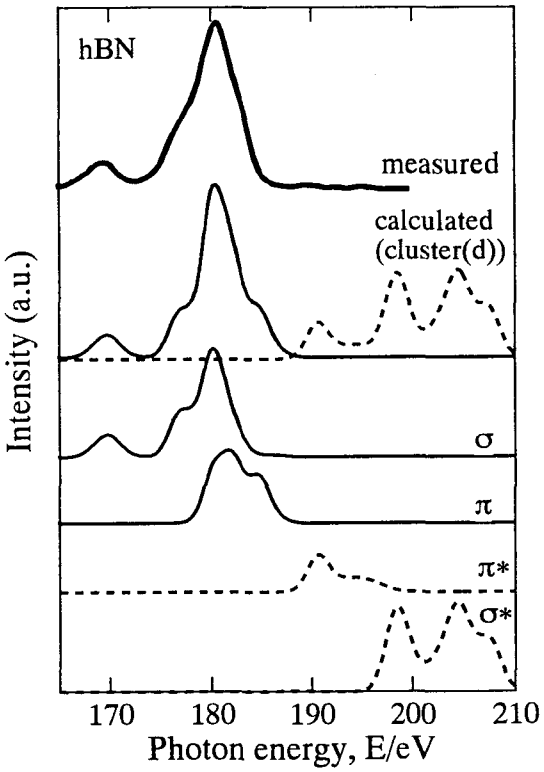

Fig. 6-11. B K x-ray emission spectra measured (top) on h-BN powder by an EPMA and calculated (the second from the top) for h-BN cluster model (d) shown in Fig. 6-3 by the DV-Xα method. In lower sides, σ, π, π* and σ* subbands are separately shown.

method is also preferentially oriented perpendicular to the substrate surface, and that the origin of its strong high-energy satellite band near 190 eV is attributed to the preferential orientation of its BN crystal. Thus, it was attempted to calculate the polarized B K x-ray emission spectrum of h-BN using Eq. (6-1) proposed by A.Mansour *et al.* [1, 21], based on the spectrum calculated by the DV-Xα method from the h-BN cluster model (d) shown in Fig. 6-3.

Figure 6-11 shows separately the σ, π, π* and σ* subbands and the B K x-ray emission spectrum calculated from the h-BN cluster model (d) by the DV-Xα method, together with the spectrum of h-BN measured by an EPMA. In Fig. 6-11, the top thick solid curve shows the measured spectrum, and the calculated spectrum is denoted at the second from the top by the solid and broken curves, which are obtained by the sum of the σ and π, and of the π* and σ*

subbands, respectively. Because the photon energy of the calculated spectrum is generally inconsistent with that of the measured one [8], the calculated subbands are arranged in Fig. 6–11 so that the main peak position of the spectrum obtained by the sum of the σ and π subbands corresponds to that of the measured one. But, the measured and calculated spectra agree well on the photon energy difference between the main and satellite bands. The measured B K x–ray emission spectrum of h–BN composes of the main band, the low– and high–energy satellite bands (near 170, 190 to 195 eV), corresponding to the σ and π subbands, the σ subband near 170 eV and the π* subband of the calculated spectrum, respectively. As described in section 6–2, therefore, the main band originates due to the electron transition to the *1s* from the σ and π orbitals of boron, the low–energy satellite band near 170 eV due to the electron transition to the *1s* from the σ orbitals near 170 eV formed as a result of the hybridization of the boron *2p* orbital with the nitrogen *2s* orbital, and the high–energy satellite band near 190 to 195 eV due to the electron transition to the *1s* from the π* orbitals after the excitation of one of the *1s* electrons to the π* orbital which is an unoccupied one in BN. There is no satellite band associated with the σ* orbital of boron, which is also an unoccupied one in BN, in the measured spectrum, since the σ* orbital lies in the continuum beyond the ionization limit [17].

Next, the polarized B K x–ray emission spectra of h–BN, *i.e.*, the spectra detected at different take–off angles θ from the *c* axis, were calculated using Eq. (6–1). The results obtained are shown in Fig. 6–12. The main and low–energy satellite bands of the polarized emission spectra were calculated at take–off angles of 15, 30, 45, 60 and 90 degrees from the σ and π subbands shown in Fig. 6–11, and were normalized by setting the calculated maximum intensities of the main bands to 100. The relative intensity of each low–energy satellite band was denoted in Fig. 6–12 in percentage against the maximum intensity of the main band.

The relative intensity of this satellite band measured on the h–BN standard sample is 16.6 % of the main band, and corresponds approximately to the calculated value. The high–energy satellite band was also calculated at each take–off angle from the π* subband shown in Fig. 6–11 by Eq. (6–1). Here, the contribution of the σ* subband to the high–energy satellite band was ignored, that is, $I_{\sigma}(E)$ was regarded as 0, because the intensity of the σ* subband near 190 eV

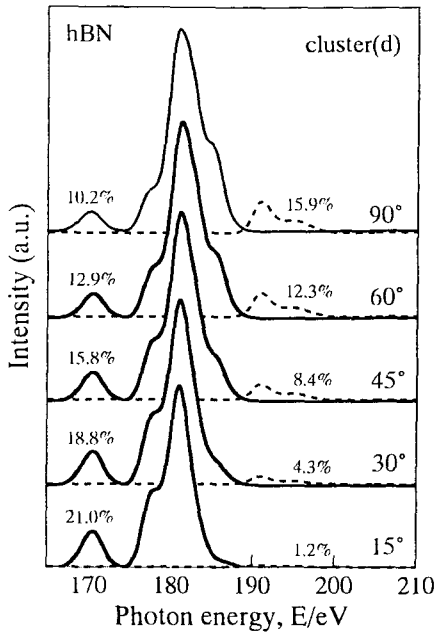

Fig. 6-12. Polarized B K x-ray emission spectra of h-BN at take-off angles of 15, 30, 45, 60 and 90 degrees which were calculated for h-BN cluster model (d) shown in Fig. 6-3, using the DV-Xα method and Eq. (6-1).

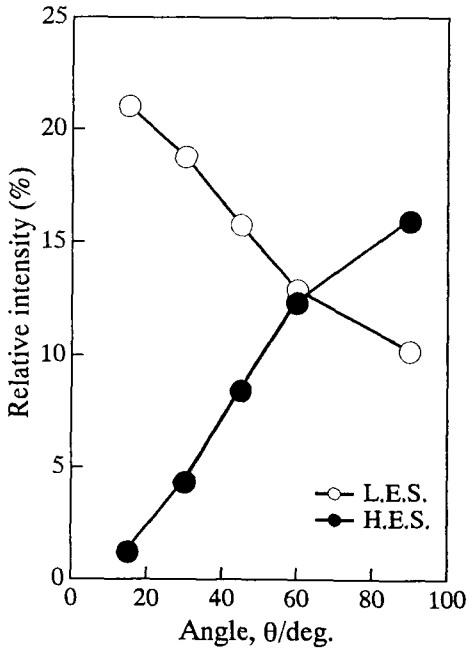

Fig. 6-13. Changes in relative intensities of the high- and low-energy satellite bands with the take-off angle.

was very weaker than that of the π^* subband. As mentioned above, since the high-energy satellite band differs from the main and low-energy satellite bands in the x-ray emission mechanism, the calculated intensity of the high-energy satellite band cannot be directly compared with those of the main and low-energy satellite bands. Therefore, the intensity of the high-energy satellite band calculated at a take-off angle of 45 degrees was assumed to be 8.4 in percentage as the relative intensity against the intensity of the main band. The value of 8.4 is the maximum relative intensity of the high-energy satellite band obtained from the mechanically ground h-BN powder (see section 5-4), and was used as the value of the intensity of the high-energy satellite band calculated at a take-off angle of 45 degrees, because the spectrum calculated at a take-off angle of 45 degrees corresponds to that of h-BN crystals with perfectly random orientation and because thoroughly mechanically ground h-BN powder is considered to be virtually randomly oriented. The relative intensities of the high-energy satellite bands at the take-off angles except 45 degrees were estimated by the product of the intensities which were calculated at each take-off angle from the π^* subband of h-BN by Eq. (6-1) and the fraction of the measured maximum relative intensity of the high-energy satellite band of the mechanically ground h-BN powder to the calculated intensity at a take-off angle of 45 degrees. The calculated relative intensity of each high-energy satellite band is also denoted in percentage in Fig. 6-12.

It is seen in Fig. 6-12 that both low- and high-energy satellite bands change in their relative intensities with the take-off angle, that is, as the take-off angle increases, the former relative intensity decreases whereas the latter one increases. So, the relative intensities were plotted as a function of the take-off angle in Fig. 6-13. It is seen in Fig. 6-13 that the relative intensities change almost lineally with the take-off angle. Supposing that the B K x-ray emission spectrum of h-BN is detected at a take-off angle of 90 degrees (parallel to the basal plane of h-BN crystal), the high-energy satellite band increases its relative intensity more than tenfold, while the low-energy satellite band reduces that to about half, compared with the relative intensity of the high-energy satellite band calculated at a take-off angle of 15 degrees (approximately perpendicular to the basal plane of h-BN crystal). The changes in the relative intensities of the low- and high-energy satellite bands are mainly attributable to the contribution of σ and π^*

subbands, respectively, and especially, the high-energy satellite band changes remarkably in the relative intensity with the take-off angle.

The polarized B K x-ray emission spectra calculated at several take-off angles were discussed in comparison with the EPMA-measured spectrum of the initially deposited BN film which composed of an sp^2-bonded phase. This BN film was deposited on a silicon substrate for 1 minute under the condition of c-BN film formation by the ion-plating method. Figure 6-14 shows the measured B K x-ray emission spectrum of this BN film, compared with the spectrum calculated at a take-off angle of 90 degrees (parallel to the basal plane of h-BN crystal). In comparison between the measured and calculated spectra, both spectra differ considerably from each other in the relative intensity of the high-energy satellite band, although both spectra agree approximately on that of the low-energy satellite band. Here, the relative intensity 8.4 of the high-energy satellite band was used as that of this satellite band calculated at a take-off angle of 45 degrees by supposing that the value of 8.4 was obtained from the h-BN crystals with perfectly random orientation. As described in section 3-3, on the B K x-ray emission spectrum of h-BN powder used as a standard sample, the relative intensities of the low- and high-energy satellite bands are 2.9 and 16.6 in percentage to the intensity of the main band, respectively. The spectrum of the h-BN standard sample were measured by an EPMA using the flat plane of a thin disk into which the h-BN standard sample was pressed. As the high-energy satellite band changes in the relative intensity with the h-BN crystallite size, judging from the relative intensity of the low-energy satellite band, the measured spectrum of the h-BN standard sample corresponds to the spectrum calculated at a take-off angle of about 40 degrees rather than of 45 degrees. Therefore, the basal plane of the h-BN standard sample is considered not to be perfectly randomly oriented but to be somewhat oriented parallel to the flat plane of the disk. It is often observed that graphite and h-BN with a layered structure exhibit the preferential orientation of the basal planes parallel to the pressed surface [24]. The B K x-ray emission spectrum of the mechanically ground h-BN powder was measured using the flat plane of its disk produced with the same procedure as that of h-BN standard sample. It is, therefore, possible that the basal plane of the mechanically ground h-BN powder was also somewhat oriented parallel to the flat

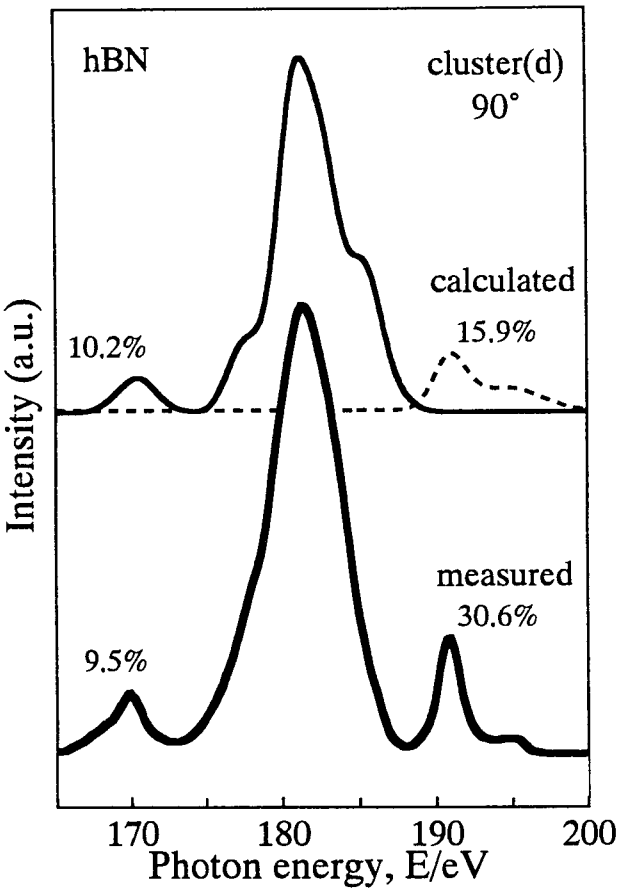

Fig. 6-14. Comparison of measured B K x-ray emission spectrum (bottom) of the initially deposited BN film with the calculated spectrum (top) of h-BN cluster model (d) at a take-off angle of 90 degrees.

plane of the disk, like that of the h–BN standard sample. Thus, supposing that the relative intensity of the high–energy satellite band calculated at a take–off angle of 40 degrees is 8.4 in percentage to the intensity of the main band, the high–energy satellite band calculated at a take–off angle of 90 degrees increases the relative intensity from 15.9 to about 21. Furthermore, supposing that the initially deposited BN film composes of smaller h–BN crystallites than the mechanically ground h–BN powder, and that the relative intensity of the high–energy satellite band calculated at a take–off angle of 40 degrees is 10.0, the relative intensity of the high–energy satellite band calculated at a take–off angle of 90 degrees further increases to about 25, and is considerably close to that of the initially deposited BN film. Thus, supposing that the initially deposited BN film composes of fine h–BN crystallites, the relative intensity of the high–energy satellite band of this BN film is approximately consistent with that of the high–energy satellite band calculated at a take–off angle of 90 degrees. And this consistency shows that the h–BN crystallites in the initially deposited BN film are preferentially oriented.

The B K x–ray emission spectrum of the initially deposited BN film was measured almost perpendicular to the substrate surface. The mechanically ground h–BN powder with the strongest high–energy satellite band (the relative intensity of 8.4) was considered from a result of the x–ray diffraction measurement to compose of h–BN crystallites with a size of about 1.1 nm. Therefore, it is considered that the initially deposited BN film composes of fine h–BN crystallites with a size of less than 1.1 nm and its basal plane is preferentially oriented perpendicular to the surface of the substrate. Conversely describing, the extremely strong high–energy satellite band of this BN film is considered to be emitted due not only to the size effect of h–BN crystallite but also to the preferential orientation of h–BN crystal.

In summary, in order to verify theoretically the polarized emission spectrum of h–BN, using the calculated B K x–ray emission spectrum of h–BN by the DV–Xα method, the contributions of the σ, π and π* subbands to its spectral feature were estimated at the different take–off angles from the *c* axis of h–BN crystal. In the case of the low–energy satellite band, the relative intensity can be estimated using the calculated intensities of this satellite band and the main band, and is in good agreement with the measured one. On the other hand, in the case of the high–energy

satellite band, the relative intensity cannot be directly estimated using the calculated intensities of this satellite band and the main band, because of the difference in the x-ray emission mechanism between both bands. Therefore, assuming that the intensity of this satellite band calculated at a take-off angle of 45 degrees corresponds to the relative intensity measured on the mechanically ground h-BN powder, the relative intensities at the take-off angles except 45 degrees were estimated by the product of the intensities which were calculated at each take-off angle from the π^* subband of h-BN by Eq. (6-1) and the fraction of the measured maximum relative intensity of the high-energy satellite band of the mechanically ground h-BN powder to the calculated intensity at a take-off angle of 45 degrees. Consequently, it is found that the calculated B K x-ray emission spectra at the different take-off angles are in considerably good agreement with the measured ones. The high-energy satellite band due to the contribution of the σ subband increases remarkably its relative intensity with increasing the take-off angle, whereas the low-energy satellite band decreases its relative intensity. And the polarized emission spectrum of h-BN was verified from the theoretical calculations of the B K x-ray emission spectra at the different take-off angles. In comparison of the measured B K x-ray emission spectrum of the initially deposited BN film with the calculated spectra, the extremely strong high-energy satellite band of this film is found to be emitted due to the size effect of h-BN crystallite and to the preferential orientation of h-BN crystal, and it is verified that this BN film composes of fine h-BN crystallites of less than 1.1 nm and that its basal plane is preferentially oriented perpendicular to the substrate surface.

References

[1] A.Mansour and S.E.Schnatterly, Phys. Rev., **B36**, 9234(1987).

[2] A.Rosén, D.E.Ellis, H.Adachi and F.W.Averill, J. Chem. Phys., **65**, 3629(1976).

[3] H.Adachi, *Ryoshi-Zairyo-Kagaku-Nyumon* (means an introduction to quantum chemistry for materials), (Kyoritsu-Shuppan, Tokyo, 1991).

[4] J.Kawai, K.Maeda, M.Takami, Y.Muramatsu, T.Hayashi, M.Motoyama and Y.Saito, J. Chem. Phys., **98**, 3650(1993).

[5] J.Kawai and M.Motoyama, Phys. Rev. **B47**, 12988(1993).

[6] J.Kawai, (to be published).

[7] Y.Muramatsu, M.Ohshima, J.Kawai and H.Kato, Nucl. Instrum. Methods Phys. Rev. **B42**, 559(1993).

[8] J.Kawai and K.Hashimoto, Advan. X-Ray Chem. Anal. Jpn., **23**, 151(1992).

[9] H.Adachi and K.Taniguchi, J. Phys. Soc. Jpn., **49**, 1944(1980).

[10] H.Adachi, H.Nakamatsu and T.Mukoyama, Advan. X-Ray Chem. Anal. Jpn., **23**, 19(1992).

[11] M.Morinaga, N.Yukawa and H.Adachi, Bull. Jpn. Inst. Met., **27**, 165(1988).

[12] Joint Committee on Powder Diffraction Standards (JCPDS, Swarthmore, PA), pattern 34-421.

[13] Joint Committee on Powder Diffraction Standards (JCPDS, Swarthmore, PA), pattern 25-1033.

[14] Joint Committee on Powder Diffraction Standards (JCPDS, Swarthmore, PA), pattern 26-773.

[15] P.K.Lam, R.M.Wentzcovitch and M.L.Cohen, Mater. Sci. Forum, **54&55**, 165(1990).

[16] C.R.Aita, Mater. Sci. Forum, **54&55**, 1(1990).

[17] S.Luck and D.S.Urch, Physica Scripta, **41**, 970(1990).

[18] F.S.Galasso, *Structure and Properties of Inorganic Solids* (Pergamon, Oxford, 1970), p.96 and 140.

[19] T.A.Friedmann, P.B.Mirkarimi, D.L.Medlin, K.F.McCarty, E.J.Klaus, D.R.Boehme, H.A.Johnsen, M.J.Mills, D.K.Ottesen and J.C.Barbour, J. Appl. Phys., **76**, 3088(1994).

[20] E.Cartmell and G.W.A.Fowles, *Valency and Molecular Structure* (Butterworth, London, 1977), p.157.

[21] A.Mansour, S.E.Schnatterly and R.D.Carson, Phys. Rev., **B31**, 6521(1985).

[22] D.J.Fabian, *Soft X-Ray Band Spectra* (Academic Press, London, 1968).

[23] G.Dräger, W.Beier, O.Brümmer and P.Krönert, Kristal und Technik, **9**, 1921(1974).

[24] M.Motoyama and G.Hashizume, J. Spectrosc. Soc. Jpn., **29**, 92(1980).

[25] G.Dräger and O.Brümmer, Phys. Stat. Sol., **B124**, 11(1984).

[26] A.Mansour and S.E.Schnatterly, Phys. Rev. Lett., **59**, 567(1987).

[27] Chr. Beyreuther, R.Hierl and G.Wiech, Berichte der Bunsen-Gesellschaft, **79**, 1081(1975).

[28] F.C.Brown, R.Z.Bachrach and M.Skibowski, Phys. Rev., **B13**, 2633(1976).

[29] A.Zunger, A.Katzir and A.Halperin, Phys. Rev., **B13**, 5560(1976).

[30] R.D.Leapman and J.Silcox, Phys. Rev. Lett., **42**, 1361(1979).

[31] J.Barth, C.Kunz and T.M.Zimka, Sold State Commun., **36**, 453(1980).

[32] B.M.Davies, F.Bassani, F.C.Brown and C.G.Olson, Phys. Rev., **B24**, 3537(1981).

[33] R.D.Leapman, P.L.Fejes and J.Silcox, Phys. Rev., **B28**, 2361(1983).

[34] R.D.Carson and S.E.Schnatterly, Phys. Rev. Lett., **59**, 319(1987).

[35] J.Robertson, Phys. Rev., **B29**, 2131(1987).

[36] J.Pirenne and P.Longe, Physica, **30**, 277(1964).

[37] G.D.Mahan, Phys. Rev., **B15**, 4587(1977).

[38] R.S.Crisp, J. Phys., **F13**, 1325(1983).

[39] D.J.Kester, K.S.Ailey, R.F.Davis and K.L.More, J. Mater. Res., **8**, 1213(1993).

[40] A.K.Ballal, L.Salamanca-Riba, C.A.Taylor and G.L.Doll, Thin Solid Films, **224**, 46(1993).

[41] D.L.Medlin, T.A.Friedmann, P.B.Mirkarimi, P.Rez, M.J.Mills and K.F.McCarty, J. Appl. Phys., **76**, 295(1994).

Chapter 7
General Discussion and Conclusions

The synthesis of c-BN film by the reactive ion-plating method was investigated. The ion-plating apparatus used in this study was equipped with a pair of magnets for generating a magnetic field parallel to the electric field between the anode and the hot cathode, in order to promote the ionization of the species such as boron and nitrogen and the reaction between the species. The BN films were deposited on a silicon substrate by varying various ion-plating parameters, and mainly analyzed by Fourier transform infrared spectroscopy (FTIRS) and selected area electron diffractometry (SAED). Consequently, the deposition condition required for the c-BN film formation by this ion-plating apparatus could be clarified, and it was found that the Ar/N_2 gas flow ratio introduced into the deposition chamber and the self-bias voltage applied to the substrate were important parameters for the c-BN film formation. Because it was difficult to distinguish between c-BN and w-BN with FTIRS and to observe the weak diffraction rings from the (200) and (222) planes of c-BN with SAED, the BN films that were presumed to be a c-BN film by FTIRS and SAED were further analyzed by electron energy loss spectroscopy (EELS), x-ray diffractometry (using the attachment for a thin film) and Raman spectroscopy. The EELS spectrum of the BN film almost corresponded to that of c-BN, and four x-ray diffraction peaks were observed from the BN film to correspond to the (111), (200), (220) and (311) planes of c-BN. In particular, two Raman peaks were observed from the BN film to correspond to the TO and LO (transverse and longitudinal optics) modes of c-BN lattice. There is no report that the Raman peaks corresponding to c-BN have been observed from c-BN films produced by various PVD and CVD techniques, so far as the author knows. Therefore, it is considered that the c-BN film have been undoubtedly deposited by the reactive ion-plating method. However, the results of the analyses of these films by FTIRS, SAED and EELS also showed that the ion-plated c-BN film surely contained a small amount of sp^2-bonded BN phase like h-BN. The same phenomenon has been reported on c-BN films deposited by other PVD and CVD tech-

niques [1 - 7]. Hereafter, the sp^2–bonded BN phase will be referred to as a hexagonal–like BN phase which is a general name for h–, r–, t– and a–BN phases, because it is unknown which of h–, r–, t– and a–BN phases corresponds to the sp^2–bonded BN phase.

Cubic BN films deposited by various PVD and CVD techniques are generally identified not by x–ray diffractometry and Raman spectroscopy but by FTIRS and SAED, because the c–BN films are thin films with submicron thickness and compose of the fine crystallites with a size of less than 10 nm. In this study, the ion–plated c–BN films were characterized with soft x–ray spectroscopy, *i.e.*, using B K x–ray emission spectrum, in addition to these analytical methods. It was clarified that the B K x–ray emission spectrum of BN changes in the spectral features , such as the peak position, FWHM and asymmetric index of the main band, and the relative intensities of the low– and high–energy satellite bands depending on the crystal structure, and that the phase identification of BN films, which are very thin films with a thickness of less than submicron and compose of the fine crystallites with a size of less than 10 nm, can be carried out by the B K x–ray emission spectral feature. However, it was also found that the ion–plated BN films, which were identified as c–BN films by FTIRS, SAED, EELS, x–ray diffractometry and Raman spectroscopy, exhibit certainly the stronger high–energy satellite band near 190 eV (near 6.5 nm in wavelength) than c–BN powder synthesized at high temperature and pressure.

On the other hand, the BN films were deposited by varying the deposition time under the condition that a c–BN film formed, and their B K x–ray emission spectra were measured by an EPMA. Consequently, the initially deposited BN films were found to compose not of a c–BN phase but of an sp^2–bonded BN phase like h–BN, *i.e.*, a hexagonal–like BN phase, and to exhibit the extremely strong high–energy satellite band near 190 eV. Thus, using the BN film deposited for 7 minutes under the condition that a c–BN film formed, the B K x–ray emission spectra were measured with synchrotron radiation by varying the take–off angle, since the lower take–off angle measurement is more surface–sensitive. The B K x–ray emission spectra measured at the take–off angles of less than 12.5 degrees for the film surface were in perfect agreement with that of the c–BN powder, and it was found that the c–BN film forms in the upper region of the film and the hexagonal–like BN film with about 30 nm thickness in the lower region, *i.e.*, at the

interface between the c-BN film and the substrate. It was, furthermore, found that the reason why the c-BN film certainly contains a small amount of hexagonal-like BN phase and exhibits the stronger satellite band near 190 eV than the c-BN powder is attributed to the presence of the initially deposited hexagonal-like BN film. Recently, it has been proposed from the results of the cross-sectional high-resolution TEM observations of c-BN films deposited by several other PVD techniques that such a hexagonal-like BN film exists at the interface between the substrate and the c-BN film [2, 4, 6]. Therefore, it is implied that the presence of hexagonal-like BN film participates in the formation of c-BN film.

Since B K x-rays are emitted by the electric dipole transition of an electron from the boron *2p* orbital, which forms a valence molecular orbital in BN, to the boron *1s* orbital after the photoionization of one of the *1s* electrons, the B K x-ray emission spectral feature of BN reflects the *2p* density of states (DOS) of the molecular orbital. It is accordingly considered that the extremely strong high-energy satellite band of the initially deposited hexagonal-like BN film reflects the *2p* DOS of the molecular orbital. However,the extremely strong high-energy satellite band as observed in the present study has not been reported so far. Thus, it was attempted to ascertain the origin of the extremely strong high-energy satellite band from the calculation of the *2p* DOS with the discrete variational Hartree-Fock-Slater (DV-Xα) method. Consequently, one reason for the origin of extremely strong satellite band was found to be due to the size effect of the BN crystallite and another reason due to the polarized B K x-ray emission. In other words, it was found that the initially deposited hexagonal-like BN film composes of the fine crystallite with a size of less than 1.1 nm and that its basal plane is preferentially oriented perpendicular to the substrate surface. It has been recently also proposed from the results of the cross-sectional high-resolution TEM observations of c-BN films deposited by other PVD techniques that the basal planes of hexagonal-like BN films are preferentially oriented perpendicular to the substrate surface [4, 6]. In the cases of the depositions of c-BN films by every PVD techniques, the hexagonal-like BN film may be considered to play a role as the precursor of c-BN film, because the hexagonal-like BN film is always deposited at the initial stage prior to the growth of c-BN film under the condition that a c-BN film forms.

In this study, it is required for the c–BN film formation to apply negative self–bias voltages of 15 ~ 65 V to the substrate. The BN films deposited at negative self–bias voltages of less than 15 V are sp^2–bonded BN films, *i.e.*, hexagonal–like BN films, and the relative intensities of their low– and high–energy satellite bands to the peak intensity of the main band are about 13 and 9 in percentage, respectively. Therefore, these relative intensities indicate that the basal plane is randomly oriented to the substrate surface when the depositions are performed at negative self–bias voltages of less than 15 V. On the other hand, in the case of the hexagonal–like BN film deposited at the initial stage prior to the growth of c–BN film at negative self–bias voltages of 15 ~ 65 V, its basal plane is always preferentially oriented perpendicular to the substrate surface, because of the difference in the energy of ions impinging to the growing film. Hence, it is considered that the preferential orientation of the basal plane of the initially deposited hexagonal–like BN film would be required for the c–BN film formation.

The deposition process of an ion–plating method is in competition with the resputtering of the growing film due to ion bombardment. It is known that the sputtering yield of a single crystal depends on the crystal plane and becomes larger with the denser one [8]. Since the basal plane of h–BN is the most dense crystal plane, the atoms in the basal plane should be more easily sputtered by ion bombardment than ones in the prismatic plane. In other words, the atoms in the basal plane oriented parallel to the substrate surface should be more easily sputtered by ion bombardment than ones in the basal plane oriented perpendicular to the substrate surface. When the growing hexagonal–like BN film is bombarded by ions with high energies of 15 ~ 65 eV, the preferential orientation of the initially deposited hexagonal–like BN film is taken place and the c–BN film is formed by the reactive ion–plating method. Therefore, it is considered that the reason why the basal plane of the initially deposited hexagonal–like BN film is preferentially oriented perpendicular to the substrate surface is due to the difference in the sputtering yield between the basal planes oriented parallel and perpendicular to the substrate surface by the bombardment of ions with high energies of 15 ~ 65 eV. That is to say, the basal planes oriented perpendicular to the substrate surface would be mainly left without resputtering under the deposition condition that the c–BN film forms. On the other hand, in the case of the hexagonal–like

BN film deposited at negative self-bias voltages of less than 15 V, both basal planes oriented perpendicular and parallel to the substrate surface would be left without resputtering, because of the low-energy ion bombardment.

Although there have been several arguments about the growth mechanism of c-BN film, unfortunately, its mechanism has not been made clear yet. C.Weissmental *et al.* [9, 10] proposed that a c-BN film is formed due to the thermal spike, *i.e.*, the generation of high temperature and pressure on an atomic scale, caused by ion-bombarding the growing film. According to the model of the growth mechanism of c-BN film proposed by C.Weissmental *et al.*, the c-BN film formation should be dependent on the energy transferred into the growing film from the impinging ions to the film. However, D.J.Kester *et al.* [4] proposed from the result of the synthesis of c-BN film using the ion-beam of nitrogen and various inert gases that the c-BN film formation is dependent not upon the energy but upon the momentum transferred into the film through ion bombardment, since there are distinctly the upper and lower threshold values with respect to the transferred momentum for the c-BN film formation. The upper and lower threshold values are observed due to the ion bombardment which is too high to deposit the BN film (complete resputtering of the deposited film) and which is too low to form the c-BN film, respectively. In this study, the c-BN film could be deposited on the initially deposited hexagonal-like BN film with the preferential orientation which was caused by the resputtering, when the growing hexagonal-like BN film is bombarded by the ions with energies of 15 ~ 65 eV. The c-BN film could not be deposited by the bombardment of ions with energies of less than 15 eV, and the complete resputtering of the deposited film was taken place by the bombardment of ions with energies of more than 65 eV. Therefore, these results would support the model of the growth mechanism of c-BN film proposed not by C.Weissmental *et al.*, but by D.J.Kester *et al.*. A.Weber *et al.* [11] further proposed from the result of the synthesis of c-BN film by electron cyclotron resonance (ECR) plasma deposition that the initially deposited hexagonal-like BN film is transformed into a c-BN film *via* a w-BN film by ion-bombarding the growing film. According to the model of the growth mechanism of c-BN film proposed by A.Weber *et al.*, w-BN should be present in the film. However, there was no evidence that w-BN was present in the c-

BN films deposited by the reactive ion-plating method in this study.

On the other hand, D.R.McKenzie *et al.* [12] proposed from the results of theoretical analysis on intrinsic stress generated in a c-BN film deposited by a reactive ion-plating method that the formation of c-BN film is attributed to the strong compressive stress generated in the film through ion bombardment,. In other words, they described that ion impacts cause a local melting of small regions of the h-BN film and the melted regions solidify as c-BN under the influence of the compressive stress, of which the magnitude is certainly great enough to generate conditions which lie inside the stability region of c-BN in the phase diagram of BN as shown in Fig. 7-2. According to their estimation of the intrinsic stress in the film, the compressive stress is generated in the film with ion impacts, and is attained to the maximum value of about 8 GPa by bombarding the growing film with ions with an energy of about 20 eV. The compressive stress decreases abruptly and exponentially with decreasing and increasing the ion energy from 20 eV, respectively. In this study, the minimum and maximum intensities of the self-bias voltage required for the c-BN film formation are -15 and -65 V, respectively. And the magnitudes of the compressive stress generated by bombarding the growing film with ions with energies of 15 and 65 eV are estimated to be about 5 and 3 GPa, using the compressive stress *v.s.* ion energy curve calculated by them (see Fig. 7-1). The substrate temperature during the deposition was measured in this study to be about 250 degrees. Since the phase boundary between h-BN and c-BN has not been determined at low temperature, judging from the phase boundary between graphite and diamond determined by Berman *et al.* [13] from a thermodynamic analysis, a c-BN phase is stable over about 2 GPa at 250 degrees (see Fig. 7-2). Therefore, the conditions required for the c-BN film formation obtained in this study are considered to lie inside the stability region of c-BN phase in the phase diagram of BN as shown in Fig. 7-2.

It is known that the generation of compressive stress is in competition with the annealing of the stress by the energy from the impact, and that some film thicknesses would be needed to store the strong intrinsic stress in many metallic and ceramic films [14]. This is considered to be the reason why the c-BN film grew on the initially deposited hexagonal-like BN film with about 30 nm thickness, that is, the c-BN film began to grow after about 2 minutes from the onset of

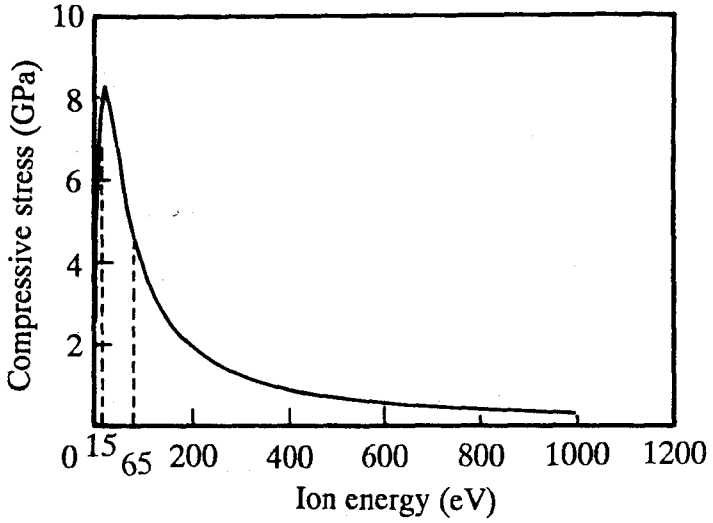

Fig. 7-1. Compressive stress produced in h-BN film, calculated by D.R.McKenzie *et al.*, is shown as a function of ion impact energy.

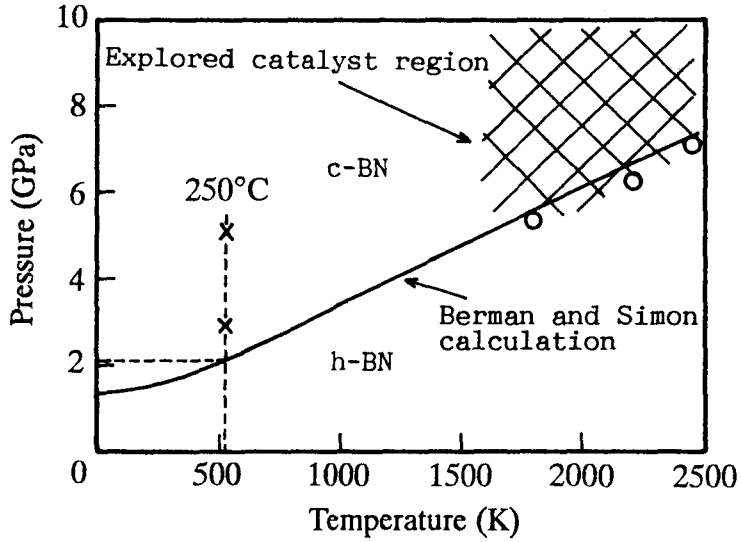

Fig. 7-2. The phase diagram of BN in the P-T plane. The circles and cross hatching show the region in which c-BN has been found to be the stable phase. The symbols x show the region in which c-BN film has been deposited by the reactive ion-plating method.

deposition, when the deposition was performed at a self-bias voltage of -65 V. It was, further, confirmed that the c-BN film began to grow within 1 minute from the onset of deposition because of the small annealing effect of the stress and the fast deposition rate, in the cases of the depositions at self-bias voltages of -15 and -40 V.

The compressive stress is considered to be the biaxial stress in a thin film, and h-BN has a larger compressibility in the direction of the *c* axis than of the *a* and *b* axes. Therefore, it is considered that it is the most stable in terms of free energy to lay the *c* axis in the biaxial compressive stress field, *i.e.*, to orient the basal plane perpendicular to the film surface. This is considered to be another reason why the basal plane of the initially deposited hexagonal-like BN film is preferentially oriented perpendicular to the substrate surface, *i.e.*, the film surface. In other words, it is considered that the preferential orientation of the hexagonal-like BN film perpendicular to the substrate surface should be needed to store the strong compressive stress required for the c-BN film formation in the film.

Consequently, it is considered that the c-BN film formation with the reactive ion-plating method is attributed to the preferential orientation of the basal plane of the initially deposited hexagonal-like BN film composed of fine crystallites and the strong compressive stress generated in the hexagonal-like BN film by bombarding the growing BN film with ions with energies of 15 ~ 65 eV. And the growth mechanism of c-BN film is considered as follows (see Fig. 7-3).

First, the hexagonal-like BN film is deposited on a silicon substrate and then the preferential orientation of this film is taken place with the progress of deposition. Simultaneously, the compressive stress is steadily stored in the film by bombarding the growing film with ions with energies of 15 ~ 65 eV, such as argon, nitrogen and boron ions. Second, when the magnitude of the compressive stress attains to a critical value of the stress which makes a c-BN phase stable, c-BN begins to form near the growing surface of film. D.R.McKenzie *et al.* [12] assumed that the melting and solidification of the film were caused near the growing surface of film by ion impacts. However, it is considered that c-BN would be able to form without the melting, because boron and nitrogen atoms near the growing surface of film would be certainly agitated by ion impacts and the energy of the impinging ions to the growing film is larger than the bond

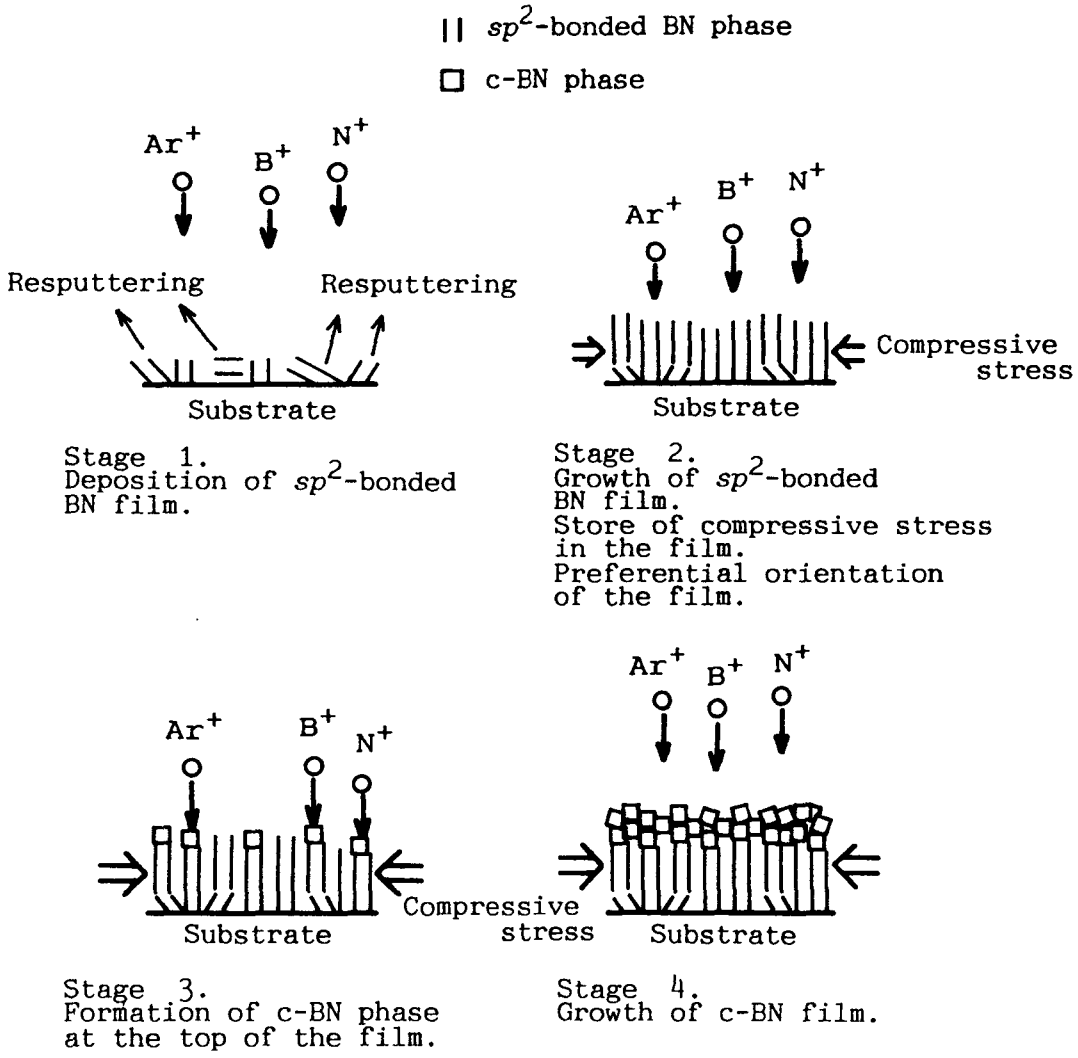

Fig. 7-3. Schematic diagram of the growth mechanism of c-BN film deposited by the reactive ion-plating method.

energy of h-BN (about 4 eV) [15]. Cubic BN continues to grow with the progress of deposition and the film will become covered with c-BN. After the film has become covered with c-BN, c-BN is considered to keep growing without ion impacts, because c-BN film can be deposited without applying a self-bias voltage to the substrate after about 5 minutes' deposition with applying a self-bias voltage of -65 V.

In this study, the deposition conditions required for the formation of c-BN film by the reactive ion-plating method were investigated, and the microstructure of the ion-plated c-BN film was analyzed by soft x-ray spectroscopy. Furthermore, the growth mechanism of ion-plated c-BN film was discussed. These are described in 6 chapters.

In chapter 2, the deposition conditions of c-BN film were investigated using the reactive ion-plating method with a hot cathode plasma discharge in a parallel magnetic field. It was found that there were the appropriate ranges for the c-BN film formation in both terms of the self-bias voltage applied to a substrate and of the Ar/N_2 gas flow ratio introduced into the deposition chamber throughout the deposition. These facts imply that bombarding the growing BN film with ions, such as argon and nitrogen ions, plays a significant role for the c-BN film formation. The c-BN film could be deposited at self-bias voltages of -40 ~ -60 V, Ar/N_2 gas flow ratios of 2.0 to 3.0, an ionization current of 14 A and electron-beam powers (for boron evaporation) of 1.8 ~ 2.0 kW by the reactive ion-plating method. The deposited c-BN films were identified by FTIRS, SAED, EELS, x-ray diffractometry (using the attachment for a thin film) and Raman spectroscopy. In particular, since the two Raman peaks corresponding to a c-BN phase were observed from the deposited c-BN film, the c-BN film is considered to be undoubtedly deposited by the reactive ion-plating method. However, the deposited c-BN films contain a hexagonal-like BN phase as a second phase, and impurities such as argon, oxygen, and carbon in small amounts. The deposited c-BN film composed of the fine crystallite with a size of less than 30 nm and with random orientation.

In chapter 3, the soft x-ray spectroscopic analysis was investigated on boron carbide, boron oxide, boron nitrides with different crystal structures, sodium tetrafluoroborate and the ion-plated BN films using their B K x-ray emission spectra measured by an EPMA. It was found

that the B K x-ray emission spectrum changes in the spectral features such as the peak position, FWHM and asymmetric index of the main band, the peak positions and relative intensities of the low- and high-energy satellite bands with variation in the chemical bond of boron. In particular, since the low-energy satellite band changes distinctly in the peak position with kinds of atoms/ions combined to boron, its peak position is very useful to identify boron compounds. Although sodium tetrafluoroborate is easily decomposed by electron-beam irradiation, its B K x-ray emission spectrum could be almost correctly measured by an EPMA, with continuous moving the analytical area of the sample during the measurement. In the case of boron nitrides, their B K x-ray emission spectra also change in the spectral features depending on the crystal structure, and the spectral feature can be used to distinguish between c- and w-BN phases or among h-, r-, t- and a-BN phases, whereas these BN phases can not be distinguished by the infrared absorption spectra. Using h- and t-BN samples with the anisotropic layered structure like graphite, though it was attempted to observe the polarized B K x-ray emission spectra, the polarized emission spectra could not be clearly observed from the h- and t-BN samples The B K x-ray emission spectra of the ion-plated c-BN films were found to exhibit surely the stronger high-energy satellite band near 190 eV than the c-BN sample synthesized at high temperature and pressure, because of the contribution of the strong high-energy satellite band of the initially deposited hexagonal-like BN film to that of the c-BN film.

In chapter 4, the adhesion improvement of c-BN film to a silicon substrate and the atmospheric degradation of c-BN film were investigated. Consequently, it was found that the adhesion strength of c-BN film to the substrate is increased exceedingly by depositing the buffer interlayer with gradually increasing nitrogen concentration between the substrate and c-BN film on the substrate which has been implanted with both boron and nitrogen ions. On the other hand, it was found that the c-BN film is broken to pieces and peeled off from the substrate on exposure to air. To prevent the c-BN film from breaking and peeling off from the substrate in air is a important subject which must be settled in future.

In chapter 5, in order to investigate the formation process of c-BN film, the BN films were deposited by varying the self-bias voltage and deposition time, and were mainly analyzed by the

soft x-ray spectroscopy. It was found that it is necessary to apply negative self-bias voltages of 15 ~ 65 V to the substrate for about 5 minutes after the onset of deposition in order to form the c-BN film, and that the c-BN film keeps growing without applying the self-bias voltage to the substrate after about 5 minutes' deposition with applying a self-bias voltage of -65 V. Furthermore, it was found that the non-cubic BN film, *i.e*, the hexagonal-like BN film, forms on the substrate at the initial stage of deposition, followed by the growth of c-BN film on the hexagonal-like BN film. The initially deposited hexagonal-like BN film was confirmed by the synchrotron-radiation measurements to have about 30 nm thickness and to exist between the substrate and the c-BN film. The initially deposited hexagonal-like BN film exhibited a extremely strong high-energy satellite band near 190 eV, and it is considered that the reason why the ion-plated c-BN film exhibits surely the stronger high-energy satellite band than the c-BN powder synthesized at high temperature and pressure is due to the contribution of the extremely strong one of the initially deposited hexagonal-like BN film to that of the c-BN film. On the other hand, it was confirmed from the DV-Xα calculation of the *2p* DOS of h-BN that the high-energy satellite band becomes stronger as the h-BN crystallite smaller. However, the origin of the extremely strong high-energy satellite band could not be explained only from the size effect of h-BN crystallite. The initially deposited hexagonal-like BN film is considered to compose of the fine crystallite of less than 1.1 nm, because its relative intensity of high-energy satellite band was stronger than that of mechanically ground h-BN powder with a crystallite size of about 1.1 nm.

In chapter 6, in order to ascertain the origin of the strong high-energy satellite band, it was, further, attempted to reproduce the B K x-ray emission spectrum of h-BN with the detailed DV-Xα calculation of the *2p* DOS in the molecular orbital. Consequently, it was found that the B K x-ray emission spectrum can be approximately reproduced by the DV-Xα calculation, and that the origins of the main band and the low- and high-energy satellite bands are due to the electron transition to the *1s* from the *2p* σ and *2p* π orbitals, from the *2p* σ orbital near 170 eV formed as a result of the hybridization of the boron *2p* orbital with the nitrogen *2s* orbital, and from the *2p* π* antibonding orbital after the excitation of the electron in the inner occupied orbit-

al to this antibonding orbital, respectively. Furthermore, as a result of the calculation of the polarized B K x-ray emission spectrum of h-BN, it was found that the high-energy satellite band becomes stronger as the take-off angle of which measurement is taken from the *c* axis of h-BN crystal increases, whereas the low-energy satellite band becomes weaker, and that the origin of the strong high-energy satellite band of the initially deposited hexagonal-like BN film is due to the polarized B K x-ray emission. In comparison of the measured B K x-ray emission spectrum of the initially deposited hexagonal-like BN film with the calculated spectra at the different take-off angles, the basal plane of the initially deposited hexagonal-like BN film was found to be preferentially oriented perpendicular to the substrate surface.

In chapter 7, the growth mechanism of ion-plated c-BN film was discussed. Consequently, it was considered that the c-BN film formation with the reactive ion-plating method is attributed to the preferential orientation of the basal plane of the initially deposited hexagonal-like BN film composed of fine crystallites and the compressive stress generated in the film by bombarding the growing BN film with ions with energies of 15 ~ 65 eV such as argon and nitrogen ions. Furthermore, it was considered that the preferential orientation of the initially deposited hexagonal-like BN film is taken place due to the resputtering of the growing film caused by ion impacts, and needed to store the strong compressive stress in the film.

References

[1] K.Inagawa, K.Watanabe, K.Saitoh, Y.Yuchi and A.Itoh, Surf. Coat. Technol., **39/40**, 253(1989).

[2] D.R.McKenzie, D.J.H.Cockayne, D.A.Muller, M.Murakawa, S.Miyake, S.Watanabe and P.Fallon, J. Appl. Phys., **70**, 3007(1991).

[3] H.Yokoyama, M.Okamoto and Y.Osaka, Jpn. J. Appl. Phys., **30**, 344(1991).

[4] D.J.Kester and R.Messier, J. Appl. Phys., **72**, 504(1992).

[5] D.J.Kester, K.S.Ailey, R.F.Davis and K.L.More, J. Mater. Res., **8**, 1213(1993).

[6] D.L.Medlin, T.A.Friedmann, P.B.Mirkarimi, P.Rez, M.J.Mills and K.F.McCarty, J. Appl. Phys., **76**, 295(1994).

[7] T.Ichiki, T.Momose and T.Yoshida, J. Appl. Phys., **75**, 1330(1994).

[8] A.Kinbara, *Sputtering Phenomena* (Tokyo-Daigaku-Shuppan-Kai, Tokyo, 1985), p.77.

[9] C.Weissmantel, K.Bewilogua, D.Dietrich, H.-J.Erler, H.-J.Hinneberg, S.Klose, W.Nowick and G.Reisse, Thin Solid Films, **72**, 19(1980).

[10] C.Weissmantel, Thin Solid Films, **92**, 55(1982).

[11] A.Weber, U.Bringmann, R.Nikulski and C.-P.Klages, Surf. Coat. Technol., **60**, 493(1993).

[12] D.R.McKenzie, W.D.McFall, W.G.Sainty, C.A.Davis and R.E.Collins, Diamond Relat. Mater., **2**, 970(1993).

[13] R.Berman and F.Simon, Z. Elektrochem., **59**, 333(1955).

[14] K.L.Chopra, *Thin Film Phenomena* (Robert E. Krieger, Florida, 1979), p.278.

[15] E.Cartmell and G.W.A.Fowles, *Valency and Molecular Structure* (Butterworth, London, 1977), p.116.

List of Publications

[1] Conditions for Formation of BN Film by Ion-Plating Method.
H. Kohzuki, K. Yamada, K. Yamagishi, and Y. Okuno,
J. Jpn. Soc. Powder Metall., **38**, 435(1991).

[2] B K X-Ray Emission Spectra of Boron in Its Compounds.
H. Kohzuki and M. Motoyama,
Advan. X-Ray Chem. Anal. Jpn., **23**, 43(1992).

[3] Characterization of BN Powder and BN Films by EPMA.
H. Kohzuki and M. Motoyama,
J. Jpn. Inst. Metals, **56**, 565(1992).

[4] Characterization of Ion-Plated BN Films from X-Ray Emission Spectra of Boron.
H. Kohzuki and M. Motoyama,
J. Jpn. Inst. Metals, **56**, 572(1992).

[5] Atmospheric Degradation of BN Films Deposited by Ion-Plating Method.
H. Kohzuki, M. Motoyama, Y. Okuno, and K. Yamada,
J. Jpn. Soc. Powder Metall., **40**, 449(1993).

[6] Improvement of Adhesion of Cubic Boron Nitride Film on Silicon Substrate.
H. Kohzuki, Y. Okuno, and M. Motoyama,
Proceedings of the 2nd International Conference on the Applications of Diamond Films and Related Materials, 631(1993).

[7] Effect of Self-Bias Voltage on Formation of c-BN Film.
H. Kohzuki, T. Ishihara, Y. Okuno, and M. Motoyama,
J. Jpn. Soc. Powder Metall., **41**, 57(1994).

[8] Soft X-Ray Spectrochemical Analysis of Boron Nitride Thin Film Structure.
H. Kohzuki, M. Motoyama, S. Shin, A. Agui, H. Kato, Y. Muramatsu, J. Kawai,
and H. Adachi,
Advan. X-Ray Chem. Anal., Jpn., **26**, 175(1995).
(*Proceedings of the 5th Workshop on Total Reflection X-Ray Fluorescence Spectroscopy and Related Spectroscopical Methods*).

[9] Adhesion Improvement of Cubic Boron Nitride Film on Silicon Substrate.
H. Kohzuki, Y. Okuno, and M. Motoyama,
Diamond Films Technol., **5**, 95(1995).

[10] X-Ray Spectroscopic Analysis of Boron Nitride Clusters Deposited by Ion-Plating Method.
H. Kohzuki, M. Motoyama, T. Kaneyoshi, Y. Kowada, J. Kawai, and H. Adachi,
Proceedings of the 7th International Symposium on Small Particles and Inorganic Clusters,
(to be published).

[11] Discrete-Variational Hartree-Fock-Slater Calculations of Polarized B K-Emission Bands from Hexagonal Boron Nitride Thin Film.
H. Kohzuki, T. Kaneyoshi, Y. Kowada, M. Motoyama, and F. Kanamaru,
Physica B, (to be submitted).

Acknowledgments

The studies presented in this thesis have been carried out at Hyogo Prefectural Institute of Industrial Research during 1988–1995.

The author wishes to express his sincerest gratitude to Professor Fumikazu Kanamaru of Osaka University for his direction, valuable suggestions and discussions in every aspect of the work. It cannot be overstated that Professor Kanamaru's kind generosity has encouraged the author very much. The author is greatly indebted to Professor Hitoshi Watarai and Professor Tomoji Kawai of Osaka University for their helpful discussions and comments. The author would like to express his sincere thanks to Dr. Shinichi Kikkawa, Associate Professor of Osaka University, and Dr. Masao Takahashi, Assistant of Osaka University for their valuable suggestions, discussions and hearty encouragement.

The author is greatly indebted to Dr. Muneyuki Motoyama for his direction, insightful discussions and encouragement throughout this research in Hyogo Prefectural Institute of Industrial Research.

The author wishes to express his gratitude to Associate Professor Jun Kawai of Kyoto University, Assistant Yoshiyuki Kowada of Hyogo University of Teacher Education, and Mr. Takahiro Kaneyoshi of Hyogo Prefectural Institute of Industrial Research for help with DV-Xα calculations of B K x-ray emission spectra. The author would also like to express his appreciation to Dr. Shik Shin and Dr. Akane Agui of Tokyo University, Dr. Hiroo Kato of National Laboratory for High Energy Physics, and Dr. Yasuji Muramatsu of NTT Interdisciplinary Research Laboratories for measurements of B K x-ray emission spectra using synchrotron radiation, to Professor Shinichi Nakajima, Associate Professor Hiroshi Harima and Assistant Kenji

Kisoda of Osaka University for measurements of Raman spectra, to Dr. Masato Tomita of NTT Interdisciplinary Research Laboratories for measurements of EELS spectra, to Associate Professor Akifumi Onodera of Osaka University for supplying the samples of boron nitride powders used in this work, and to Mr. Tuguo Ishihara of Hyogo Prefectural Institute of Industrial research for measurements of infrared absorption spectra.

It is also a pleasure for the present author to acknowledge the hospitality, collaboration and helpful advice of Dr. Yukinobu Hayashi, Mr. Yasuo Okuno, Mr. Toshiaki Nishioka, and all the other members of Hyogo Prefectural Institute of Industrial Research.

Finally, the author sincerely thanks his family for their affectionate encouragement throughout this work.

Hidenori Kohzuki

1995